Trim optimization for ships in service

A grey-box model approach using operational voyage data

R.H. Zwart

MSc thesis Marine Technology - Ship design, production and operations

A digital copy of this thesis can be retrieved at the TU Delft repository: SDPO.20.010.m

TUDelft

Trim optimization for ships in service

A grey-box model approach using operational voyage data

by

R.H. Zwart

to obtain the degree of Master of Science
at the Delft University of Technology,
to be defended publicly on Wednesday June 17, 2020 at 14:00 AM.

An electronic version of this thesis is available at `http://repository.tudelft.nl/`.
Front picture from unsplash.com (open source)

T̃U Delft

Abstract

The IMO has set the goal that greenhouse gas emissions from international shipping should peak as soon as possible and should be reduced by 50% by 2050 compared to 2008, consistent with the Paris Agreement of the United Nations (2015). Trim optimization is an approach considered by the industry to improve the energy efficiency of ships, having a potential in both reducing operational costs and to decrease the emissions of the ship. Potential fuel consumption reduction by trim optimization is 0.5 to 3 % and to up to 7% in extreme cases.

Stolt Tankers, a shipping company active in the chemical tanker market, wants to increase the energy efficiency of their ships in operation by trim optimization. For a limited number of ships, trim tables from model scale towing tests are available, but these are not used and the accuracy of these tables are unknown. The objective of this research was to develop a method to decrease fuel consumption by trim optimization, by a dynamic fuel consumption estimation model based on available operational data, that can be integrated in the voyage management system of Stolt Tankers.

A dynamic fuel consumption estimation model has been developed, using mainly the noon report data of the C-38 ship class, consisting of six sister vessels of 38 000 DWT chemical tankers. Quality of noon report data is an issue: human error in observing and recording data causes noise and a mismatch exists between the snapshot of conditions on one hand, and the 24 hr averaged sailing speed and recorded shaft power or fuel consumption on the other hand. A data pre-processing framework has been developed and applied to integrate and transform the data, clean and filter the data and to prepare the data to be used for the neural network.

A grey-box model (GBM) approach is followed, combining a white-box model (WBM) with a black-box model (GBM) approach, by using a regression model together with an artificial neural network (ANN). Advantages of using a GBM approach is that less historical data is required than for a BBM, extrapolation qualities may be improved and unreasonable results can be avoided. The model has been able to extract the effects of speed through water, mean draft, trim, sea water temperature, wind force, sea state and swell state and their relative direction to the ship and days since last hull cleaning and propeller polishing.

The model has shown to perform optimal using the regression model of Lutzen and Kristensen (2013), combined with a multiple layer feed-forward neural network, consisting of 1 hidden layer with 15 neurons. The model is able to estimate the shaft power with an average accuracy of 6.58 % for a random test set of the noon report data. It is able to extract the effect of trim on shaft power and to consider the effect of weather and fouling conditions. Model results show that about 1 to 2% of shaft power per 0.50 m can be saved, with trim by bow being the optimal trim.

Sea trials have been performed to validate the model performance. Based on these sea trial results, it is concluded that the model performs most accurate for conditions that are represented by a high quantity of historical data. The model can be applied for speeds between 12 and 14 knots and for mean draft conditions of 9.5 m and more. Within this range, the effect of trim and weather conditions are followed with reasonable accuracy. It is confirmed by the sea trial that trim by bow is the optimal trim, with a much stronger magnitude of the effect of trim on shaft power. A difference of 6 to 8% in shaft power was found for a change in trim of 0.50 m. This shows that the potential fuel savings indicated by the model can be even more significant in practice, compared to the model results.

Compared to similar models in available literature, the model presented in this research has a higher accuracy on a random test set of noon report data. However, no indications are observed that would confirm any of the possible advantages of using a GBM over a BBM approach. Therefore it is more likely that the quality of the filtered noon reports has contributed to this, as well as the unique feature selection. Further model modifications may increase the applicability, but the model performance with the goal of trim optimization remain limited, caused by the drawbacks inherent to using noon report data.

Preface

Using marine technology to improve daily ship operations is what challenges me. Trim optimization for ships in service is therefore fully within my personal interest, which made and kept me enthusiastic to work on this project for the entire duration. The result is this master thesis, required to complete the MSc program Marine Technology at Delft University of Technology.

The support I received during the project was a major contribution to both the result and how I experienced working on it. Austin Kana, I would like to thank you for enthusiastic attitude from the first meeting onwards, the confidence you gave me and for the clear and supportive feedback. Our regular meetings and your extensive involvement helped me keeping on the track. Also, I would like to thank professor Hans Hopman for the critical and well-thought questions during the progress meetings, which pushed me to provide a well-thought answer.

I am very grateful for the opportunity given by Stolt Tankers to work on such a relevant and practical problem. Jordi Bogaard, thank you for your endless support to provide me all information I needed, enabling to test the model by actual sea trials, getting to know the company and for your enthusiastic reactions on the research results. I highly enjoyed our weekly coffees and your sense of humor.

Finally, my deepest gratitude goes to my parents. Your limitless support made it possible to enjoy my study as much as I did. You are always ready for me and willing to help me making the right decisions. Thank you for everything.

R.H. Zwart
Delft, June 2020

Contents

List of Figures

List of Tables

I

Part I: Introduction and problem analysis

1

Introduction

Decreasing the operating expenses from fuel consumption reduction is of special interest for shipping companies. Generally, the bunker fuel cost dominates the expenses of a ship with annual fuel costs being in the order of millions (Du et al., 2019, Leifsson et al., 2008). For a shipping company having multiple ships in the fleet, this means that a marginal saving of fuel costs can result in a significant saving in annual fuel costs. Fuel efficient operations help shipping companies to lower their operational cost and thereby to maintain or increase their competitive position in the market.

Moreover, the IMO (2019a) has set the goal that greenhouse gas (GHG) emissions from international shipping should peak as soon as possible and should be reduced by 50% by 2050 compared to 2008, consistent with the Paris Agreement of the United Nations (2015). In the third IMO study to GHG emissions (IMO, 2014), it is estimated that the international shipping industry emitted 796 million tonnes of CO_2 in 2012, accounting for about 2.2% of the total CO_2 emissions caused by human for that year, while transporting almost 90% of the global trade (Islam and Guedes Soares, 2019). Due to the estimated growth of the world maritime trade, the research of IMO states that the emissions from international shipping could grow between 50% and 250% by 2050. Coraddu et al. (2017) states that GHG emissions from the combustion of oil-based fuels are directly proportional to fuel consumption, which makes improving the ship energy efficiency one of the possible solutions to reduce GHG emissions. Similarly, shipping also contributes to air pollution, mainly in the form of sulphur oxides (SO_X), nitrogen oxides (NO_X) and particulate matter (PM).

To reduce GHG emissions, the Marine Environment Protection Committee (MEPC) of IMO adopted a strategy, in which shipping companies are supported to improve the energy efficiency operational index (EEOI) of their ships in operation. This is done by the Ship Energy Efficiency Management Plan (SEEMP). The SEEMP establishes a mechanism to improve the energy efficiency of the ship's operation and to provide an approach for shipping companies to manage ship and fleet performance over time (Kishev et al., n.d., Lu et al., 2015, Yuan and Nian, 2018).

Trim optimization is one of the approaches considered by the industry to improve the energy efficiency of ships, having a potential in both reducing operational costs and to decrease the emissions of the ship. Trim optimization is the selection of trim with the goal of fuel consumption reduction, by ballast water management and load distribution, which can be done without significant changes to the ship structure (Coraddu et al., 2017, Gao et al., 2019, Islam and Guedes Soares, 2019).

Stolt Tankers, a subsidiary of Stolt-Nielsen Ltd., is a shipping company active in the chemical tanker market who wants to increase the energy efficiency of their ships in operation by trim optimization. For a limited number of ships, the effect of trim on propulsion power is known from model scale towing tests, but for the majority of ships, the effect is not known. The goal of this research is to develop a method able to determine the effect of trim on the propulsion power of the ship, to enable trim optimization for all ships in operation by Stolt Tankers.

1.1. Description of the concept trim optimization

Trim is defined as the draft at the stern (or aft of the ship, denoted as T_{aft}), minus the draft at the bow (or forward, denoted as T_{fwd}), as shown in formula 1.1, all in metres. Hence, positive trim is defined as trim by stern, which means that the aft of the ship has a larger draft compared to the rest of the ship. Negative trim is often called trim by bow. In this research, optimal trim is defined as the trim condition at which the required propulsion power is minimized.

$$trim = T_{aft} - T_{fwd} \tag{1.1}$$

Typically, the optimal trim can be determined by consulting trim tables. Trim tables are generated from the results of model scale towing tests, or in some cases from computational fluid dynamics (CFD) simulations. During these tests, the required power is measured for combinations of draft and trim and for a range of speeds. The results of these tests are the trim tables. In this way, the optimal trim condition for a certain mean draft for each measured speed can be determined. An illustration is given by figure 1.1. This example represents a trim table for a speed of 13.0 knots. It can be seen that the values represent the trial condition specified as 0 Beaufort. The green color represents a reduction in required propulsion power. For this speed, the observed trend is that negative trim generally increases the required propulsion power, except for partial load conditions, where a slight trim to the stern seems to have a small favourable effect as well. If a draft condition of $T = 10m$ is considered, it can be seen that for the specified condition, the propulsion power in even keel condition is predicted to be 4009 kW. Trimming the vessel by bow with $-0.50m$ will result in a decrease in required propulsion power of 97 kW compared to even keel. Trim by stern with $1.50m$ will result in an increase of required propulsion power of 185 kW. The extreme values in this example shows that 7 % in required propulsion power can be saved when taking even keel as a reference, as done in formula 1.2.

$$\Delta P[\%] = \frac{|P_{fwd} - P_{evenkeel}| - |P_{aft} - P_{evenkeel}|}{P_{evenkeel}} \times 100 \tag{1.2}$$

In the past years, alternatives to trim tables in the field of trim optimization have emerged. A number of commercial trim optimization tools have been developed and entered the market, which vary in price, user friendliness, fundamental approach and performance (Architect, 2014). A number of these tools is reviewed in chapter 3.

Draught (even keel)	Difference in PD /kW with respect to even keel condition (Trial Prediction, Bft. 0) Trim (Ta-Tf) /m:									PD /kW (even keel)
	1.50	1.25	1.00	0.75	0.50	0.25	0.00	-0.25	-0.50	
6.50	161	155	145	127	97	53	0			3567
6.60	155	147	135	117	88	47	0			3570
6.70	149	139	125	106	79	42	0			3573
6.80	143	130	115	96	70	37	0			3577
6.90	138	122	105	85	61	32	0			3580
7.00	132	114	96	75	53	27	0			3584
7.10	127	107	86	66	44	22	0			3588
7.20	122	99	77	56	36	18	0			3592
7.30	117	92	69	47	29	13	0			3597
7.40	112	86	61	39	21	9	0			3602
7.50	108	80	53	31	15	5	0			3608
7.60	104	74	47	24	9	2	0			3614
7.70	101	69	41	17	3	-1	0			3621
7.80	98	65	35	12	-2	-4	0			3629
7.90	96	61	30	7	-6	-7	0			3637
8.00	94	59	27	3	-10	-9	0			3646
8.10	93	56	24	0	-12	-10	0			3656
8.20	92	55	22	-2	-14	-11	0			3667
8.30	93	55	21	-3	-15	-12	0			3679
8.40	93	56	22	-3	-15	-12	0			3692
8.50	95	57	23	-2	-14	-11	0	-15	-44	3706
8.60	97	60	26	1	-12	-10	0	-17	-48	3721
8.70	101	63	30	5	-9	-8	0	-20	-51	3737
8.80	104	68	35	10	-5	-6	0	-22	-55	3754
8.90	109	73	41	16	0	-3	0	-24	-58	3772
9.00	114	80	48	23	6	0	0	-26	-62	3791
9.10	120	86	56	30	13	4	0	-29	-65	3811
9.20	126	94	64	39	20	8	0	-31	-69	3831
9.30	132	102	73	48	27	12	0	-33	-72	3852
9.40	139	111	83	58	35	17	0	-35	-76	3874
9.50	146	120	93	68	44	22	0	-38	-79	3895
9.60	154	129	104	79	53	27	0	-40	-83	3918
9.70	161	139	115	90	62	32	0	-42	-86	3940
9.80	169	148	126	101	72	37	0	-44	-90	3963
9.90	177	158	138	113	81	43	0	-46	-94	3986
10.00	185	168	149	124	91	48	0	-49	-97	4009

stern trim ←|→ bow trim

Figure 1.1: Trim table for one single speed (V = 13.0 knots) (HSVA, 2014).

1.2. The potential of trim optimization in reducing fuel consumption

The MEPC (n.d.) estimates that optimization of trim and draft can reduce the fuel consumption by 0.5% to 3% on main engine fuel consumption for most vessel types. For ships with partial loads, this can be as high as 5%. In other literature, Coraddu et al. (2017) concludes that improvements exceeding 2% in fuel consumption for a handymax chemical tanker can be achieved. In a case study from DNV-GL (2013), where the benefits of a commercial optimization tool (the ECO Assistant of DNV-GL) was tested, savings were recorded between 2% and 14% for different draft and speed combinations of a handymax bulk carrier. Furthermore, Yuan and Nian (2018) states that trim optimization for a VLCC leads to around 1.8% change in fuel consumption, Du et al. (2019) states that trim optimization could save 5-6% bunker fuel for a 9000 TEU containership and Gao et al. (2019) states a save in bunker fuel of 3-7% for a PCTC from on-board measurements. Based on this, it can be concluded that the effective reduction of fuel consumption by trim optimization can be significant, but depends on the ship type, operational profile and freedom in trimming.

In addition to the above, the potential of effective trim optimization on fuel savings can be estimated by analyzing the results of the model scale towing tests of one ship class of Stolt Tankers (the C38 class) of which trim tables are available. The results are shown in appendix J, with graphs showing the effect of trim for three mean drafts and trim tables valid for a range of speeds. In these tables, propulsion power is considered, which is directly related to fuel consumption (as will be shown in chapter 4). It is observed that trim by bow reduces propulsion power of around 7 % for all tested speeds at a mean draft of 10 m, compared to 1.50 m trim by stern. In practice, ships sometimes sail with a trim by stern exceeding 1.50 m. When smaller trim values are considered, the difference in propulsion power is less, which confirms that the effective reduction in fuel

consumption depends on the operational profile.

The potential of trim optimization can be quantified in terms of savings in operational cost and reduction in CO_2 emissions for Stolt Tankers in particular. This is done by formula 1.3 and 1.4 for one single ship. The savings in operational cost and CO_2 are listed in table 1.1. The following assumptions have been made:

- The fuel consumption (FC) of a chemical tanker is estimated to be 26 MT per day;

- The vessel sails 183 days per year, which is the average days at sea for a chemical tanker of 20.000 DWT and above (IMO, 2014);

- Approximately 80% of the total fuel consumption is used for propulsion power (based on noon report data for the C38 class), denoted as π_{prop};

- Potential decrease in power (ΔP) is varied between 2% and 7%;

- CO_2 conversion factor C_f is 3.2060 $\frac{t}{t}$ for MDO (approximate value for low-sulphur fuel oil) (IMO, 2014);

- The price (P_{fuel}) of MGO/MDO is around 600 USD/MT, which is the approximate fuel price of MGO in Singapore, November 2019 (Ship and Bunker, 2019).

$$\Delta_{fuelcosts} = FC \cdot \text{yearly sailing days} \cdot \pi_{prop} \cdot P_{fuel} \cdot \Delta P \tag{1.3}$$

$$\Delta_{CO_2-emissions} = FC \cdot \text{yearly sailing days} \cdot \pi_{prop} \cdot C_f \cdot \Delta P \tag{1.4}$$

Table 1.1: **Potential of trim optimization, quantified for a single large chemical tanker.**

Potential of trim optimization	2%	7%
Yearly fuel cost savings	USD 46.000	USD 160.000
Yearly CO_2 reduction	244 tons CO_2	854 tons CO_2

1.3. Chemical tanker fleet description

Stolt Tankers is a shipping company that operates a fleet of 104 chemical and parcel tankers. The assets are deployed globally, with over 70 deep-sea ships and regional fleets in Europe, Asia and the Caribbean, coastal fleets in Asia and with inland barging services in Europe and the US Gulf.

The relative size of the chemical tankers in the world fleet can be defined by deadweight tonnage (DWT), using the analysis of UNCTAD (2019). In this analysis, a complete division of the world fleet by principal ship type of seagoing vessels of 100GT and above is presented, including offshore drillships and floating production, storage and offloading units, but excluding military vessels, yachts, waterway vessels, fishing vessels and offshore fixed and mobile platforms and barges. In early 2019, the total number of ships in the world fleet was 95 402, accounting for 1.92 billion DWT. The division of ships is shown in figure 1.2. Within this structure, chemical tankers are within the group of *other ship types*. The same structure is used in an analysis of the world fleet division by DWT, based on the data of UNCTAD (2019), and is shown in figure 1.3. It can be concluded that chemical tankers contribute to approximately 2.34 % of the world fleet by DWT, with a total capacity of 46 297 000 DWT.

Within the group of chemical tankers, the fleet of Stolt Tankers in total had a capacity of 2 687 thousand DWT (Intelligence, 2019), at approximately the same moment of measurement of UNCTAD (2019), early 2019, representing approximately 5.80% of the chemical tanker fleet.
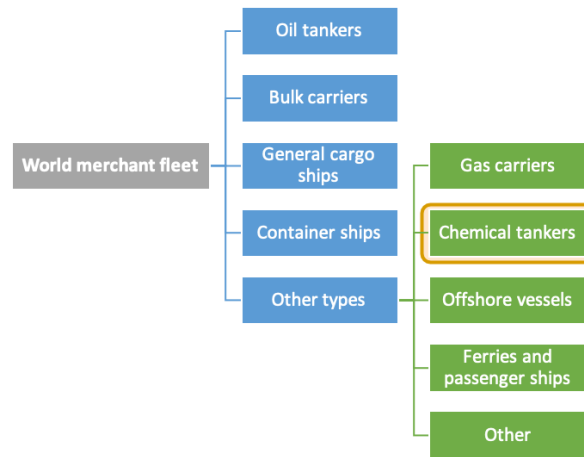
Figure 1.2: World fleet by principal ship type.
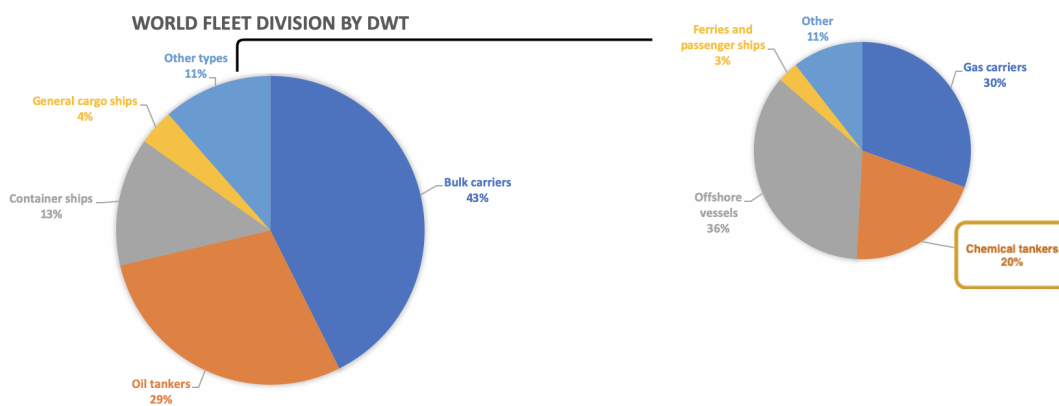
Figure 1.3: World fleet division by (DWT).

1.4. Structure of report

This chapter has described the concept of trim optimization, drivers to use this technology to reduce fuel consumption and a description of the chemical tanker fleet. Chapter 2 and 3 covers the problem analysis and a literature review to solution approaches.

The remainder of this report is organized as following. Part II of the report consists of a technical background of the problem and the solution approach. In part III, the method and model is defined. This model will be tested with a case study on one of the ship classes of Stolt Tankers. Finally, part IV consists of the discussion and conclusion.

2

Problem analysis

It has been introduced that Stolt Tankers wants to use trim optimization to reduce the fuel consumption of their ships in service. In this chapter, the problem is analysed in section 2.1 to section 2.4. As a result of this, the problem is defined in section 2.5. The available data is described in section 2.6. Next, the research objective is described in section 2.7.

2.1. Availability of trim tables

In paragraph 1.1, it is explained that trim tables can be consulted to determine the optimal trim. However, one of the problems is the availability of these documents. From contact with staff within Stolt Tankers[1] and research within the database of Stolt Tankers for any trim information, the availability of trim tables for the ships of Stolt Tankers is determined. As far as known, trim tables are available for two ship classes of the fleet of Stolt Tankers: the D37 class and the C38 class, with 9 and 6 ships within the class, respectively. This means that in total 15 ships of the fleet can consult the trim tables. For the remaining ships, it can be that the required model tests were never performed, or that the ship is acquired second-hand, without acquiring the trim tables.

It can be concluded that one of the problems of sailing at optimal trim, is the unavailability of trim tables. Therefore, one of the objectives of the research is to construct a method that can generate trim tables for all ships commercially operated by Stolt Tankers.

2.2. Uncertainty of accuracy of existing trim tables

Differences are expected in optimal trimming conditions between the conditions suggested by trim tables and the optimized trim conditions on full scale and realistic conditions, due to scaling effects from model scale at calm water conditions to ship scale, with possible dynamic effects from weather and sea conditions. In paragraph 3.1, these effects are explained in more detail.

As a result, the accuracy of the existing trim tables is uncertain. Consequently, it is uncertain if the existing trim tables provide trim conditions that minimizes fuel consumption on full scale and in realistic conditions. The influence of dynamic factors on the optimal trim condition supports the need for a dynamic trimming method.

---

[1] Explicitly mentioned in e-mail conversation with L. de Jong from the 'New Building and Technical' department, on 21-10-2019.

2.3. Integration of trim in voyage management

In paragraph 2.1 it is found that trim tables are available for only a small part of the ships of the fleet. This raises two questions. The first question is if the information of optimal trim values from the available trim tables is adopted in the operating process for the relevant ships. The second question is how the ship is trimmed without considering trim tables and what role trim optimization plays within the current process. Therefore, an exploratory research is performed to understand the role of trimming from the perspective of fuel consumption in the current loading and trimming process.

From a conversation with the superintendent of ships including the C38 class[2], it is clear that the available trim tables are not used at all. Instead, the trim of the ship is determined by numerous other reasons, dominated by the limited freedom in stowage of cargo.

A brief survey[3] to ask if the trim tables are available on board and if these are used in ship operation, was sent to the crew of C38 and D37 ship class (for which trim tables have been developed). All questions and received answers are shown in appendix F. Generally, these trim tables were not available on board nor part of daily ship operation. Two ships within the D37 ship class, such trim tables, or an equivalent in the loading computer, are available on board, but are not actively used. From the answers of the D37 ship class, it is known from experience that trim by bow generally increases the attained speed for a given engine power setting. Main reasons mentioned for not taking optimal trim into account are the limitations inherent to the cargo stowage.

The ship operators are responsible for the initial stowage plan and determine which tank is allocated to which cargo. If the limited freedom in stowage of cargo is dominating the trim condition, the role of the operator on the trim condition of the ship is important. A conversation with one of the operators of other types of ships[4] made clear that the integration of trim in the cargo stowage plan is limited to the prevention of excessive trim, not only during transit, but between (un)loading ports as well.

On-board of the ships, it is the chief officer who is responsible for the stowage of the cargo and the trim of the ship. From a conversation with the chief officer[5] of one of the ships, the concept of trim on-board of ships is better understood. Firstly, the chief officer explained that the trim of the ship is mostly dominated by the stowage of the cargo, draft limitations in ports and safety. In addition to this, the chief officer can trim the ship. The trim situation of the ship is monitored with the loading computer, which provides the current draft at the bow and stern and the loading condition of the cargo, fuel, fresh water and ballast tanks. It was stated that it is unclear how the ship is trimmed optimal related to fuel consumption. According to the chief officer, both trim by stern and trim by bow can be argued to be the preferable trim condition regarding fuel consumption and that the trim condition depends on the crew's preference and characteristics of the ship, such as manoeuvrability, course-keeping and sea-keeping characteristics. He furthermore explained that he normally trims the ship by stern between 0.5 and 1.0 meter in port (known as static trimming), which will result in a trim condition that can be described as close to even keel or slightly trim by bow during sailing, as a result of dynamic trimming effects.

It can be concluded that trim optimization is not integrated in the voyage operations procedures. Neither the crew or the operators consult trim tables or consult any structured methods to optimize trim with the goal of fuel consumption reduction. The trim of the ship is done based on experience and preference of the crew. This practice indicates that the trim of all ships in the fleet is done in a sub-optimal way from the perspective of fuel consumption.

2.4. Limitations for sailing at optimal trim

Sailing at optimal trim conditions is limited by a number of factors. During the exploration study to the trimming process on ships and in the operations department, some of these are already mentioned, such as

---

[2]Conversation with P. Brant, senior superintendent of the European fleet, which includes ships of the C38 class (one of the two ship classes with trim tables available), on 30-10-2019.

[3]Performed by e-mail in January and February 2020.

[4]Conversation with M. Speksnijder, operator of the Inter-European fleet, on 30-10-2019.

[5]Conversation on board of the Stolt Osprey with the chief officer of the Stolt Osprey, on 09-10-2019.

manoeuvrability, course-keeping, sea-keeping characteristics and limited freedom in stowage of the cargo. In order to decrease fuel consumption by trim optimization, these limitations should be identified as complete as possible. The impact of trim optimization will furthermore depend on to which extent these limitations can be overcome.

2.5. Problem definition

Based on the problem analysis, the problem is defined in table 2.1. The problem is that all ships of Stolt Tankers sail at sub-optimal trim conditions, with the consequence of extra fuel consumption with associated costs and emissions. The trimming process of ships is dominated by cargo limitations and any information on optimal trim from the perspective of fuel consumption minimization is not integrated in the voyage management. The solution can be found in a method that can generate dynamic trim tables, based on a dynamic fuel consumption prediction model. Limitations should be identified and overcome. The trim optimization method is to be integrated in the voyage management. Figure 2.1 shows the identified sub-problems, the requirements for the solution and the ultimate objective. The figure also shows how the sub-problems are related to each other.

Table 2.1: **Summary of problem analysis and problem definition.**

Sub-problem	Problem specification		Solution requirement
1. (see 2.1)	Trim tables from model testing are available for only 15 ships of the 104 ships of the fleet.	→	A method is to be constructed that is able to generate trim tables for the 89 ships of which trim tables are not available.
2. (see 2.2)	Uncertainty exists regarding the performance of the available trim tables. The uncertainty is caused by scaling effects between model and full scale, and because of the neglected influence of weather and sea conditions on optimal trim.	→	A method is to be constructed that is able to verify the performance of existing trim tables. The trim optimization method should also incorporate the influence of weather and sea conditions.
3. (see 2.3)	Trim optimization from the perspective of reducing fuel consumption is not integrated in the voyage management. Instead, trimming is done by the crew's experience.	→	The trim optimization should be integrated in the voyage management system in order to actually reduce fuel consumption.
4. (see 2.4)	Freedom in trimming the ship is limited by (partly) unknown factors.	→	Factors that limit the freedom of the trim of ships should be identified, quantified and, if possible, solved.

2.6. Available data to solve the problem

The amount of unique ship parameters and recorded parameters from voyage reports is comprehensive. Table 2.2 provides an overview of different types of data sources and aims to provide a indication of available data.

The voyage reports are part of daily operations and for that reason, the database of Stolt Tankers has an extensive record of voyage reports and hence a comprehensive database of operational voyage data. All the data from the voyage reports are collected and integrated in the voyage management system of the company,
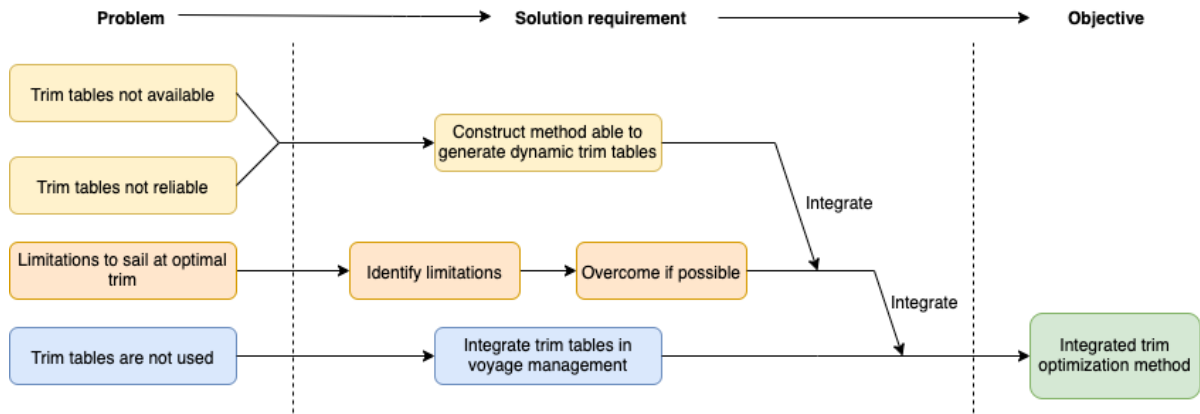
Figure 2.1: Definition of the problem.

Table 2.2: **Description of available data.**

Type of data	Source	Description of data or examples
Ship design specifications	Inhouse ship specifications brochure, general arrangement, loading manual, hydrostatic tables, loading computer, sea trial results	ship design parameters, hull shape information, length centre of buoyancy, propulsion system, engine performance, cargo holds arrangement
Maintenance data	Inhouse maintenance database	Date of last hull cleaning, propeller fouling
Voyage report data	Noon reports	Operational: draft, load, trim, heading, speed, shaft power Environmental: temperature, wind, sea and swell state and directions
Trim tables	Model scale test results	Trim tables of two ship classes

called Veslink. The data is available for ships in the Stolt Tankers Joint Services (STJS) pool, which is the pool that arranges the commercial management for the ships that are owned by Stolt Tankers and others. This pool consists of ±75 ships.

It should be noted that the raw data of the voyage report is generally considered to be noisy. Sources of error can either be technical failures of the sensors and because of human error, for example in estimating, recording or calculating values for certain fields in the ship log. Also, the recording of weather and sea conditions is done based on a snapshot once every 24 hours. This observation may differ from the average weather and sea condition over the past 24 hours, and thus may not provide an accurate value of the past 24 hours.

Another source of error can be the difference in actual draft and the indicated (and recorded) draft. The draft is indicated by the loading computer on-board the ships, which calculates the forward draft, mean and aft based on the loading levels of the tanks and the hydrostatics of the vessel. Although the indicated values are regularly checked by the crew by reading the draft marks while the ship is in port, an error may still be introduced due to the large sized reading marks and the presence of small waves.

Pressure distribution around a ship hull surface at a constant speed differs from hydrostatic pressure. As a result, the ship experiences a hydrodynamic lift and pitch moment, known as sinkage and trim (Ma et al., 2016). This dynamic trim effect is confirmed by crew of two ship classes within Stolt Tankers. However, it is the static trim condition indicated by the loading computer that is recorded in the noon reports[6].

---

[6]Mentioned in e-mail contact with the crew of ships of the C-38 and D-37 ship class of Stolt Tankers in February 2020.

2.7. Research objective

The objective of this master thesis is:

To develop a methodology to decrease fuel consumption by trim optimization, by a dynamic fuel consumption estimation model based on available operational data, that can be integrated in the voyage management system of Stolt Tankers.

The methodology should fulfill the following requirements. The model should:

- estimate the required power for propulsion, with sufficient accuracy to extract the effect of trim;

- be able to generate trim tables considering he effect of dynamic factors;

- be based on available data within Stolt Tankers;

- deal with errors in voyage report data;

- be able to be used for a range of ship types within the fleet.

The methodology will be tested in a case study. Based on these results, the research questions can be answered. If these are answered and the methodology requirements are met, the research objective is fulfilled. The coherence of the research objective, methodology requirements and research questions is illustrated by figure 2.2.

1. What methods exist to generate trim tables?

2. How can the required shaft power of a ship under specified conditions be estimated?

3. At which trim condition is the required shaft power minimized?

4. How accurate are trim tables based on model scale towing tests?

5. What limitations exist to trim a ship?

6. How can the proposed method for trim optimization be integrated in the voyage management system?
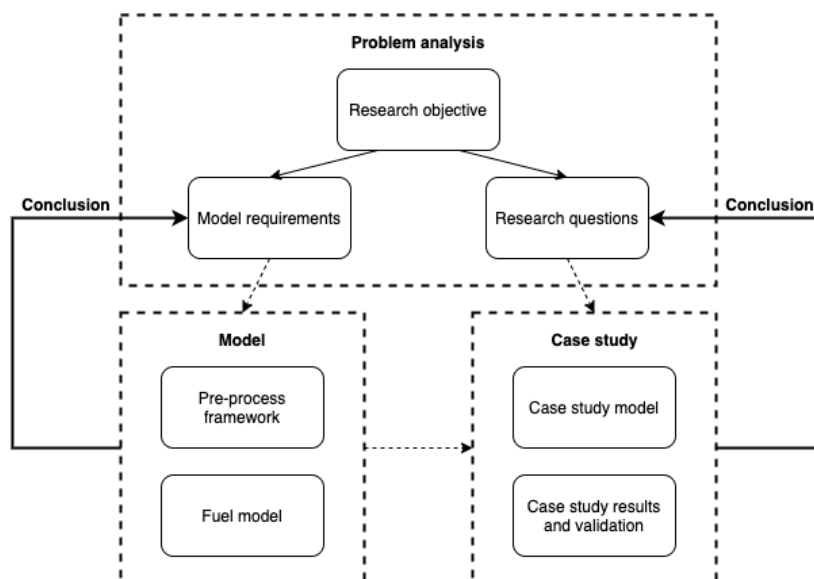
Figure 2.2: Coherence of research objective.

3

Solution approaches

This chapter answers research question 1: *What methods exists to generate trim tables?* by providing an literature review.

Performing full ship scale sea trials for different speeds, draft and trim conditions to develop trim tables is one of the possible approaches. However, this would require comprehensive sea trials in uncontrollable conditions, idling the ship operations and to be repeated for every ship.

A number of alternative approaches exist, either based on model scale test results or full ship scale data from daily ship operations and focused on a single ship (class) or using a generic approach. These characteristics are used to organize the different approaches in a matrix, as done in figure 3.1. The different approaches are discussed in the following sections and tested upon the method requirements of section 2.7.

Figure 3.1: Solution matrix. The numbers refer to the corresponding paragraph.

3.1. Trim tables from model towing tests or CFD simulations

Trim tables can be constructed from model towing tests and CFD calculations. For a range of combinations of speed and draft, the required propulsive power is determined for a range of trim conditions. The result is a range of trim tables, of which an example is illustrated in figure 1.1.

3.1.1. Trim tables based on model scale towing tests

To scale the results from model tests to values true for full scale, the model and actual ship should satisfy with similarity constraints. These constraints, together with the challenge to satisfy these, is explained in Larsson and Raven (2010). However, within the scope of this section, a brief review is presented here.

The three similarity constraints consists of:

- Geometric similarity: The model and the ship should be geometrically similar, which is a challenge especially for the full scale ship;

- Kinematic similarity: All velocities in the flow are to be scaled by the same factor. It means that the streamlines around the hull will be similar at model and full scale;

- Dynamic similarity: All forces of the flow are to be scaled by the same factor. Force vectors thus have the same direction at both scales.

As a consequence, the Reynolds and the Froude number should be the same for the model and ship, which can not be fulfilled simultaneously. This results in scaling effects on the hull resistance between model and ship.

Besides scaling effects on hull resistance, Starke and Bosschers (2012) describes a scaling error due to a difference in the wakefield of the propeller. Due to a different Reynolds number of the model and ship, the boundary layer is different as well. The smaller Reynolds number of the model, has the consequence that the boundary layer is relatively big, hence resulting in a different wake field of the propeller.

Trim tables from model scale towing tests are performed for calm water conditions. However, the influence of trim on the fuel consumption depends on weather and sea conditions (Abouelfadl and Abdelraouf, 2016, Coraddu et al., 2017, Du et al., 2019, Islam and Guedes Soares, 2019). Consequently, it can be the case that the trim tables provide inaccurate, non-optimal trim conditions when the ship is sailing in other conditions than calm water.

3.1.2. Trim tables based on CFD calculations

An alternative to model testing in a towing tank, is to simulate the flow around the ship using computational fluid dynamics (CFD). Trim tables can hence also be generated by performing CFD simulations. By using this approach, the resistance of the ship is calculated for different trim angles and speeds as well.

These CFD simulations can be done on model scale and, with recent developments in computational power, on full scale. CFD simulations on model scale are well validated by experimental measured data (Jasak et al., 2019), but suffer from scale effects as well and simplifications, such as to use an actuator disk instead of the actual propeller, disregarding the free surface or not to calculate the dynamic sinkage and trim of the vessel (Ponkratov and Zegos, 2015). The accuracy of CFD simulations on model scale have been 0.50-5.8% Gao et al. (2019) and 0.10-8.9% Islam and Guedes Soares (2019) compared to results from experimental data. The feasibility of trim suggestions using CFD simulation on model scale have been shown by Labanti et al. (2016) and Sherbaz and Duan (2014).

State of the art CFD simulations perform ship scale simulations and avoid simplifications by using more computational power. This is done by Castro et al. (2011) for a KRISO containership, but the results were not validated due to a lack of data from sea trials. In the work of Ponkratov and Zegos (2015), the CFD simulation

was validated with data from sea trials, but here the results were calculated for a fixed sinkage and trim. Still, the method showed sufficient agreement for the power prediction (a difference of approximately 2.8%), which was better than the estimation from model tests. Mikkelsen et al. (2019) have compared the results of ship scale CFD simulation with model scale towing tests and sea trial data for one single ship. It was found that the extrapolated towing tank results are overestimating the power by approximately 3-9%, while the ship scale CFD simulations overestimates the delivered power by 0-5%. It was noted that sea trial results always depend on factors such as wind and waves, which are uncontrollable and not modelled in the CFD simulation. This study shows that ship scale CFD simulations are capable in estimating the calm water power requirement in a more accurate way compared to the method of model towing tank tests.

It can be concluded that generating trim tables based on model scale towing tests and CFD simulations is feasible. It provides sufficient accuracy, although scaling results will always results in an error of a few percents. Full ship scale CFD simulations potentially increase the accuracy, but more validation is needed. In all cases, dynamic effects are hard to model and the tests or simulations are to be done for every ship design.

3.2. Regression analysis

Another approach to determine the effect of trim on fuel consumption found in literature is to perform a regression analysis on the available data. This can be based on continuous on-board measurements, or on data from noon reports.

A regression analysis on continuous on-board measurements is performed by Perera et al. (2015a,b). The ship was equipped with sensors that could measure the propeller shaft power and torque, the fuel consumption and instruments of the navigational parameters of the ship. The scatter plot of this research is shown in figure 3.2. Based on this, the authors state that for an approximate draft of 11-12 m, a considerable increase in fuel consumption can be observed at a trim around 2 m.
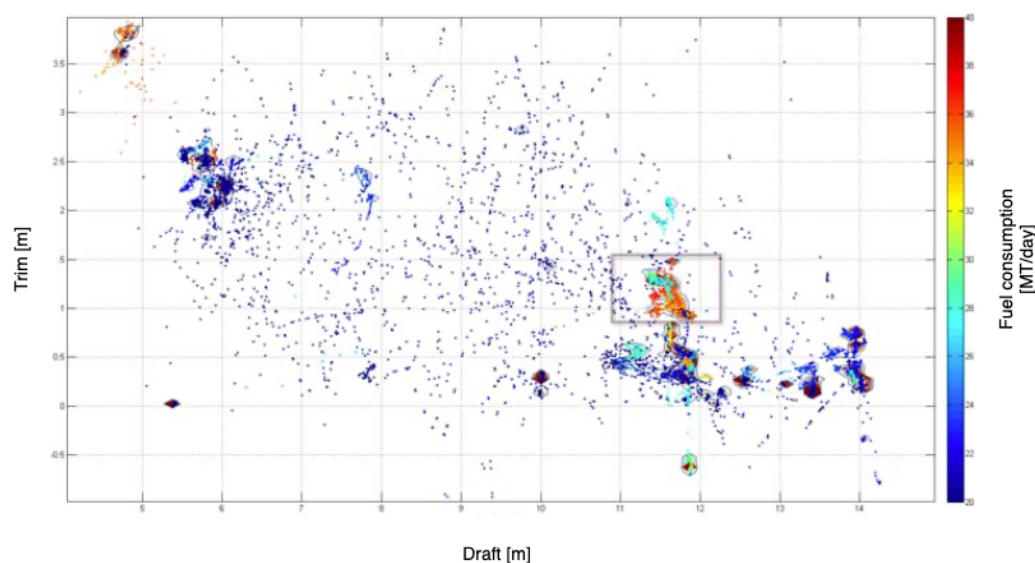
Figure 3.2: Example of a scatter plot of fuel consumption against trim and draft condition, from the work of Perera et al. (2015b).

Some significant disadvantages for using this approach can be identified. Firstly, it is noticed that the approaches are only capable in identifying a range in operational settings that would relate to a difference in fuel consumption in an ambiguous way. These approaches would not be able to generate trim tables, since no relation between fuel consumption (or power requirement) and trim can be identified. Moreover, the effect of multiple other parameters that influence the fuel consumption, such as the influence of weather, sea and fouling, are not considered simultaneously. The work of Coraddu et al. (2017), Safaei et al. (2019), Soner et al. (2019), Yuan and Nian (2018) and Du et al. (2019) emphasize the influence of wind and waves on the

fuel consumption of the ship. As a consequence, the same trim and draft condition can result in a significant different fuel consumption than expected, due to different weather conditions. So, this approach lacks in the ability to generate trim tables as a function of speed, draft and weather conditions.

Bialystocki and Konovessis (2016) performed a statistical approach based on continuous data from on-board measurements is applied as well. Although the effect of trim is not part of interest in this paper, this is technically possible and the paper shows the characteristics of such a solution approach. A trend analysis is performed to estimate the fuel consumption of a ship by means of a second-order polynomial as a function of speed, see figure 3.3. Also, the effect of weather was considered separately, which would result in a similar polynomial for different wind forces. Instead of the effect of weather, the effect of trim could be considered. For example, the fuel consumption as a function of speed could be measured for one single mean draft condition, for various trim settings. Although this would result in a direct relation between fuel consumption and trim condition, this approach is unable to adopt other effects simultaneously, therefor fails to isolate the effect of trim. This straightforward approach is therefore not suitable to use generate trim tables in an accurate way.
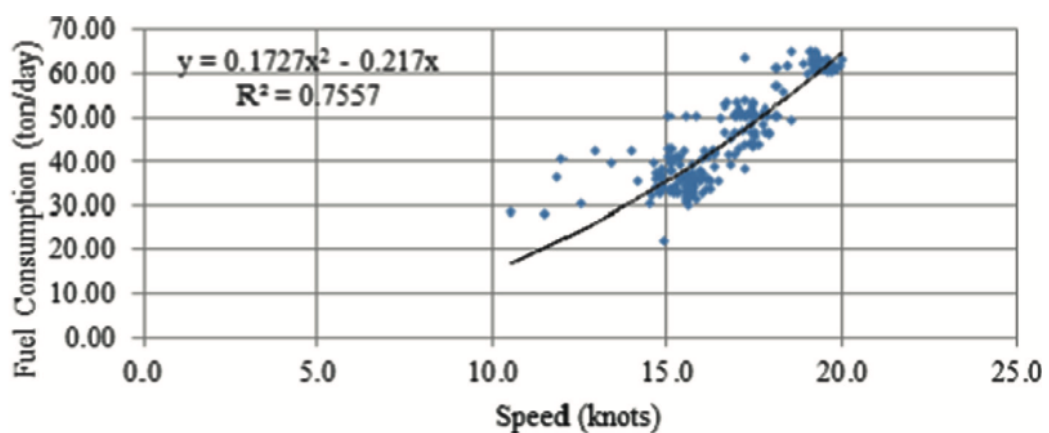
Figure 3.3: Example of a trend analysis of ship speed and fuel consumption, from the work of Bialystocki and Konovessis (2016).

Additionally, a similar linear regression approach can be done based on noon report data. This is done, for example, by Safaei et al. (2019). However, in this research the effect of trim is neglected as well. Instead, a linear relation between fuel consumption and ship speed, displacement and weather state, has been found for a VLCC. The presented relation shows insufficient accuracy due to the linear method, against the nonlinear physical relation of the ship speed and the fuel consumption.

It can be concluded that regression analyses are not able to generate accurate dynamic trim tables, since no relation between trim and fuel consumption can be established, while simultaneously taking into account other effects.

3.3. Commercial trim optimization tools

Another group of solution approaches are commercial trim optimization tools. It is this type of solutions that is of increasing interest by ship owners and suggested by the IMO to support the implementation of energy efficiency technologies to enhance the EEOI. A number of solutions is available these days. Besides costs and interface, these commercial trim optimization tools differ in the fundamental working principle and source of information, which make it possible to categorize these tools in the solution matrix of figure 3.1. The evaluation is this paragraph is structured by data source of the tool, starting with model scale towing tests. It must be noted that descriptions of the working principle behind the software is often limited and supplied by commercial parties. As a consequence, it is difficult to analyze the exact working principle or source of data of the tool and special care should be taken considering the validity of the information. In paragraph 3.3.1 to 3.3.3, a number of such commercial trim optimization tools are evaluated.

3.3.1. Commercial trim tools based on model tests

Within the box of model scale towing tests as the source of data for the trim optimization tool, two suppliers are considered.

CruiseMax is a trim optimization tool developed by *Herbert-ABS Software Solutions*. The applied method for this tool is to conduct model tests in calm water, in which relevant speeds and drafts for the operational profile of each vessel class are covered. This tool combines the optimized trim condition with the specific loading and regulatory requirements of the vessel, by connecting the tool with the loading software *CargoMax* which is developed by *Herbert-ABS* as well, hence suggesting operational attainable trim settings (Herbert-ABS, n.d.).

Sea Trim, developed by FORCE Technology is a trim optimization tool that makes use of a series of model tests as well. Trim tests have been performed for almost 300 vessels of various ship types, including tankers, container vessels (the majority of the tested models), LNG carriers, RoRo vessels and ferries. In the program, advice is given regarding optimal trim based on the initial entered forward and aft draft, typically taken from the ship loading computer, and the planned vessel speed. If the trim condition is not optimal, the tool gives a guidance where the optimal trim can be found. This tool does not consider operational constraints which have to be considered during shipping. However, the *Sea Trim* software is able to be connected to a loading software, if supported by the manufacturer. Additionally, the trim optimization tool can also be delivered with a loading software developed by FORCE Technology as well (FORCE-Techology, n.d., Reichel et al., 2014).

Trim optimization tools based on a series of model scale towing tests, like *Sea Trim*, will have scaling effects as described in paragraph 2.2. Furthermore, this approach is not ship specific and does not consider weather and sea conditions.

3.3.2. Commercial trim tool based on CFD simulations

DNV-GL has developed *ECO Assistant*, which is trim optimization tool that uses data from CFD simulations as input for the optimal trim condition. The approach of this tool requires a geometry model of the ship, which has to be created ship-specific, if not already available, from available cross-sections and main dimensions or from 3D scanning. The *ECO Assistant* software makes use of the state-of-the-art CFD approach of performing numerical sea trials on ship scale. DNV-GL states it has confirmed the results from the CFD simulations in multiple sea trials and by in-service measurements, thereby increasing the validity of this approach, which is one of the drawbacks of this kind of CFD simulations as is described in paragraph 3.1. By the CFD simulations, a matrix is constructed of speed, draft and trim values. The discrete data sets are connected by smooth interpolation, called multi-dimensional response surface. According to DNV-GL, the *ECO Assistant* can be interfaced with any loading computer and cargo planning system. Furthermore, the trim performance of vessels equipped with *ECO Assistant* can be monitored in performance management system of DNV-GL, *ECO Insight* (DNV-GL, 2013, n.d.). An important advance of this approach is that it does not require interfacing with on-board systems or sensors, which makes the installations more cost effective, especially for sister ships or fleets (Architect, 2014).

Another, though only briefly documented tool, is the trim curve generation tool developed by *GreenSHIP*. This tool makes use of CFD simulations as the datasource as well (GreenFramework, n.d.), yet insufficient information is available to evaluate this commercial tool.

Tools that optimizes trim based on ship specific ship scale CFD simulations, such as *ECO Assistant*, cover most of the drawbacks described in paragraph 3.1. On the other hand, it requires more than the available data and does not consider weather and sea conditions.

3.3.3. Commercial trim tools based on continuous on-board measurements

Instead of using tank testing or CFD simulations, the trim optimization tool *Eniram Trim* uses actual data from vessel operations. The tool requires highly accurate sensors (usually not readily available on-board of ships) that measures the actual trim during sailing and compares this to the optimal trim condition. It

collects data on vessel performance from multiple, different on-board systems and combines that with the trim information by using advanced modelling techniques (Govindan, 2019). It is not explicitly mentioned how the optimal trim condition is determined for this tool.

A similar approach is adopted in the trim optimization tool of Marorka (n.d.). By collecting data in a continuous way, the effect of operational parameters, such as trim, on the ship performance is presented. Also for this tool, it is not explicitly mentioned how the optimal trim is determined.

The approach of *Eniram Trim* and *Marorka* is able to consider the effect of weather and sea conditions, it requires high-frequency data sampling from specific on-board sensors, which have to be installed additionally on each ship to optimize trim. This approach is capable to consider the effect of weather and sea conditions.

3.4. Dynamic fuel consumption estimation models

A dynamic fuel consumption prediction model, in short the *fuel model*, can be used to estimate the fuel consumption for a range of trim conditions, with dynamic trim tables as result. The method of using the fuel model is illustrated in figure 3.4. Within the field of fuel consumption models, three types of models can be distinguished: white-box models (WBMs), black-box models (BBMs) and grey-box models (GBMs). A review of these models according to the structure of figure 3.5 is given in this section.
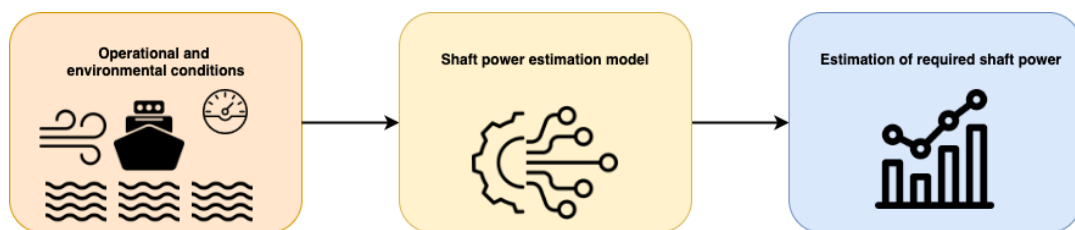
Figure 3.4: Working principle of a dynamic fuel consumption estimation model. By changing trim conditions, the effect of trim on required power and fuel consumption can be researched.
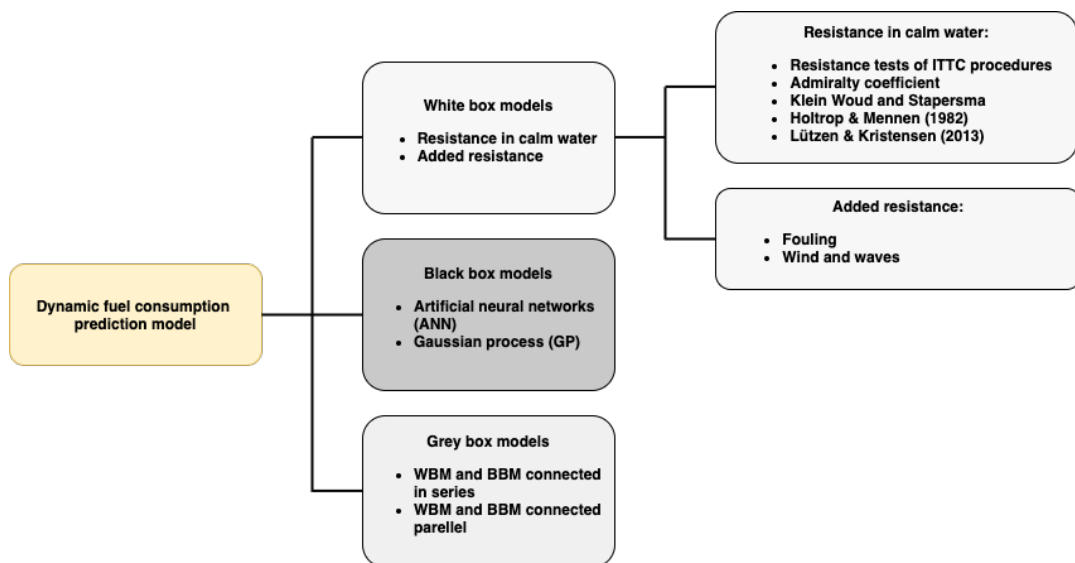
Figure 3.5: Overview of models to estimate the power or fuel consumption.

3.4.1. White box model (WBM)

Fuel consumption can be modelled by applying physics-based relations and relations found by regression analysis from model and full-scale experiments. This approach is known as white-box modelling. These models are most often used in the design phase to estimate the power requirements. WBMs are generally rather tolerant to extrapolation, but the margin of error to estimate the fuel consumption for a specific ship in realistic sailing conditions, especially considering wind and waves, may be large (Coraddu et al., 2017, Leifsson et al., 2008). Models exist to estimate both the calm water resistance and the added resistance due to waves and wind.

Calm water resistance

In recommended procedures for resistance tests from the International Towing Test Conference (ITTC) of Resistance Committee of the 27th ITTC (2014), the total resistance of a ship can be modelled with a non-dimensional total resistance coefficient. The drawback of this coefficient and is that the wetted surface has to be known, which is typically not readily available (Klein Woud and Stapersma, 2012).

Simple alternatives are the Admiralty coefficient of formula 3.1 (MAN Diesel and Turbo, 2011) or the method of Klein Woud and Stapersma (2012), shown by formula 3.2. Sea trial results can be used for the reference power and speed. Here, A is the Admiralty coefficient and ∇ is the displacement in m^3 and Δ is the displacement in t.

$$A = \frac{\nabla^{\frac{2}{3}} \cdot V_S^3}{P_P} = \frac{\nabla_{ref}^{\frac{2}{3}} \cdot V_{S_{ref}}^3}{P_{P_{ref}}} \tag{3.1}$$

$$P_E = R \cdot V_S = c_1 \cdot V_S^3 \qquad \text{with,}$$
$$c_1 = C_E \cdot \rho^{\frac{1}{3}} \cdot \Delta^{\frac{2}{3}}$$
$$C_E = \frac{P_{E_{des}}}{\rho^{\frac{1}{3}} \cdot \Delta_{des}^{\frac{2}{3}} \cdot V_{S_{des}}^3} \tag{3.2}$$

More comprehensive regression models to estimate the required propulsion power have been developed as well. A well-known regression model is the Holtrop and Mennen (1982) method. Here, a regression analysis is performed based on model scale towing tests. In the method, the resistance is subdivided in a frictional resistance (R_F) with form factor k for the hull, the resistance of appendages R_{APP}, a wave making and wave breaking resistance R_W, an additional pressure resistance for ships with a bulbous bow R_B, an additional pressure resistance of the immersed transom R_{TR} and a model-ship correlation resistance R_A, but all applicable for calm water in ideal trial conditions. The method is furthermore able to consider the effect of trim, by considering the draft forward and aft and by the shift in the length centre of buoyancy. Regarding the estimations for the propeller efficiency, the effective blade area ratio and propeller-pitch ratio are to be known, which causes problems when this information is unknown and when a controllable pitch propeller is used.

Lutzen and Kristensen (2013, 2012) have developed a regression model to estimate the required propulsion power, based on the work of Harvald (1983) but modified for tankers and bulk carriers. This method subdivides the resistance into a frictional resistance, an incremental resistance C_A (to include the effect of roughness of the surface of the ship, which is not present at the ship model), an air resistance coefficient C_{AA} and a residual resistance C_R. This method requires less input parameters compared to the Holtrop and Mennen (1982) method, but does not account for trim.

All these methods however, exclude the effect of the increase of frictional resistance due to fouling over time, although the effect can be significant. The fuel consumption increases at least 10% on average when the ship's hull is lightly fouled, and up to 35% under heavily fouled conditions. The rate of biofouling complex as it is affected by many environmental factors, including pH-value and nutrient abundance physical factors, such as the micro texture. An advanced model is presented by Uzun et al. (2019). This model can be approximated

in a linear way by an increase in power demand of 8-9% per year. An increase of frictional resistance over time can be included in this way. This is also done by Aldous et al. (2015), in which an incremental resistance increase of 5% per year is assumed.

Added resistance

Prediction of the added resistance of a ship due to wind and waves is complex and depends on many parameters. However, empirical formulas to consider the effect on propulsive power are available. The influence of the added resistance can be quantified in either an increment of resistance and hence the required power or as a loss of speed.

Townsin et al. (1993) have developed approximate values to quantify the effect of wind and waves on the ship speed. The speed loss is a function of the ship displacement, the wind force and the wind direction in respect to the ship. Lu et al. (2015) have improved the accuracy of this model by including ship specific characteristics. Meng et al. (2016) have modified the model of Townsin et al. (1993) as well, by taking the wind force and wave height in meters as input. The coefficients within this model are based on container ships, which makes the model less useful for chemical tankers.

Another considered method are the new guidelines for speed and power trials. With the goal to standardize the sea trial procedures and correction for the weather conditions, guidelines are established with the assistance of the Sea Trial Analysis-Joint Industry Project (STA-JIP), the ITTC, IMO and leading shipowners. The results are the guidelines of "ITTC - Recommended Procedures and Guidelines, Analysis of speed/power trial data" of the Specialist Committee on Performance of Ships in Service 27th ITTC (2014). The guidelines are subdivided in short waves, where reflection is considered and long waves, where ship motions due to waves are considered (van den Boom et al., 2013). The approximation of the added resistance of long waves are complex and require specific information of the hull and waves, including inertia moments and wave length and is only relevant for head waves with an angle between 0° and 45 ° with respect to the bow direction.

It can be concluded that the WBMs can be used to make an initial approximation of the power requirement in calm water. The models differ in complexity and required input. Most models to estimate the added resistance due to wind and waves are unpractical to use for this research. The model of Townsin et al. (1993), or variants on that model of Lu et al. (2015) or Meng et al. (2016) could be used to estimate the speed loss caused by wind and waves, but would require an additional method to translate this in an increase in required power.

3.4.2. Black box model (BBM)

Another approach is to observe data to predict the output of a system given some input data, without the requirement of knowledge of the system. This approach is described as black-box modelling. A BBM gives a functional relationship between system input and output, which does not represent any physical significance, and can be more effective to model trends in process behavior (Zhang, 2010). Moreover, a BBM can be more accurate than a WBM, but requires large amounts of data for training and often suffer from poor extrapolation qualities (Leifsson et al., 2008, Parkes et al., 2018, van Ballegooijen et al., 2018, Yang et al., 2019).

In recent literature, BBMs are used to estimate the fuel consumption based on either noon reports or on high frequency sampling of operational data. This have been done with artificial neural networks (ANNs) and Gaussian processes (GPs), which are considered as machine learning approaches. Machine learning approaches play a central role in extracting information from raw data collected from ship data logging systems (Coraddu et al., 2017). The capabilities of an ANN to model the fuel consumption based on noon report data using multiple parameters including trim and weather conditions, have been shown by Bal Besikci et al. (2016), Du et al. (2019), Parkes et al. (2018), Pedersen and Larsen (2009a,b), Petersen et al. (2012). In these cases, it is found that the use of an ANN performed better in comparison to pure WBMs. Bal Besikci et al. (2016) has shown good estimation qualities based on 233 noon reports, using 8 input parameters including trim and weather conditions. However, the number of observations has a significant effect on the uncertainty of the prediction, with more data reducing the uncertainty (Parkes et al., 2018).

Petersen et al. (2012) investigate and compare the use of an ANN and GP, by using an operational high-

frequency dataset of a ferry over a period of two months. In all tests performed in the paper, the performance of the ANN is a little better than the GP. Additionally, Pedersen and Larsen (2013) and Yuan and Nian (2018) used a GP as a BBM for estimating the fuel consumption of a ship based on noon report data. It was found that similar accuracy can be obtained, although a GP is not appropriate for the analysis of large datasets, because the complexity increases with the amount of input parameters to the third power (Pedersen and Larsen, 2013). Moreover, in the case of an ANN, it is suggested that larger networks will improve the ability to extrapolate beyond the available input data Parkes et al. (2018). This makes the use of a ANN more effective than a GP for modeling fuel consumption based on noon report data.

However, extrapolation remains an important weakness of a pure BBM. This weakness is caused by data scarcity. In the case of conducting experiments or calculations, a predetermined matrix of required data points can be chosen in such a way that there is a knowledge base covering all operational conditions of a ship, even those that are rarely encountered. In the case of a data-driven approach, which is true for a pure BBM based on noon report data, the model will learn from data obtained in the past operation which may be limited in variation. Hence, the BBM may not accurately predict the fuel consumption in new conditions because it does not have the data to do so. Ideally, the model learns realistic relationships between the input variables and power or fuel consumption, while taking into account the external conditions. If this is done successfully, the model can predict the optimal trim even when the ship sails in new, unseen conditions for which no data is available yet (van Ballegooijen et al., 2018). Therefore, the abilities of a WBM and a BBM should be combined.

3.4.3. Grey box model (GBM)

Grey-box models (GBM) aim to combine the advantages of both a WBM and a BBM. The goal is to retain knowledge from the WBM about the physical behaviour of the ship regarding the propulsion power and resistance, while the BBM integrates what is known from the specific operational data of the ship (Leifsson et al., 2008, Yang et al., 2019).

A comparison between WBMs, BBMs and GBMs for predicting ship fuel consumption is made by Yang et al. (2019), presented by table 3.1. Based on this comparison and the review of WBMs and BBMs (in paragraph 3.4.1 and 3.4.2), the following reasons for using a GBM for this research are identified:

- More accurate than a WBM by considering ship specific, real operational conditions;

- Less historical data required than a BBM;

- A certain degree of extrapolation capacity;

- Can avoid unreasonable results because of over- or underfitting on available data.

The performance of a GBM in predicting fuel consumption of a ship, and the improved extrapolation capacity of a GBM over a BBM especially, can be illustrated by the work of Leifsson et al. (2008). In this research, a GBM was constructed to model the fuel flow rate (samples every 15 seconds) of a cargo ship that operates between Iceland and Northern Europe. The ship typically operates with speeds between 18 and 20 knots. Figure 3.6 shows the fuel consumption for two types of voyages. It is seen that when the vessel operates at different sailing speed than normal operations, the GBM predicts the fuel consumption closer to the actual data than the BBM, indicating better extrapolation results. It is also noticed that for this voyage, the WBM outperforms the GBM. However, Leifsson et al. (2008) states that overall, the root mean squared error (RMSE) of the WBM is more than three times as big as the GBM. In another voyage, the ship encountered unusual environmental conditions. Leifsson et al. (2008) state that the WBM failed to follow the operational data well, because the effect of environmental components, such as ocean waves, are not modeled by the WBM.

A WBM and a BMM can be combined in two ways, serial-modeling and parallel modeling, as can be seen in figure 3.7 based on Leifsson et al. (2008). In serial grey-box modelling, the BBM is provided with an initial estimation of the fuel consumption, which can be seen as an additional parameter for the BBM. In parallel grey-box modelling, the BBM models the residual of the measured and calculated fuel consumption. The authors evaluated both ways, and found marginal difference in outcome between the two.

Table 3.1: **Comparison between WBM, BBM and GBM used for prediction of ship fuel consumption.**

Approach	Advantage	Disadvantage
WBM	Can interpret prediction results and system behavior	Accuracy of predictions depends on assumptions and uncertainties implicit in the models
	Can extrapolate beyond the given data range	Requires complete beforehand system understanding
	Does not require historical data	
BBM	Does not require beforehand system understanding	Require large amount of historical data
	More accurate compared to WBMs	Poor model interpretability
		Poor extrapolation capacity
		May result in unreasonable results (overfitting and under-fitting)
GBM	Higher accuracy than WBMs	Limited model interpretability
	Less historical data required than BBMs	Requires beforehand system understanding
	A certain degree of extrapolation capacity	
	Can avoid unreasonable results	
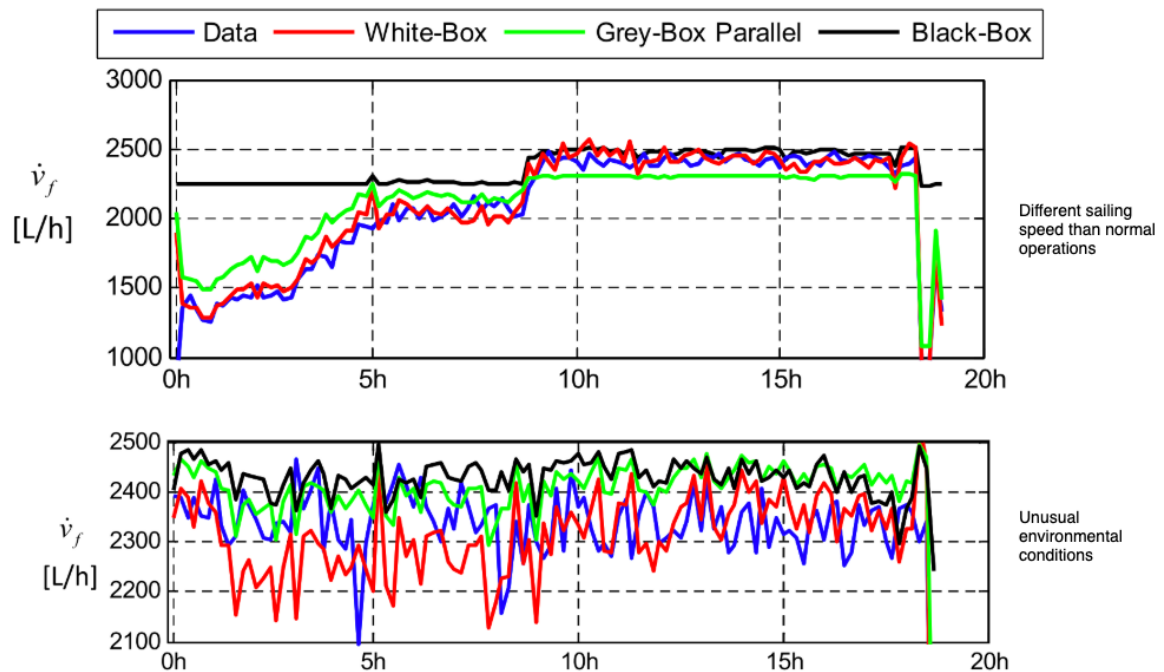
Figure 3.6: Comparison of the performance of a WBM, BBM and GBM in modeling fuel consumption, (figures from Leifsson et al. (2008))

3.4.4. Conclusion regarding dynamic fuel consumption model

A dynamic fuel consumption prediction model based on operational data from noon reports overcomes the drawbacks of trim tables based on model scale towing tests or CFD simulations. It is able to provide dynamic trim optimization, by taking into account dynamic factors such as the effect of weather and sea conditions and fouling. Taking noon reports as source of data overcomes the need for the installation of additional
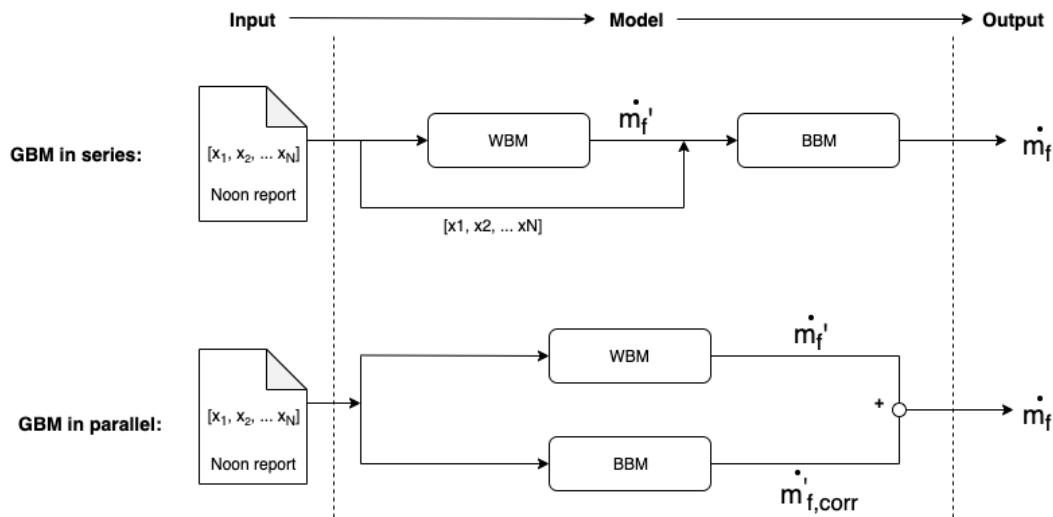
Figure 3.7: Serial grey-box modelling (above) and parallel grey-box modelling (below), based on Leifsson et al. (2008).

sensors. Moreover, no scaling effects occur when ship scale operational data is used.

A GBM shows superior ability to comply with the above stated requirements in comparison to a pure WBM or pure BBM, mainly due to the fact that the effects are determined ship specific and can handle the complexity of the effect of weather, while having the ability to extrapolate as well. Based on the literature review on existing approaches, the GBM will consist of a regression model (WBM) and a neural network (BBM) in series (top scheme in figure 3.7), thus feeding the neural network with an initial estimate based on a physics-based model.

The WBM will be based on Lutzen and Kristensen (2013) and Holtrop and Mennen (1982). A comparison between the two methods to use as a WBM is shown in table 3.2. Based on this, it cannot be concluded yet which one will perform better. Both methods will be used and will be compared in their ability in the GBM in estimating required shaft power and generate accurate trim tables. A WBM to model the effect of weather on fuel consumption, is not needed since this part is captured by the neural network. The capability in doing has been shown in relevant literature (Bal Besikci et al., 2016, Du et al., 2019, Parkes et al., 2018, Pedersen and Larsen, 2009a,b).

Table 3.2: **Comparison to use the method of Lutzen and Kristensen (2013) and Holtrop and Mennen (1982) as a WBM to estimate the required shaft power.**

Method	Advantage	Disadvantage
Lutzen and Kristensen (2013)	Less input parameters Modified for tankers and bulkers	Excludes the effect of trim
Holtrop and Mennen (1982)	Includes the effect of trim Accounts for hull shape with parameters	More input parameters

3.5. Ideally and actually available data

The data ideally available for the fuel model consists of the data requirements for both parts of the model; the WBM and the BBM. The power prediction method of Holtrop and Mennen (1982) and Lutzen and Kristensen (2013) requires ship design parameters and propulsive parameters. The propulsive parameters are usually not known, but Lutzen and Kristensen (2013) provide approximation formulas, as well as Carlton (2018) and

Molland et al. (2011). The ideally available data for the fuel model is listed in table 2.2. The ANN model considers the dynamic effects as well and mainly requires the environmental parameters and the operational parameters. The environmental and operational parameters are known from the noon reports.

Noise in data from the noon reports may be present as a consequence of human error. This can be missing data or flat lines in the data, suggesting unrealistic data recordings. An illustration of this is given in figure 3.8. The draft condition may differ from day to day, for example as a result of fuel and fresh water consumption. The flat line in draft during the first voyage compared to the changing draft and trim in the second voyage, indicate that the consistency of draft recording may differ. Results from a survey to the ships (see appendix F) made clear that for some voyages only the draft condition at departure and arrival is determined, since that is required to be known regarding draft limitations in ports. It can be concluded that the frequency of updating draft conditions differ from ship to ship.
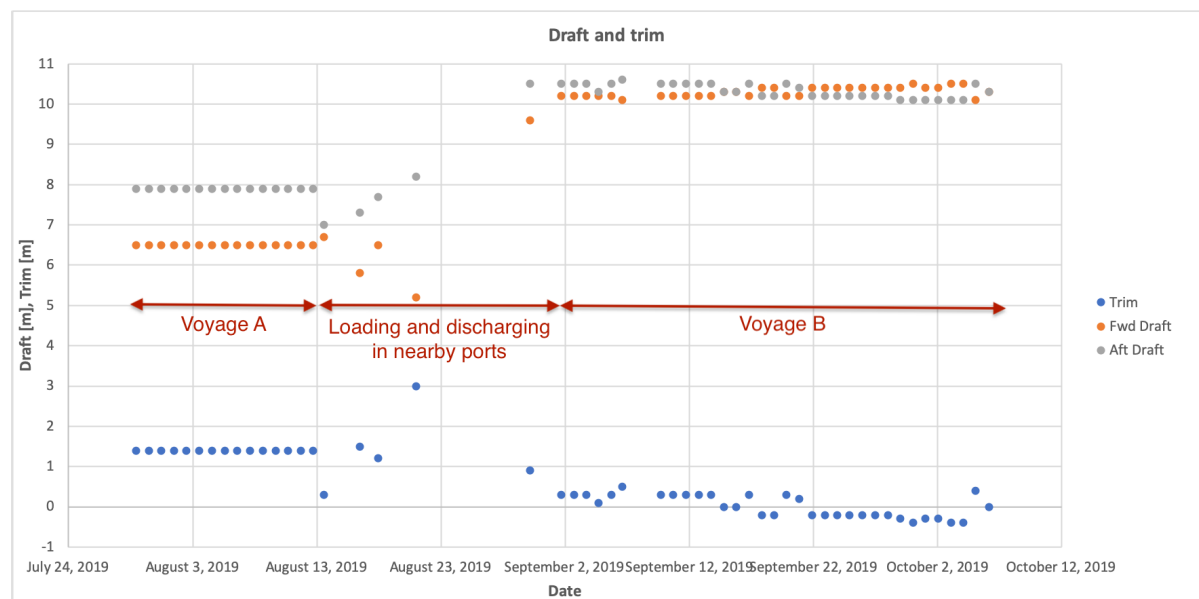
Figure 3.8: Recordings of draft fore and aft of two consecutive voyages.

Pedersen and Larsen (2013) describes that the use of hind-cast weather data in addition to the noon report data has a significant impact on the estimation accuracy, since it overcomes the human error in observing the environmental conditions. Pedersen and Larsen (2013) states that for the data from noon reports without hind-cast weather data, there seems to be a significant benefit using more data, since the prediction errors decrease with time for most of the data set. Hind-cast weather data is not available during this research.

Based on the available data as described in section 2.6, it can be concluded that all ideally available data is present. In special cases where data is missing, practical and appropriate approximations formulas are available. Hind-cast weather data would improve the data quality if available, but data from noon reports may be sufficiently accurate.

3.6. Gap to literature

Considering the available relevant literature on fuel estimation models, a literature gap is recognised which explains the contribution of this work. Despite the growing attention on using machine learning tools in extracting knowledge from noon report data, the proven ability of ANN in estimating fuel consumption based on this data and the demonstrated additional competence of grey-box modelling, no research is available yet on this subject. This gap in literature is shown in figure 3.9. The method proposed in this work aims to contribute by showing the ability of a grey box model using ANN with the objective of trim optimization for ships in service.

Figure 3.9: Relevant literature on fuel consumption models, showing the literature gap.

3.7. Conclusion of solution approaches

The different solution approaches to generate trim tables are shown in figure 3.1. These are evaluated in table 3.3 with the methods requirements, which have been determined in section 2.7.

Based on this, it is concluded that static trim tables, regression analyses and commercial trim optimization tools do not comply with the method requirements. A dynamic fuel consumption prediction model (or *the fuel model*), as described in 3.4.4 and with the working principle as illustrated in figure 3.4, is likely able to comply with all the requirements.

Table 3.3: **Evaluation of solution approaches based on method requirements.**

Method requirement	Dynamic fuel consumption model	Static trim tables	Regression analyses	Commercial trim optimization tools
Sufficiently accurate	Likely	Uncertain	No	Unknown
Dynamic fuel consumption modelling	Yes	No	No	No
Dynamic trim optimization	Yes	No	No	No
Use available data	Yes	No	Yes	No
Solution effective for multiple ships	Yes	No	No	Yes
Deal with error in available data	Requires data pre-processing	Unknown	Requires data pre-processing	Not applicable

3.8. The gain for Stolt Tankers

The gain for Stolt Tankers, by providing the proposed method successfully, is threefold. First of all, the method can potentially generate trim tables for any ship class within the fleet of the company, and provide a solution to incorporate these results in the voyage management procedures. Moreover, the proposed method can overcome the drawbacks from existing trim tables, since the generated trim tables can cope with weather and

sea conditions, whereas the existing trim tables are based on model towing tests in calm water condition. All together, this can result in a significant saving in fuel costs, providing the company a opportunity to improve the competitiveness of the company and reduce the emissions of shipping.

Secondly, part of the method will consist of a multi-variable dynamic fuel consumption prediction model. The model will be able to quantify the relationship between fuel consumption and its determinants, including speed, trim and weather conditions. This model can be used to accurately predict the fuel consumption of a voyage. It can also be used as an accurate model to internally compare the energy efficiency of the ships in the fleet to find abnormalities in fuel consumption.

Finally, the dynamic fuel consumption prediction model can be the basis for weather-routing, speed optimization and scheduling of hull and propeller cleaning.

II

Part II: Technical background

4

Effect of trim on fuel consumption

The subject of trim optimization requires the understanding of how trim influences the power demand and consequently the fuel consumption of a ship. Change of trim has an effect on both the ship's resistance and the propulsive efficiencies. These effects are considered in paragraph 4.2 and 4.3 respectively. Paragraph 4.1 starts with an introduction to ship's resistance and propulsion.

4.1. Basic formulas on ship's resistance and propulsion

The power required to drive the ship at a certain speed without any propulsive losses, is the effective power in calm water (P_E) of the ship, which is the total resistance times the speed (see formula 4.1) (Larsson and Raven, 2010). The total resistance of a ship can be divided into multiple resistance components.

Knowledge about resistance of ships originates from model towing tests, since the resistance of individual resistance components cannot be measured directly on full scale. Different approaches to describe the total resistance exists, which is extensively described in the work of Bertram (2000) and Larsson and Raven (2010). A comprehensive overview of resistance decomposition is provided in figure 4.1. Decomposition into a wave resistance (R_W, dependent on the Froude number) and a viscous resistance (R_V, dependent on the Reynolds number) is the description most directly related to physical phenomena (Larsson and Raven, 2010), shown by formula 4.2.

Neither with of ship scale tests, nor with model towing tests, the individual contribution of the wave resistance can be determined directly (Bertram, 2000). However, the viscous resistance and the total resistance, can be determined from model towing tests. This can be done using formula 4.3 to 4.6, in which resistance coefficients are defined (Bertram, 2000, Larsson and Raven, 2010, Reichel et al., 2014).

$$P_E = R_T \cdot V_S \tag{4.1}$$

$$R_T(Fn, Rn) = R_W(Fn) + R_V(Rn) \tag{4.2}$$

$$C_T = C_R + (1 + k)C_{F_0} \tag{4.3}$$

$$C_T = \frac{R_T}{\frac{1}{2} \cdot \rho \cdot V_S^2 \cdot S_W} \tag{4.4}$$

31
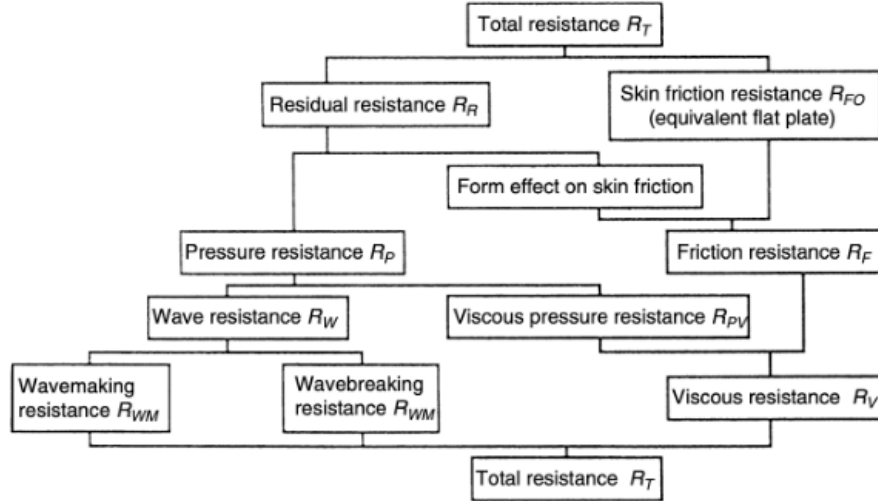
Figure 4.1: Overview of resistance decomposition (Bertram, 2000).

$$C_{F_0} = \frac{0.075}{\left(log(Rn) - 2\right)^2} \tag{4.5}$$

$$Rn = \frac{V_S \cdot L_{WL}}{\nu} \tag{4.6}$$

Here, P_E is the effective towing power in kW, R_T is the total resistance in N, V_S is the ship speed in $\frac{m}{s}$, R_W is the wave-making resistance in N, R_V is the viscous resistance in N, C_T is the total resistance coefficient, C_{F_0} is the flat plate equivalent frictional resistance, k is the form factor, S_W is the wetted surface of the hull in m^2, Rn is the Reynolds number, Fn is the Froude number and L_{WL} is the waterline length in m and ν is the kinematic viscosity in $\frac{m^2}{s}$.

Consequently, shaft power and brake horse power of the engine can be calculated using the relevant efficiencies of the propulsion chain as described by Klein Woud and Stapersma (2012), shown by formula 4.7 and 4.8

$$P_S = \frac{P_E}{k_p \cdot \eta_O \cdot \eta_R \cdot \eta_H \cdot \eta_S} \tag{4.7}$$

$$P_B = \frac{P_S}{k_e \cdot \eta_{GB}} \tag{4.8}$$

Here, η_O is the open water propeller efficiency, η_R is the relative rotative efficiency, η_H is the hull efficiency, η_S is the shaft efficiency, η_{GB} is the gearbox efficiency, k_p is the number of propellers and k_e is the number of engines per propeller.

4.2. Change in ship resistance

According to Reichel et al. (2014), the residual resistance is most affected by change in trim, where frictional resistance is less influenced by trim. A significant part of the residual resistance is the wave making resistance. Górski et al. (2013) describes the influence of immersion of the bulbous bow and transom, based on model tests and CFD simulation.

Immersion of the bulbous bow has a strong influence on the resistance of a ship. The function of the bulbous bow is to generate a wave system that favourably interferes with the wave system generated by the bow of the ship. The interference with the wave pattern is dependent on the draft and speed of the ship. A bulb located too close to the free surface generally creates a strong, unfavourable wave system. On the other hand, increased bulb immersion would result in a less developed wave system. Consequently, changing the trim enables to adapt the bulb immersion to the actual draft and speed (Górski et al., 2013).

Resistance of the flow around the stern part depends on the speed and the immersion of the transom, similar to the situation of the bow of the ship. From the work of Górski et al. (2013), it is clear that a turbulent flow, combined with a significant drop in pressure, can be observed when the velocity of the flow around the transom is below a certain (unspecified) threshold. This pressure drop results in a significant increase in resistance. Emergence of the transom, by trimming by bow, may prevent this situation by preventing the occurrence of flow separation (Iakovatos et al., 2014).

The frictional resistance plays a role as well. Trim by bow results in a reduction in wetted surface, hence a decrease in the frictional resistance, as can be explained by formula 4.5 (Górski et al., 2013, Iakovatos et al., 2014). Also, the frictional resistance coefficient C_F is dependent on L_{WL}, as can be seen in formula 4.6. Reichel et al. (2014) states that for most cases, L_{WL} will vary up to ± 5 %, which can result in ± 0.5 % change in required power. In addition to the hull friction, the change of resistance of appendages at trim conditions should be considered, such as bilge keels, the rudder construction and shaft brackets. These elements are orientated in such a way that the flow is in line with the orientation of the appendage. This way, the appendage resistance is limited to additional frictional resistance. At trimmed conditions however, a form factor should be considered. The appendage resistance at trimmed conditions will therefore be expected to be higher compared to even keel condition (Górski et al., 2013).

4.3. Change in propulsive characteristics

Klein Woud and Stapersma (2012) describes a number of propulsive efficiencies (see formula 4.7 and 4.8), which are affected by a change in trim.

The hull efficiency (η_H) (see formula 4.9) is a function of the thrust deduction factor (t) and the wake fraction (w). The trust deduction represents the difference in total produced thrust by the propeller(s) and the pure towing resistance of the hull. The remaining part has to overcome the added resistance of the propeller. Hence, a deduction(factor) is needed to go from thrust (T) to resistance (R_T), both in N (Klein Woud and Stapersma, 2012). The trust deduction is calculated with formula 4.10. If R_T changes due to trim and if the speed is kept constant, T will change as well. However, t will not remain constant. According to Reichel et al. (2014), t changes with trim up to ± 15% and peaks when the propeller submergence decreases to a critical level. However, the effect of change in thrust deduction is relative to the change in the wake fraction.

The wake fraction represents the difference between the ship's speed and the velocity of the water at the propeller location (both in $\frac{m}{s}$). The latter is called the advance velocity (V_A) and is usually lower than the ship's speed. The reason for this is that the entrained water in the boundary layer of the ship has a certain speed. The boundary layer at the ship's stern has a considerable thickness, in which the propeller is normally located. The difference in these two speeds, as a ratio of ship's speed is called the wake fraction and can be calculated with formula 4.11 (Klein Woud and Stapersma, 2012). If the ship's speed remains constant, the wake fraction only changes if the speed of water at the propeller inflow changes. In the tests of Reichel et al. (2014), the wake fraction increases for bow trim conditions up to 20% (which would increase η_H, hence favourable) and decreases for stern trim conditions with up to 10%. Considering the possible change in w and t, η_H can change ± 2%.

$$\eta_H = \frac{1-t}{1-w} \qquad\qquad (4.9)$$

$$t = \frac{k_p \cdot T - R_T}{k_p \cdot T} \qquad\qquad (4.10)$$

$$w = \frac{V_S - V_A}{V_S} \qquad (4.11)$$

The open water (η_O) efficiency of the propeller depends on the curvature in the open water diagram and the advance ratio 'J' (see formula 4.12). Here, n is the engine speed in rps and D is the propeller diameter in m. Change in trim will change V_A. Since the curve of η_O is inclined, η_O will vary depending on J. Change in η_O can be $\pm 2\%$ (Reichel et al., 2014).

$$J = \frac{V_A}{n \cdot D} \qquad (4.12)$$

The relative rotative efficiency (η_R) covers the difference between the actual situation of the propeller in a non-uniform velocity field and the open water situation, see formula 4.13 (Klein Woud and Stapersma, 2012, Reichel et al., 2014). Here, P_O is the propulsive power in open water (with uniform flow), P_P the actually delivered power by the propeller. $K_{Q_{openwater}}$ is the torque coefficient in open water and $K_{Q_{ship}}$ the torque coefficient for the situation that the propeller is behind the ship. Since the flow at the propeller will be slightly different due to trim, η_R can vary up to 2% from even keel condition (Reichel et al., 2014).

$$\eta_R = \frac{P_O}{P_P} = \frac{K_{Q_{openwater}}}{K_{Q_{ship}}} \qquad (4.13)$$

Finally, as can be seen in formula 4.8, the difference between P_B and P_E is caused by η_S and η_{GB}, together known as the transmission energy. These efficiencies are not considered to be effected by change in trim. Klein Woud and Stapersma (2012) considers these efficiencies to be rather constant and in the case of η_{GB}, the value is dominated by the type of gearbox.

In addition to the above and to formula 4.8, Górski et al. (2013) argues that under trimmed conditions, the direction of the force generated by the propeller is not parallel to the direction of the ship motion and hence, the effective thrust is deduced.

4.4. Engine fuel consumption

The required power directly relates to the fuel consumption, which is of particular interest within the field of trim optimization. Fuel consumption ($\dot{m}_f$ in $\frac{kg}{s}$) is a function of the required brake power, the performance of the engine and the lower heating value of the fuel (LHV in $\frac{MJ}{kg}$). The performance of the engine can be quantified in terms of specific fuel consumption (sfc in $\frac{kg/s}{kW}$) or in the engine efficiency (η_E). The engine performance is dependent on the engine speed and engine load and is specified by the engine manufacturer. Eventually, the fuel consumption can be calculated with formula 4.14 (Stapersma, 2002).

$$\dot{m}_f = \frac{P_B}{\eta_E \cdot LHV} = P_B \cdot sfc \qquad (4.14)$$

4.5. Conclusion of the effect of trim on required power

A summary of the effect of trim on the required power and eventually the fuel consumption, as described in paragraph 4.1 to 4.4, is summarized in table 4.1. Here, the items of the ship resistance and the propulsive characteristics that are influenced by a change in trim, are listed accordingly with the favourable trim to decrease the power demand. Also, the potential effect on the required power is given, if known.

Based on this, it is expected that generally, trim by bow will decrease the required power and thus has a favourable effect on fuel consumption. However, for many influenced items it is hard to determine the effect on the required power.

Table 4.1: **Effect of trim on required power.**

Ship resistance item	Physical effect	Favourable trim	Potential difference
Immersion of bulbous bow	Change in wave pattern	Depends on design, speed and draft	Unknown
Immersion of transom	Prevention of pressure drop at transom due to turbulent flow	Trim by bow	Unknown
Change in frictional resistance	Change in wetted surface	Trim by bow	± 0.5 %
	Change in waterline length	Trim by bow	± 0.5 %
Introduction of form factor for appendages	Change in orientation of appendages	Even keel	Unknown

Propulsive characteristics	Physical effect	Favourable trim to decrease fuel consumption	Potential difference in required power
Hull efficiency	Change of thrust deduction by 15% Change of wake fraction by up to 20%	Unknown Trim by bow	Together ± 2%
Open water efficiency	Change in advance ratio due to change in advance velocity	Unknown	± 2%
Relative rotative efficiency	Change in actual delivered thrust by propeller	Unknown	±2 %
Thrust direction	Change shaft orientation	Even keel or trim by stern	Unknown

5

Freedom and limitations in ship trim

Limitations to trim a ship have been identified. Research question 5 (*What limitations exist to trim a ship?*) can be answered with figure 5.1, in which an overview of limitations is given. The groups of limitations are covered one by one in the remainder of this chapter.
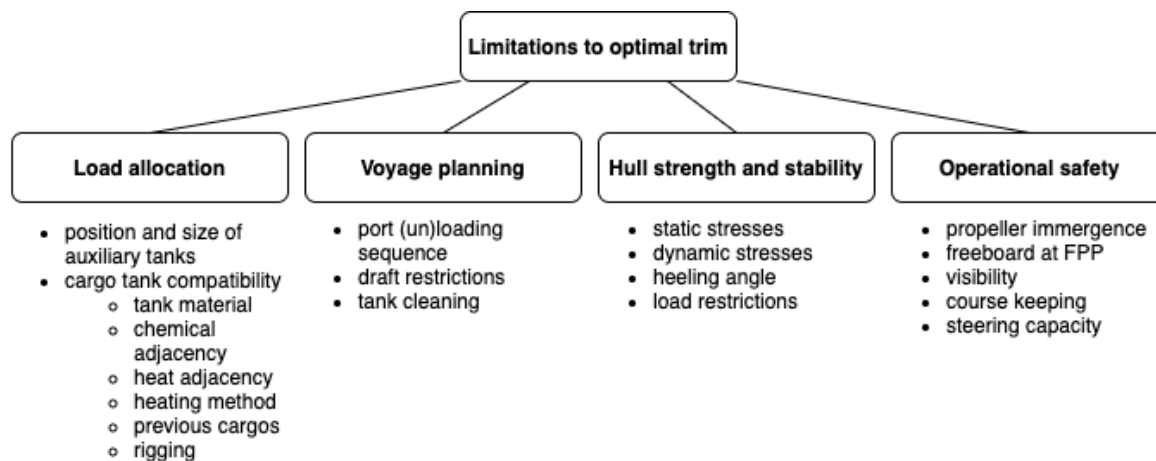
Figure 5.1: Breakdown of limitations to sail at optimal trim. These limitations are considered in the remainder of this chapter.

5.1. Limitations in load allocation
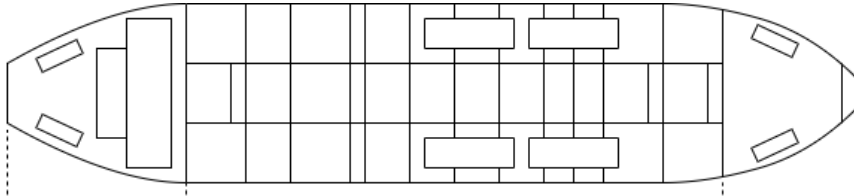
Figure 5.2 shows a simplified illustration of the C38 class chemical tanker and a breakdown of all tanks on board. The types of tanks are grouped by cargo, fuel and oil, water, ballast and miscellaneous tanks. Based on the loading computer of the ship, the maximum load and the number of tanks are shown in the figure. The length-location of the tanks and its capacity in tons are shown as well. In most load conditions, the challenge is to trim the ship forward, since the ship tends to trim to stern automatically, mainly due to the weight of the hull and machinery located on the aft of the ship.

The figure provides an overview of which tanks play a role in changing the trim forward from the perspective of trim optimization. Naturally, the trim changes with every change in load of each tank, but not all of these tanks can or will be used for trim optimization. Tanks that contain loads which are (up to a certain degree) controllable, are marked yellow in figure 5.2, which are the following:

- Cargo: cargo load is the most significant in terms of total weight and dominates the trim condition.

Cargo allocation can be used as a tool for trim optimization, especially in part load conditions.

- HFO: HFO storage tanks are mainly located in the aft and has two storage tanks in the fore peak, with a capacity of 266 tons when loaded 98%.

- Technical fresh water: Tanks with ±450 tons capacity is placed in the aft and tanks with more than double the capacity is located in the fore peak.

- Ballast water: 22 tanks for ballast water are divided over the midship, and one tank placed in the fore-peak. Adding ballast water to trim the ship to the bow is only feasible in part load conditions: in full load condition the additional deadweight can not be carried and in ballast condition, the ballast tanks are filled already. However, adding ballast water also increases the mean draft and displacement, which negatively affects the fuel consumption.

	AFT	MIDSHIP	FORE
Cargo		± 38000 tons (over 43 tanks)	
Fuel & oil			
HFO	1834 (12)		293 (3)
MDO	201 (2)		
MGO	141 (4)		
Fuel oil other	411 (3)		
Lube oil	121 (9)		
Sludge	45 (1)		
Water			
Potable fresh	686 (2)		
Technical fresh	458 (1)		990 (3)
Bilge	110 (3)		
Grey and black	129 (2)		
Ballast			
Ballast		15604 (22)	1322 (1)
Heeling		1082 (2)	
Miscellaneous	284 (10)		

Figure 5.2: Simplified illustration of the C38 class chemical tanker and its maximum load and approximated length location of all tanks at 100% load.

Four scenarios within the identified options are investigated on its effect on trim for three loading conditions - full, partial and ballast:

1. Cargo re-allocation: feasible in partial load condition. The load of one normal-sized tank of 1113 ton is re-allocated to a tank which is ±0.5 L_{PP} forward.

2. HFO storage to fore tanks: 266 tons is re-allocated from aft tanks to fore tanks, which is the maximum capacity of the forward tanks.

3. Technical fresh water: 458 tons of technical freshwater (FW) from aft to forward tanks. This is the full capacity of the aft-located tank.

4. Ballast water (re-)allocation: 900 tons of ballast water is allocated to the ballast tank in the fore-peak.

The results of these four trim scenarios for different loading conditions are shown in table 5.1. It is concluded that trim is significantly changed by cargo re-allocation, but is only possible in part-load conditions. However, freedom in allocation of cargo is limited by multiple factors which will be covered in the next section. Changing the location of fuel and technical fresh water can be the most feasible way to change the trim, yet this method is subject to re-allocation of fuel from aft to fore tanks. Fuel re-allocation trims the ship ±0.50 m forward, and technical fresh water ±1.00 m forward. Adding ballast water can only be used in part load conditions. This method can trim the ship more than a meter forward, but will result in additional displacement as well. In normal ballast conditions, forward located ballast tanks will already be in use to comply with other limitations.

Table 5.1: **Options to change trim in three load conditions. Change in trim has been determined using the loading computer of the** *Stolt Pride* **and considers static trim.**

Load condition		T_{mean} [m]	trim [m]
Full (~98% of DWT)		10.14	1.07
Trim scenario	**Δ Weight [t]**	**Δ T_{mean} [m]**	**Δ trim [m]**
1. Cargo (re-)allocation	Not feasible		-
2. HFO to fore tanks	266 t		-0.47
3. Technical fresh water to fore tanks	458 t		-0.96
4. Ballast water	Not feasible		-

Load condition		T_{mean} [m]	trim [m]
Partial (~70% of DWT)		10.14	1.07
Trim scenario	**Δ Weight [t]**	**Δ T_{mean} [m]**	**Δ trim [m]**
1. Cargo (re-)allocation	1113 t		-0.83
2. HFO to fore tanks	266 t		-0.50
3. Technical fresh water to fore tanks	458 t		-1.04
4. Ballast water	900 t	+0.14	-1.01

Load condition		T_{mean} [m]	trim [m]
Ballast (~55% of DWT)		10.14	1.07
Trim scenario	**Δ Weight [t]**	**Δ T_{mean} [m]**	**Δ trim [m]**
1. Cargo (re-)allocation	Not feasible		-
2. HFO to fore tanks	266 t		-0.54
3. Technical fresh water to fore tanks	458 t		-1.11
4. Ballast water	Not feasible		-

5.2. Voyage planning

The stowage plan has a significant effect on the trim condition of the ship. Limitations in allocating cargoes to tanks therefore limits the freedom in trimming the ship as well.

The general stowage process within Stolt Tankers and the role of trim in this process is explained by one

of the operators[1]. By allocating cargoes to tanks, compliance with safety regulations is the first driver in this process. As a consequence, tank allocation is limited by cargo tank compatibility, which are specified as:

- Tank material or coating: a cargo tank surface is either stainless steel or a tank with zinc coating or epoxy coating. Chemical properties of the cargo determines which type of tank can be assigned.

- Tank heating method: a cargo tank is either heated with water or oil. To prevent reaction with the cargo in case of any leakage, the chemical properties of the cargo determines which type of tank can be assigned.

- Chemical adjacency: to prevent dangerous reaction between chemicals in case of any leakage, the cargo should be compatible with the cargo in adjacent tanks.

- Previous cargoes: The previous cargoes in the cargo tank are considered and should be compatible with the cargo to be loaded.

- Heat adjacency: The temperature of adjacent tanks are limited.

Hereafter, voyage planning, port unloading sequence and operational requirements are considered:

- Tank cleaning: After the delivery of a cargo, tanks are to be cleaned. For some cargoes, it is allowed to wash at sea and dispose the remainders in the seawater under MARPOL Annex II regulation. (IMO, 2019b). If possible, the cargo is stowed in such a way that the washing can be done during transit to the next port. This is done to prevent the need to leave port, wash tanks at sea, enter the port again to load cargo and leave the port again, which would result in additional time and costs. However, washing is done with water, which means that adjacent tanks of the tank undergoes cleaning, may not be used for cargoes that restrict the presence of water in the adjacent tanks.

- Draft restrictions at ports: sequence of unloading ports and berths. Excessive trim (and hence max draft) and extreme loading conditions are prevented when the ship is partly unloaded.

The ship's crew also checks if the loading manifold is able to load and disperse the cargo to the tanks as planned, known as rigging.

The above described considerations in the process of cargo tank allocation indicates limitations in the stowage plan, and therefore also limits the freedom in trimming. A similar description of limitations to the cargo stowage of a chemical tanker is given by Stadtler (1983).

5.3. Hull strength and stability

The loading condition directly affects the structural integrity of the hull. The structural integrity is ensured by examining the static and dynamic stresses on the hull, including shear, torsion, bending moments and slamming. According to Kishev et al. (n.d.), slamming can be avoided by trimming the ship by bow. Moreover, the loading condition has an effect on the heeling angle and stability (David and Gollasch, 2015). To avoid excessive heeling, to ensure sufficient stability and satisfy requirements for structural integrity, the stowage and ballast plan has to consider these factors. As a consequence, the freedom in trimming is limited. The on-board loading computer considers these limitations for each loading configuration.

5.4. Operational safety

If the propeller operates too close to the water surface, ventilation of the propeller may occur. If this is the case, the local low pressure created by the propeller blades can draw air beneath the water surface. Ventilation is likely to happen in a condition with large negative trim, or in combination with a very light displacement condition. Especially when the ship operates in high waves with severe ship motions, ventilation of the

---

[1]Conversation with M. Speksnijder, operator of the Inter-European fleet, on 30-10-2019.

propeller may occur (Prpic-Orsic and Faltinsen, 2012). As a result, thrust is decreased, severe noise may be experienced by the crew and the engine is experiencing dynamic loads. Kishev et al. (n.d.) describes that regulation exist for a minimal draft at the aft perpendicular (T_{AP}) to avoid propeller emergence and refers to the IMO (2008) *Stability Information Manual*, the manual for ship's stability which is part of the MEPC (2008) regulation. Propeller immersion (PI) is defined by formula 5.1. When PI is more than 100%, the propeller is completely immersed. T_{AP} which satisfies this requirement can be calculated with this formula.

$$PI(\%) = \frac{I \cdot 100}{D} = \frac{(T_{AP} - a) \cdot 100}{D} \tag{5.1}$$

Here,

- *I* is the vertical distance from the bottom of the propeller to the waterline in *m*;

- *D* is the propeller diameter in *m*;

- *a* is the vertical distance from the bottom of keel to the lowest point of the tip of the propeller in *m*;

- T_{AP} is the draft at aft perpendicular in *m*.

Trim has an effect on the visibility as well. Kishev et al. (n.d.) refers to the IMO (2008) *Stability Information Manual*, in which visibility requirements are determined according to the SOLAS 1974, Chapter V, Safety of Navigation, Regulation 22, Navigation Bridge Visibility, as well as the Panama Canal restrictions. In general, the IMO requirement is that the blind spot before the ship is less than two times the ship length. For the Panama Canal, this has be less than 1.5 times the ship's length for ballast condition and less than one ship's length for full load condition. The visibility is determined with formula 5.2.

$$\text{Visibility} = \frac{sin(90 - \phi - \theta)}{sin(\phi)} \left(h_S - T_F + d_{FS} \cdot \frac{T_{AP} - T_{FP}}{L_{PP}} \right) \tag{5.2}$$

Where

$$\theta = arctan \left(\frac{T_{AP} - T_{FP}}{L_{PP}} \right) \tag{5.3}$$

$$\phi = arctan \left(\frac{h_C - h_S}{d_{CS}} \right) \tag{5.4}$$

Here,

- T_{FP} is the draft at forward perpendicular in *m*;

- T_{AP} is the draft at the aft perpendicular in *m*;

- h_S is the height of the forward end of the bow from the keel of the ship in *m*;

- h_C is the height of the steering position of the helmsman from the keel of the ship in *m*;

- d_{FS} is the horizontal distance between the forward perpendicular and the forward end of the stern in *m*;

- d_{CS} is the horizontal distance between the steering position of the helmsman and the forward end of the stern in *m*;

- L_{PP} is the length between perpendiculars in *m*.

Górski et al. (2013) mentions that significant trim by bow is not used in practice, because of the reduction of freeboard and increase in foredeck flooding, which will be especially the case in bad weather conditions. The minimum local freeboard at the forward perpendicular is specified in the regulations of the *International Convention on Load Lines* by IMO (1966). However, here the design trim condition is assumed, thus no trim limit can be quantified.

Molland (2008) divides the manoeuvrability of a ship into the directional stability, response of the ship to the movement of control surfaces (i.e. rudders), response to other control devices such as bow thrusters and the turning ability. According to Molland (2008), trim by stern increases the directional stability. It is furthermore stated that good directional stability and good manoeuvrability typically are conflicting items, meaning that a trim by stern would decrease the turning ability. This can be confirmed by Kijima et al. (1990), who investigated the turning ability for multiple loading conditions including a trim by stern condition. They found that trim by stern will have a larger turning circle than at even keel conditions.

Except for the effect of trim on manoeuvrability, the on-board loading computer considers these limitations for each loading configuration.

5.5. Conclusion on limitations in ship trim

The C-38 ship class has four ways to significantly change the ship trim, which include cargo allocation, fuel and freshwater re-allocation and the use of ballast water. Limitations to trim a chemical tanker are given by figure 5.1.

<div style="text-align: right; font-size: 4em;">6</div>

Artificial neural networks

In chapter 3, it has been concluded that the concept of artificial neural networks, or ANNs, will be used in modelling the fuel consumption based on noon report data. This chapter provides an introduction to artificial neural networks (section 6.1 and 6.2), a review of existing literature of using ANNs for fuel consumption modeling (6.3) and a proof of concept on a simplified problem (6.4).

6.1. Basic principles of ANNs

da Silva et al. (2017) describes ANNs as computational models that have the ability to acquire and maintain knowledge and can be defined as a set of processing units, represented by artificial neurons, linked by a lot of interconnections (artificial synapses) by means of vectors and matrices of synaptic weights.

6.1.1. One single neuron

Figure 6.1 illustrates one single artificial neuron. An artificial neural network consists of a multiple of these neurons, which are connected with each other. The operation within a single neuron can be divided into the following steps:

1. Input variables (x_n) are fed to the neuron;

2. Each input is multiplied by a corresponding weight (w_n);

3. The aggregate is determined of all weighted input minus the threshold value (θ);

4. A proper activation function is applied to limit the neuron output;

5. The output of the neuron is determined.

6.1.2. The neural network

In a neural network, multiple neurons as described in paragraph 6.1.1, are connected with each other. Different standard forms exist and, depending on the purpose, one of the standard forms is most appropriate. Khare and Shiva Nagendra (2007) structures the different neural networks into two groups: feedforward neural networks and recurrent networks. Within these groups, different standard forms can be distinguished.
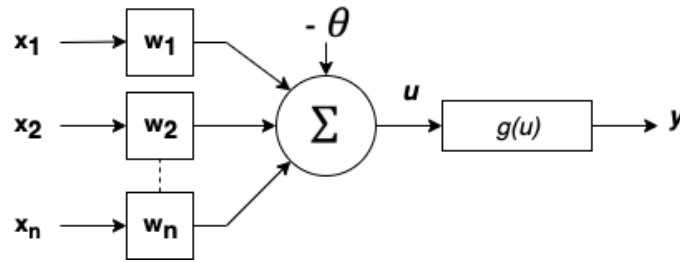
Figure 6.1: Model of single neuron (based on da Silva et al. (2017) and Khare and Shiva Nagendra (2007)).

Feedforward networks

A single layer feedforward network consists of only one neural layer, which is also the output layer. The network is defined by n input variables and m output values. Applications are pattern classification and filtering problems (da Silva et al., 2017). The network has the shape of the multiple-layer feedforward network as shown in figure 6.2, but without the hidden layers.

A multiple-layer feedforward (MLF) network consists of an input layer, one or more hidden layers and an output layer, as shown in figure 6.2. The input layer receives the input data. The hidden layer(s) perform the internal processing and are responsible for extracting patterns, which is done by the working principle of the neurons as explained in paragraph 6.1.1. The output layer is responsible for producing and presenting the final output required from the model.

Recurrent neural networks

In a recurrent network, the output of some neurons is used as an input for other neurons by means of a feedback loop, thus a previous output affects the process for the next output. Recurrent neural networks are therefore suited for problems that have a sequential nature or are time-dependent (da Silva et al., 2017). For example, recurrent neural networks are used in text sequence generation, speech recognition and text analysis (Grachev et al., 2019) or in stock price modelling (Rather et al., 2015). The networks have in common that they typically use unsupervised learning strategies. Within the group of recurrent neural networks, the following types of networks exists:

- Hopfield recurrent networks;
- Long-short term memory;
- Gated recurrent units;

- Kohonen network;
- Learning vector quantification;
- Adaptive resonance theory network

6.1.3. Training strategies

The training process consists of changing the weights and threshold of each neuron by a step by step training process. This step-wise learning process is called the training algorithm. Depending on the type of network, available data and required output, the training strategy can be chosen. Two considerations can be made:

- **Supervised or unsupervised -** In the case of supervised learning, each data sample includes the corresponding output value. The difference between the produced output and the expected output (hence the error) is calculated and used to train the network. The supervised learning strategy works well with feedforward neural networks. The unsupervised learning strategy is used when the correct output is not known and when the network is used to find any existing relations in the data (da Silva et al., 2017, Khare and Shiva Nagendra, 2007).

- **Incremental or batch training -** In the incremental training approach, the weights are updated after each unique data sample. This approach may be considered when the data is expected to change over time, for example in for the case of stock prices. In the batch training approach, all data samples are

presented in one batch (called an *epoch*) and weights are updated based on the summed error (da Silva et al., 2017, Khare and Shiva Nagendra, 2007).

6.2. Multi-layer feedforward neural networks

A MLF type of neural network is chosen with a supervised learning strategy, since this type is suited to approximate functions and the corresponding output value is known.

6.2.1. Network topology

No straight rules exist to determine the optimal topology of a MLF. The design of the network can be done in an empirical way, by investigating the performance of different network designs. Since the data is split into a training part a validation part and a test part, the performance of the trained network depends on this division. Therefore this division should be done a few times, after which a global average is taken. This process is called cross-validation (da Silva et al., 2017).

Parkes et al. (2018) states that the *accuracy* of the network is mainly determined by the number of hidden layers and neurons. As the number of units increases, more complex relations can be modelled by the network. On the other hand, a network with too few layers and neurons, can be unable to model all the (complex) relationships.

Large networks with many hidden layers and neurons can become over fitted by becoming too sensitive to certain datapoints. In this case, the model can have a low error during the training phase, but can reach a high error during testing (Parkes et al., 2018, Wilamowski, 2009).

The Fletcher-Gloss method can be used as a guideline to for the initial network topology for a MLF network with 1 hidden layer (da Silva et al., 2017), which is shown in formula 6.1). Here, n is the number of inputs, n_1 is the number of neurons in the hidden layer and n_2 is the number of neurons in the output layer.

$$2 \cdot \sqrt{n} + n_2 \leq n_1 \leq 2 \cdot n + 1 \qquad \text{(Fletcher-Gloss method)} \qquad (6.1)$$

6.2.2. The training process

The training process of a MLF network is done with the back propagation algorithm. The algorithm fits within the group of supervised, offline learning. The back propagation algorithm for a MLF is well documented in da Silva et al. (2017) and Svozil et al. (1997). This paragraph provides a brief description of this back propagation algorithm.

The back propagation algorithm consists of two stages, the forward and the backward stage. The terminology of the MLF is depicted in figure 6.2 with three neuron layers. Here:

- x_n are the input variables;

- W_{ji}^L is the weight matrix of the hidden layer L of the connection between neuron j in layer L and neuron i of layer $(L-1)$;

- I_j^L is the input vector of node j of layer L;

- Y_j^L is the output vector of node j of layer L;

- The bias of each neuron in layer L is implemented as $x_0 L$;

- y_{n_3} are the output values.
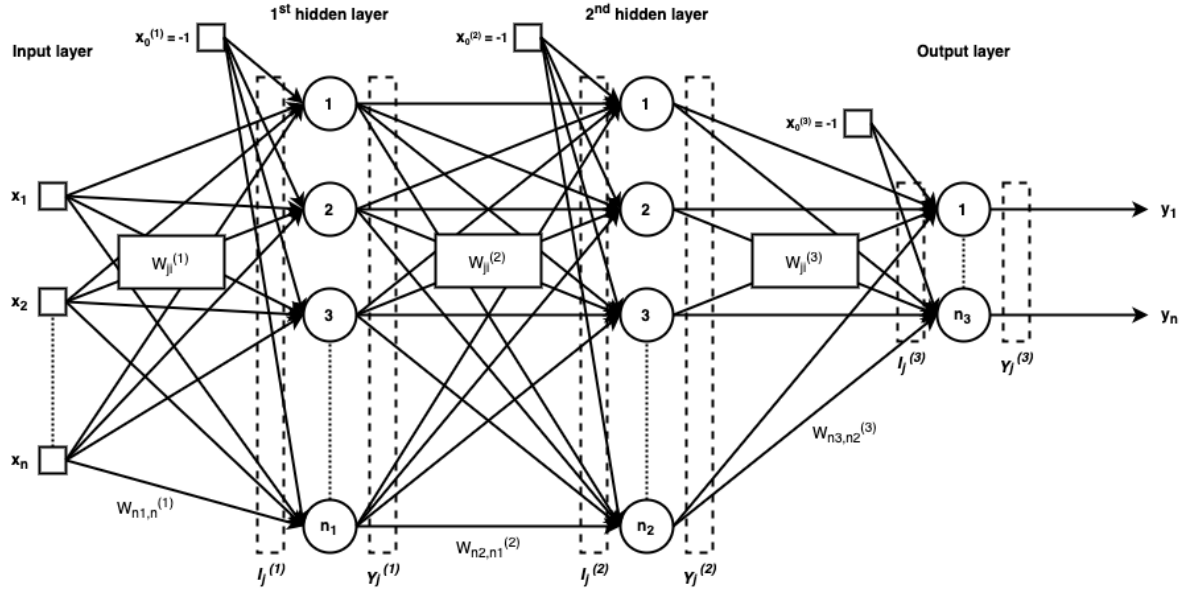
Figure 6.2: Topology of the MLF neural network (based on da Silva et al. (2017)).

Forward propagation

In the forward propagation stage, the input variables from the data samples are propagated forward through the network, where each input value is multiplied with the weight matrix W_{ji}^L. In this stage, only the output values y_{n_3} are calculated, without changing the weight matrices. Formula 6.2 and 6.3 describe this stage in the most compact way.

$$I_j^{(L)} = \sum_{i=0}^{n^{(L)}} W_{ji}^{(L)} \cdot x_i^{(L)} \tag{6.2}$$

$$Y_j^{(L)} = g\left(I_j^{(L)}\right) \tag{6.3}$$

Error calculation

Next, the calculated output is compared to the known desired output. This is done by calculating the error for each output variable. This error is used in the back propagation process of changing the weight matrices in each iteration. The error is calculated using formula 6.4. The global mean error of the network can be calculated with formula 6.5. Here, $Y_j^{(3)}(k)$ is the value produced by the jth output neuron of the network for the kth training sample, with $d_j(k)$ the corresponding desired value, p is the total number of training samples.

$$E(k) = \frac{1}{2} \sum_{j=1}^{n_3} \left(d_j(k) - Y_j^{(3)}(k)\right)^2 \tag{6.4}$$

$$E_{\mathrm{M}} = \frac{1}{p} \sum_{k=1}^{p} E(k) \tag{6.5}$$

Back propagation stage

At this point, the back propagation stage can be started. This stage can be divided into two parts. In the first part, the weight matrix of the output layer is changed, which can directly use the error as calculated

by formula 6.4. The other weight matrices are adjusted based on the change in the adjacent weight matrix. The goal of the first part of the back propagation stage is to adjust the weight matrix of the output layer to minimize the error between the produced output and the desired output. In order to adjust the matrix in the right direction, the gradient of the error with respect to the weight matrix is determined by formula 6.6. Using formula 6.2, 6.3 and 6.4, this can be rewritten into formula 6.7.

$$\nabla E^{(3)} = \frac{\partial E}{\partial W_{ji}^{(3)}} = \frac{\partial E}{\partial Y_j^{(3)}} \cdot \frac{\partial Y_j^{(3)}}{\partial I_j^{(3)}} \cdot \frac{\partial I_j^{(3)}}{\partial W_{ji}^{(3)}} \tag{6.6}$$

$$\frac{\partial E}{\partial W_{ji}^{(3)}} = - \left(d_j - Y_j^{(3)} \right) \cdot g' \left(I_j^{(3)} \right) \cdot Y_i^{(2)} \tag{6.7}$$

In formula 6.7, the first two terms can be grouped and renamed to $\delta_j^{(3)}$, the local gradient at neuron j, as shown in formula 6.8.

The change of the weight matrix is shown by formula 6.9. In addition to $\delta_j^{(3)}$ and $Y_i^{(2)}$, a minus sign is introduced since the adjustment of the weight matrix is to be done in opposite direction to the gradient. Furthermore, the learning rate parameter η can be introduced. The result is the final formula for adjusting the weight matrix of the output layer, formula 6.9. In the notation of an iterative procedure, the adjustment of the weight matrix of output layer can be written as formula 6.10. At this point, the weight matrix of the output layer is adjusted based on the error of the training sample k.

$$\delta_j^{(3)} = \left(d_j - Y_j^{(3)} \right) \cdot g' \left(I_j^{(3)} \right) \tag{6.8}$$

$$\Delta W_{ji}^{(3)} = \eta \cdot \delta_j^{(3)} \cdot Y_i^{(2)} \tag{6.9}$$

$$W_{ji}^{(3)}(t+1) = W_{ji}^{(3)}(t) + \eta \cdot \delta_j^{(3)} \cdot Y_i^{(2)} \tag{6.10}$$

In the second part of the back propagation stage, the weight matrices of the hidden layers are adjusted. As described, the computed error with the desired output can not directly be used. Instead, the adjustment of the weights is performed based on estimations of the output errors of the already adjusted neuron layer. This estimation can be done by back propagating the error, taking into account the previous adjusted weight matrix. So, the desired outcome of a neuron in the hidden layer must be calculated, using the already adjusted weights that are connected to that neuron. Similar to the first part, the goal is to adjust the weight matrix of this hidden layer in such a way that the error between the desired output (calculated by the back propagated error) and the calculated error is minimized. The derivation of the adjustment of the weight matrices of the hidden layers is more complex, but is well documented by da Silva et al. (2017). The results are given by formula 6.11 and 6.12, for the second and first hidden layer, respectively.

$$W_{ji}^{(2)}(t+1) = W_{ji}^{(2)}(t) + \eta \cdot \delta_j^{(2)} \cdot Y_i^{(1)} \tag{6.11}$$

$$W_{ji}^{(1)}(t+1) = W_{ji}^{(1)}(t) + \eta \cdot \delta_j^{(1)} \cdot x_i \tag{6.12}$$

Alternative learning algorithms

Although the back propagation algorithm will eventually converge to a minimal squared error value, the algorithm converges slowly. A range of techniques exist that reduces the convergence time, including the introduction of a momentum parameter, the conjugate gradient algorithm, the resilient-propagation method, the

Levenberg-Marquardt (LM) method, Bayesian regularization, the Broyden-Fletcher-Goldfarb-Shanno (BFGS) optimization algorithm, constrained version of quasi-Newton method, the constrained truncated Newton algorithm and hybrid models using, for example, particle swarm types of optimization techniques or genetic algorithms (da Silva et al., 2017, Ozturk and Karaboga, 2011, Pedersen and Larsen, 2009a,b, Radonjic and Vukadinovic, 2015, Svozil et al., 1997).

Stopping criteria

The goal of training the network is to find a network that minimizes the error between the predicted and the actual output value of the test data. A performance goal can be set in terms of a mean squared error (MSE) (Bal Besikci et al., 2016, Parkes et al., 2018). The MSE target may not be reached, because of noise in the data and since the test data will be different than the training data. Other stopping criteria can be used to ensure satisfactory results while limiting the calculation cost.

An increase in the error of successive epochs is a sign that a minimum is reached on the validation data and that the algorithm starts to become overfitted on the training data (da Silva et al., 2017). Overfitting will decrease the error on the training data, but this will have the consequence that the error will increase on new data. To prevent this, the number of successive increases of the error (validation failures) can be specified (da Silva et al., 2017, Parkes et al., 2018). A small number of validation failures may cause the algorithm to stop at a local minimum while the global minimum could have been reached (da Silva et al., 2017). Other ways to stop the training can be to specify the maximum number of epochs or by specifying a training time limit.

6.2.3. Training process initialising

Three sets of data will be composed from the available data points. A training set will be used to train the network. The validation set is used to perform validation, by evaluating if the performance of the trained network has reached a stopping criterion. Finally, the test set is used to evaluate the performance with new data. During data sub-sampling, it is necessary to ensure that the data points that represent the maximum and minimum values, are allocated to the training subset. Otherwise, if these extreme values are allocated to the test subset, the network tries to generalize values that are outside the domain of the input variables, causing significant errors (da Silva et al., 2017).

Depending on the learning algorithm used in the learning process, the chance exists that the error function converges to a local minimum, instead of the global minimum. To avoid that the network converges to a local minimum of the error function, the learning process can be repeated more than once with different initial weight matrices (da Silva et al., 2017).

It is recommended to scale the in- and output variables, in order to avoid saturation of the neurons. According to da Silva et al. (2017), the proportional segment principle (the Thales' theorem) is the most used. In this method, the set of values initially within a range of minimum and maximum values, i.e. $\chi \in [\chi^{min}, \chi^{max}]$, will be converted to a proportional range between -1 and 1. Input value x is normalized with formula 6.13 to the normalized input value z.

$$z = 2 \cdot \left(\frac{x - x^{min}}{x^{max} - x^{min}} \right) - 1 \tag{6.13}$$

6.3. Lessons learned from relevant applications

The considerations regarding the network architecture demonstrate the importance of a balanced number of layers and neurons and the need for an empirical approach to quantify the specific complexity. Reference values can be found in studies that applied ANN in modeling ship fuel consumption based on noon report (NR) data. The results of this study are shown in table 6.1. From the results of the references in this table, the following can be concluded:

- **Number of input variables:** The number of input variables is less than 10. Table 6.2 specifies the variables chosen in these references.

- **Number of noon reports:** The number of noon reports (after filtering) varies between 181 and 323 for a single ship. This number can be used as a reference to the amount of input data used in the model in this research. *CM* means that the input data consists of continuous measurements from on-board data. Furthermore, the data of Radonjic and Vukadinovic (2015) consists of sea trial data.

- **Percentage of data used for training:** Is either 70% or 80%, which is within the range suggested by da Silva et al. (2017).

- **Number of hidden layers:** Most references stick to one hidden layer, thereby limiting the complexity of the neural network. The way of quantifying the accuracy of the models is different for each reference, which makes comparing of results difficult. The work of Radonjic and Vukadinovic (2015) shows that a network with 2 hidden layers outperformed the network with one hidden layer. Parkes et al. (2018) compared the accuracy of the model with multiple hidden layers (each with 1, 50 or 100 neurons in it) and concluded that a 3 hidden layers provided a network with the highest accuracy.

- **Number of neurons:** In Du et al. (2019), the number of neurons in the hidden layer was equal to the number of input variables. Pedersen and Larsen (2009a) investigated the accuracy of the model for either 5, 10, 15 or 20 neurons in the hidden layer. This research found that the number of neurons was not critical, although 5 neurons was too few. This was verified by Pedersen and Larsen (2009b), where only 5 and 20 neurons were applied. Here, 20 neurons showed better results than 5 neurons. A more extensive study was performed by Parkes et al. (2018), where both the effect of the number of layers and neurons was investigated. The number of neurons was either 1, 50 or 100 for each layer. It was found that a higher number of neurons decreased the error, but both 50 and 100 neurons provided similar results. The network can get over fitted with a high number of neurons and the computational time increases with the number of neurons as well, suggesting that 50 neurons is preferred over 1 and 100 neurons.

- **Training algorithm:** No clear arguments to use one over the other are found. However, Radonjic and Vukadinovic (2015) used various training algorithms and found that the constrained truncated Newton (TNC) method found better results in the same amount of time.

Table 6.1: **Evaluation of network design in similar studies.**

ANN feature	(Du et al., 2019)	(Bal Besikci et al., 2016)	(Pedersen and Larsen, 2009a)	(Pedersen and Larsen, 2009b)	(Parkes et al., 2018)	(Radonjic and Vukadinovic, 2015)
Input variables	10	9	8	9	6	4
Data entries	242+181	223	CM	323	CM	193 sea trials
% For training	80%	70%	80%	80%	70%	80%
Hidden layers	1	1	1	1	1 to 5	1 and 2
Neurons	10	12	5 to 20	5 to 20	1 to 100	3 to 15
Training algorithm	Unspecified	LM	Bayesian	BFGS	Scaled conjugate	Various

Table 6.2 shows which parameters are selected in similar studies. The work of Radonjic and Vukadinovic (2015) is excluded from this table, since the content of this paper differs from the scope of this research. The used parameters are displayed by the unity used in the research.

6.4. Proof of concept

To show the ability of a MLF, a proof of concept is given. In this proof, the fuel consumption is modelled as a function of displacement and speed. The network is a 2-3-1 MLF neural network, so 2 input variables, 3 neurons in the hidden layer and 1 neuron in the output layer. The network topology is shown in figure 6.3.

Table 6.2: **Input parameters of fuel (or power) consumption estimation models of existing literature and the corresponding units. Empty cells represent that the variable is not selected in the corresponding model.**

Input variable	(Du et al., 2019)	(Bal Besikci et al., 2016)	(Pedersen and Larsen, 2009a)	(Pedersen and Larsen, 2009b)	Parkes et al. (2018)
Ship speed	knots	knots	knots	knots	knots
Displacement	ton				
Wave height	m	m		m	m
Wave direction	A-H	with/against		deg	
Wind speed	Bf	knots	knots	m/s	m/s
Wind direction	A-H	with/against	A-H	degrees	degrees
Current speed	knots				
Current direction	A-H				
Sea water temp.	°C		°C	°C	
Air temp.			°C	°C	
Trim	m	m		m	m
Engine speed		rpm			
Mean draft		m		m	m
Cargo quantity		ton			
Output variable	FC [MT/day]	FC [MT/h]	P_S [kW]	FC [MT/h]	P_S [kW]
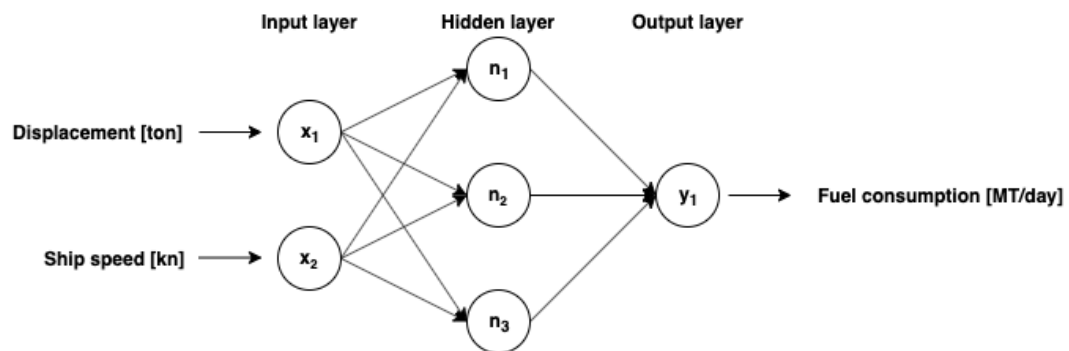
Figure 6.3: Topology of the MLF neural network used for the proof of concept.

The training data exists of 40 data samples, with random values of displacement (Δ) and ship speed (V_S), with $20\,000 \leq \Delta[t] < 30\,000$, and $6 \leq V_S[kn] < 15$. The "actual" fuel consumption is modelled as a function of the displacement and speed. Noise is introduced by a random value dependent on the displacement. The final formula is shown by formula 6.14. The described data can be found in table A.1 in the appendix.

$$FC = 0.5 \cdot \frac{\Delta}{\Delta_{max}} \cdot V_S^{2.5} + random(0...1) \cdot \frac{\Delta_{max}}{\Delta} \tag{6.14}$$

The network is trained in Matlab (version 2017b), with default settings:

- Training algorithm: Levenberg-Marquardt;

- Maximum number of epochs: 1000;

- MSE goal: 0;

- Maximum training time: infinite;

- Maximum number of validation fails (number of consecutive increases in MSE): 6;

- 80% of the data is used as training data, the remaining 20% for validation.

The network repeatedly converges to similar results. After 50 epochs, the MSE started to increase for 6 times in a row, which caused the training algorithm to stop. The final MSE of the training data was 0.19905. Additionally, the performance of the network was tested on new data, which the network had not seen before. Therefore, 10 new data samples were simulated in the same way as the training data. The trained network was used to predict the fuel consumption. The results are shown in table 6.3 and in figure 6.4. The MSE on the test data is 0.2334.

The working principle of both training an MLF and consequently use it to predict the outcome has been illustrated by applying an MLF to a simplified problem. It has been shown that a trained MLF is able to estimate the fuel consumption.

Table 6.3: **Output of trained MLF for test data, compared with the simulated actual fuel consumption.**

Δ [t]	V_S [kn]	Actual (simulated) FC [MT/day]	Estimated FC [MT/day]	Error [MT/day]
28000	10	15.80	15.26	-0.55
20000	10.5	12.17	12.09	-0.08
22000	13.5	25.28	25.49	0.21
30000	7.0	6.71	7.23	0.51
25000	8.5	9.18	8.49	-0.68
21500	9.5	10.01	9.84	-0.17
25000	14.0	31.63	31.16	-0.46
23500	9.5	11.96	10.96	-1.00
29000	12.5	27.10	27.12	0.02
23000	11.5	17.48	17.57	0.10
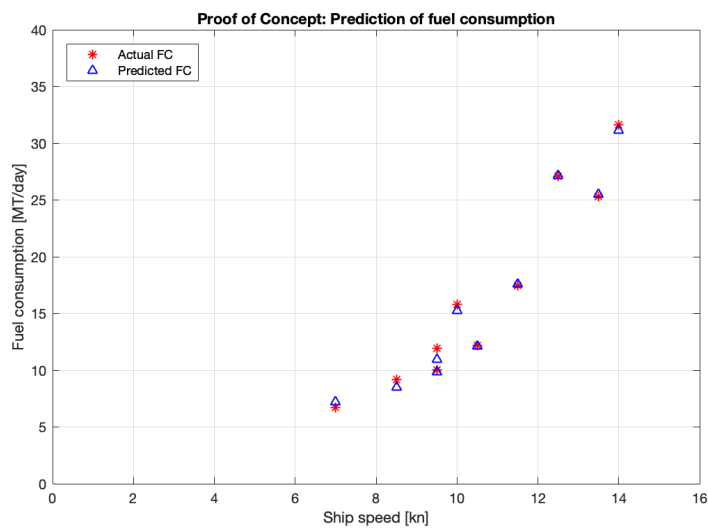
Figure 6.4: Performance of the trained neural network for the proof of concept.

III

Part III: Method and case study

7

Fuel model methodology

In this chapter, the method to fulfill the research objective and answer the research questions (as described in section 2.7) will be described. It has been explained in chapter 3 that a dynamic fuel consumption prediction model (shortly *fuel model*) based on noon report data is the solution approach that could fulfill the method requirements of section 2.7, and overcomes the drawbacks of other reviewed solution approaches.

7.1. General model description

The main solution method to fulfill the research objective and research questions of section 2.7, is to construct and use a fuel consumption estimation model. The model is made in Matlab version R2017b. The model consists of a WBM and BBM in series, using ship design parameters and voyage report data.

Two WBMs are developed. In short, the model *PLK* is based on the regression model of Lutzen and Kristensen (2013). The model *PHM* is based on the regression model of Holtrop and Mennen (1982) as far as possible. Section 7.4 describes both WBMs in more detail.

The neural network is a multi-layer feedforward neural network (MLF), which considers the result of one of the regression models as input, as well as a number of variables from the noon reports. This feature selection is part of the data pre-processing step.

The output of the GBM is the required shaft power. The predicted fuel consumption is calculated separately. This is done for two reasons. Firstly, a big difference exists in the data quality of daily fuel consumption on the one hand, and shaft power on the other. Shaft power is more reliable to use, since most ships have shaft torque meters. Together with the angular velocity of the shaft, the shaft power is calculated by using formula 7.1. Measurements on fuel consumption are less accurate. Only a few ships have fuel flow meters installed, and often the fuel consumption is calculated by measuring the fuel stock on a daily basis. Because of the size and shape of the fuel tanks, a reading error of a few cm in height can correspond to significant differences in fuel consumption. Therefore the shaft power is considered to be more reliable than the daily fuel consumption.

$$P_S = T \cdot \omega = \frac{2\pi \cdot n_e \cdot T}{60} \tag{7.1}$$

With torque (T) in [kNm], the angular velocity (ω) in $[\frac{rad}{s}]$ and the engine speed (n_e) in [rpm].

Secondly, the trim tables from model scale towing tests consider the required power as well. However, instead of shaft power P_S, the delivered propulsion power P_D is used, which includes the shaft efficiency. Fuel consumption is proportional to shaft power and is calculated separately in the post-processing, assuming a fixed specific fuel consumption. Figure 7.3 shows the relations between P_D, P_S and fuel consumption.

The fuel model can be illustrated as shown in figure 7.1. The model distinguishes a training stage and an exploiting stage.

7.1.1. Training stage

In the training stage, the MLF network is trained. The input consists of a number of variables of the noon report data and the approximated shaft power by one of the WBMs, which in turn requires noon report data and ship design parameters (as listed in table 7.1 and 7.2). Independent of the feature selection, recorded shaft power from the noon reports is one of the features to be selected from the noon reports, since this is required to perform the supervised learning strategy. If the network is trained, i.e. it has learned the relationship with the input variables and the shaft power, a function is created. This function requires the same input variables as the network, with the approximated shaft power as output. Since the performance is slightly different every time the network is trained (because of the data set sub-sampling, see 6.2.1), this process is done k times, of which the average is taken. Section 7.7 describes this process in more detail.
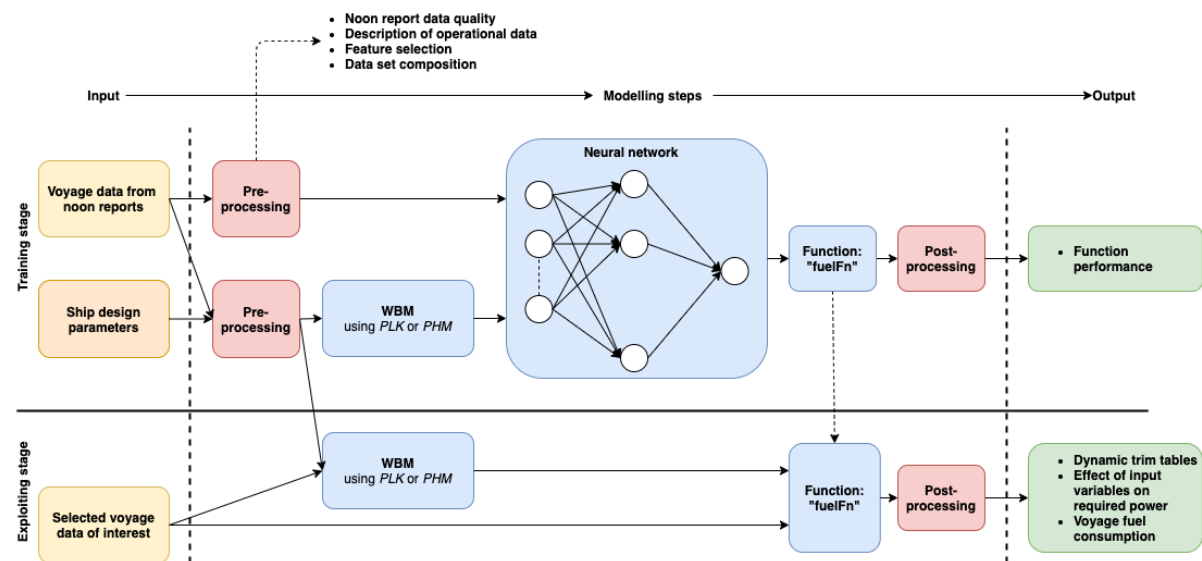
Figure 7.1: Overview of the dynamic fuel consumption prediction model.

7.1.2. Exploiting stage

The function of the trained network can be used to evaluate the effect of all input variables on the required shaft power. Therefore, one of the possibilities is to generate similar trim tables as the ones made from model scale towing tests. For a certain speed and environmental conditions, the required power can be calculated for each combination of draft and trim. This process is done k times as well and averaged, since the function will be slightly different every time the network is trained. If calm water conditions are selected, a static trim table is created. However, any sea condition can be selected, thereby generating trim tables in a dynamic way.

Other ways of exploiting the fuel model includes the evaluation of hull and propeller fouling, the effect of sea conditions and speed on required power. Therefore, this can be used as a supporting tool to investigate deviations in ship performance as well. Also, the fuel model can be used to estimate the fuel consumption for a certain voyage, taking the loading conditions and weather forecast as input.

7.2. Fuel model input

The required input data for both WBMs are listed in table 7.1 and 7.2. The input for the BBM is limited to the operational data and weather recordings. The WBMs require this data, but also additional ship parameters.

Table 7.1: **Required input data for BBM and WBMs.**

Voyage report and maintenance data		unit
Load	DWT	t
Lightweight	LW	t
Speed	V	kn
Heading	heading	°
Draft aft	T_{aft}	m
Draft forward	T_{fwd}	m
Sea temperature	-	$°C$
Wind force	-	Beaufort
Wind compass direction	-	N-NNE-NE...
Sea state	-	Douglas
Sea compass direction	-	N-NNE-NE...
Swell state	-	Douglas
Swell compass direction	-	N-NNE-NE...
Days since hull cleaning	-	days
Days since propeller cleaning	-	days

7.3. Data pre-processing framework

A data pre-processing framework is established to increase the quality of the data. Garcia et al. (2016) defines six steps of data pre-processing, which are data cleaning, transformation, integration, normalization, missing values imputation and noise identification. In this research, a sequential order is introduced to this framework, as well as the steps of feature selection and data selection.

Figure 7.2 shows the sequential order and the output of different steps. Based on the output of steps in group A, the quality of the recorded data in the noon reports will be assessed. A description of the frequency of the encountered weather and the operational profile can be given based on the output of steps in group B. The final output (group C) is used as input for the model.
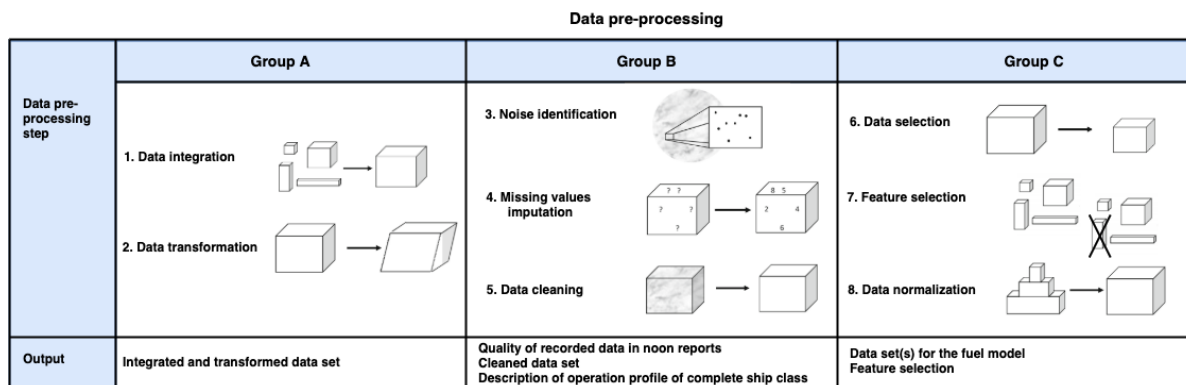
Figure 7.2: Data pre-processing framework, based on Garcia et al. (2016).

7.3.1. Data integration

The available data is composed of different data sources. Firstly, the ship parameters for the WBMs are acquired from the ship brochure, loading manual, hydrostatic tables and sea trial results. The recorded operational and environmental variables from the noon reports are acquired by downloading the noon report data from voyage management system. A dataset is constructed using Microsoft Excel.

Table 7.2: **Additional required input data for both WBMs.**

PHM			PLK		
Ship parameters		**unit**			**unit**
Waterline length	L_{WL}	m	Waterline length	L_{WL}	m
Length perpendiculars	L_{PP}	m	Length perpendiculars	L_{PP}	m
Breadth	B	m	Breadth	B	m
Wetted surface of hull	S_W	m^2	Design draft	T_{des}	m
Wetted surface of appendages	S_{APP}	m^2	Wetted surface @ design draft	S_1	m^2
Propeller diameter	D	m	Propeller diameter	D	m
Submerged transom area	A_{TR}	m^2	Afterbody form factor	F_a	-
Afterbody form coefficient	C_{stern}	-	Hull form coefficient	$C_{hullform}$	-
Bulb frontal area	A_{BT}	m^2	Waterplane coefficient	C_{WP}	-
Bulb height	h_B	m			
Lightweight ship	LW	t	Lightweight ship	LW	t
Midship area coefficient	C_M	-	Midship area coefficient	C_M	-
Waterplane coefficient	C_{WP}	-	Relative rotative efficiency	η_R	-
Form factor of appendages	k_2	-	Shaft efficiency	η_S	-
Length centre of buoyancy	lcb	%			
Relative rotative efficiency	η_R	-			
Shaft efficiency	η_S	-			

7.3.2. Data transformation

Data transformation is required to transform the input data to the required input variables of the fuel model. For example, the direction of wind, sea and swell, which are recorded in points of compass (N-NNE-NE, etc) and has to be transformed into numerical values, relative to the ship's heading.

7.3.3. Description of integrated and transformed dataset

The quality of the data in the noon reports is described by the number of empty field and unrealistic data entries. This provides insight in how many noon reports have to be deleted and for which reason.

7.3.4. Noise identification

Noise identification is done in four ways:

- Empty datafields and unrealistic values, which is different for each variable. These rules are listed in table 8.2;

- Scatter plots and boxplots are used to find outliers, which indicate noise and abnormal input values;

- Shaft power is compared with a quick estimation. The quick estimation is done by the Admiralty coefficient (see formula 3.1). If the difference is relatively big, the data entry is inspected for abnormalities as well.

7.3.5. Missing values imputation

If a missing or clearly wrong value can be logically changed to the supposed value, the value is changed manually rather than deleting the complete data sample.

7.3.6. Data cleaning

In order to limit the effect from noise on the accuracy of the fuel model, the remainder of the data entries that contain noise, is deleted from the dataset. Since the MLF requires complete data entries, the complete data entry has to be deleted when a single input value of that data entry is missing or abnormal.

7.3.7. Description of cleaned data

The cleaned data is described by means of frequency histograms, which is required to define the boundaries of the fuel model. Although a GBM has better extrapolation qualities compared to a pure BBM, the range of input data still determines the range in which the model can be applied.

7.3.8. Data selection

A trade-off exists for the dataset to be used in the fuel model. On the one hand the complete cleaned dataset can be used to train the neural network, which contains all encountered operational, weather and fouling conditions. On the other hand, the available data can be filtered for calm water conditions.

The rationale to use the complete dataset is that the effects of all input variables on shaft power can be extracted as complete as possible. This is a requirement to estimate the shaft power and fuel consumption for a wide range of sailing conditions. In addition, more data is used, therefore covering a wider range of data (including encountered trim conditions). A smaller dataset with less datapoints, will result in a model that has to extrapolate more often. Moreover, using more data seems to have a significant benefit when using noon report data without hind-cast weather data, since the prediction errors decrease with time (Pedersen and Larsen, 2013).

However, in rougher conditions, it will be the weather conditions that will dominate the shaft power and speed, of which the precise effect will be more difficult to predict with increasing sea- and swell states. Using a data set that contains calm water conditions excludes this source of error, which improves the accuracy of the fuel model. The data set representing calm water conditions fulfills the following two conditions:

- A sea state of 3 on the scale of Douglas is taken as upper bound, which relates to *slight* waves, with a wave height up to 1.25 m;

- A swell state of 2 on the scale of Douglas is taken as upper bound, which relates to *low* waves, defined as a swell height up to 2 m (lowest swell height on the scale of Douglas).

To discover the effect of this data selection, both datasets are defined and considered in the analyses. The all weather dataset is used as the reference, the small data set is considered as comparison material.

7.3.9. Feature selection

Feature selection is required for training the MLF. Introducing variables that are poorly correlated to the output variable can have the consequence that the MLF suffers from overfitting. Moreover, using input variables which are strongly correlated to each other, may result in overfitting on these variables as well. An example for this is the displacement and draught.

The feature selection is performed based on the Spearmans Rank correlation method. This method has proven effective for feature selection for a MLF in modeling ship fuel consumption by Parkes et al. (2018).

7.3.10. Data normalization

The WBMs require no additional data normalization. The neural network does require data normalization of the in- and output variables. This is done in Matlab by the 'mapminmax' function for both the input variables

and the target variable. This function normalizes the values according to the proportional segment principle, as shown by formula 6.13.

7.4. White box models in fuel model

Two WBMs are constructed, which are described in more detail in this section. A comparison between both models and the noon report data is performed in the case study.

7.4.1. WBM 1 - PLK

The WBM with the name PLK uses the regression model as documented in the work of Lutzen and Kristensen (2013). To use this model as a WBM in the fuel model, a number of modifications are made.

One of the steps in this model is to determine a residual resistance coefficient, $C_{R,diagram}$, from the graphs in the work of Lutzen and Kristensen (2013). Different graphs exist for a number of slenderness ratios and prismatic coefficients, showing the residual resistance coefficient as a function of the speed in Froude number. The slenderness ratio (M) and the prismatic coefficient (C_P) are dependent on the mean draft, therefore each noon report is considered individually, as well as the scenario of interest when the fuel model is used. The graphs are approximated by formulas, of which the result is shown in appendix C. The nearest valid approximation is taken. For example, for a slenderness ratio of $M = 5.1$ and a prismatic coefficient of $C_P = 0.78$, the graph of $M = 5.0$ and $C_P = 0.80$ is used to approximate the residual resistance coefficient.

The model of Lutzen and Kristensen (2013) provides approximations for wake fraction, thrust deduction and open water propeller efficiency as well, based on the work of Harvald (1983). Here, part of the approximation of the thrust deduction (t_1) is done with a graph, which is a function of $\frac{B}{L}$ and the block coefficient. A function is approximated, as shown in figure C.8 in appendix C. A maximum of $t_1 = 0.31$ is set, according to the boundaries of the graph of Harvald (1983).

The model of Lutzen and Kristensen (2013) provides an approximation of kinematic viscosity based on sea water density and sea water temperature. Sea water temperature has an effect on sea water density. Based on reference values of 26th ITTC Specialist Committee on Uncertainty Analysis (2011), a function is established to account for the different recorded sea water temperatures and the effect on sea water density, assuming a fixed salinity. The results are shown in table C.1 and figure C.1 in appendix C.

To account for the hull fouling in the WBM, an annual increase of 8% in required shaft power is added, based on the description given in paragraph 3.4.4. The effect of propeller fouling on required power is not approximated in the WBM, since no approximation of a relation between days since last propeller cleaning and required shaft power is found in existing literature. This effect is only accounted for in the BBM. In the case study, the accuracy of both WBMs are compared.

To generate the trim table, the required shaft power is calculated for arange of mean drafts and trim. The model of Lutzen and Kristensen (2013) requires a displacement as input. Therefore the displacement is to be estimated as a function of the draft condition. A linear relationship can be found with mean draft in the noon report data. The resulting relationship based on the noon report data of the case study vessel can be found in figure C.9 in appendix C.

7.4.2. WBM 2 - PHM

The WBM with the name PHM uses the regression model as documented in the work of Holtrop and Mennen (1982) as far as possible. This includes the resistance approximation and the effect of trim, by means of varying forward and aft draft and a shift in the length centre of buoyancy (lcb). To approximate the propulsion efficiency, the authors refer to the work of Oosterveld and Van Oossanen (1975), for which the propeller diameter, the number of blades, the effective blade area ratio and the propeller-pitch ratio is required. During the design stage, these parameters can be varied to find a suitable initial propeller design, but when applying this approach in the fuel model, problems arise. The propeller design in fixed, the effective blade area

ratio is not commonly known for every ship in operation and the propeller-pitch ratio varies in case of a controllable pitch propeller (CPP), which is not recorded in the noon reports. Moreover, approximations for the wake fraction and thrust deduction factor of the Holtrop and Mennen (1982) method have shown significant differences from values measured on model scale (which are available for the case study ship, but in general this information is considered not to be available for all ships in operation). Therefore, the propulsion characteristics, including the wake fraction, thrust deduction factor and open water propeller efficiency are approximated by the model of Lutzen and Kristensen (2013).

The model of Holtrop and Mennen (1982) requires the length center of buoyancy in respect to $\frac{1}{2}L_{WL}$, as a percentage of the waterline length. The length centre of buoyancy varies for different draft and trim conditions. Approximations can be made based on the hydrostatic tables of the ship, of which a graph is presented in figure C.7 in the appendix. Here, the length centre of buoyancy can be approximated as function of draft for different trim conditions. Linear interpolation is used to approximate the length centre of buoyancy in case the trim is not an integer value. However, in the hydrostatic tables the length centre of buoyancy is measured in metres in respect to the aft perpendicular. Formula 7.2 is used to transform the *lcb* to the definition of Holtrop and Mennen (1982). Here, *lcb* is the length center of buoyancy according to the definition of Holtrop and Mennen (1982) and LCB according to the definition in the hydrostatic tables.

$$lcb[\%] = \frac{LCB + l_{stern} - \frac{L_{WL}}{2}}{L_{WL}} \times 100 \tag{7.2}$$

with l_{stern} = waterline length behind aft perpendicular

To account for the hull fouling, an annual increase of 8% in required shaft power is added here as well, as described in paragraph 3.4.4. This model requires an estimation of the displacement as well.

7.4.3. Selection of WBM

By comparing the results for the case study of both WBMs, a decision can be made of which WBM performs best. The WBMs are compared by:

- Speed-power curve, showing the data from the noon reports, the estimations using PHM and using PLK;

- Compare the relative error of the estimations of the fuel model with the noon report data, using the optimal topology of both models;

- Compare the performance of both types of generated trim tables.

7.5. ANN decisions

It has been found in chapter 6 that a MLF neural network is the most suitable type of network for modeling the fuel consumption. Furthermore, multiple aspects in designing the neural network have been covered. The following choices have been regarding the design of the neural network:

- The data will be divided into a training set, a validation set and a test set, with a ratio of 70%, 15% and 15%, respectively. Because the performance will depend on this division (as explained in 6.2.1), the network is trained k times with as many divisions. To ensure an averaged expectation value, k is chosen to be 100. If training time increases, this number may be chosen smaller to decrease training time.

- For each data subdivision, it is ensured that the minimum and maximum input and target data (i.e. shaft power) is placed in the training data set, in accordance to the network initialising guidelines as explained in 6.2.3. First, the data is divided randomly. If the minimum and/or maximum target value is not within the training set, these values are added to the initial training set and are removed from the validation or test set.

- Final network topology will be determined in an empirical way, varying from one to four hidden layers with multiple options of nodes in each layer, cross validated by repeating the training algorithm k times. The Fletcher-Gloss method (formula 6.1) will be used as a guideline for the number of neurons. Since the number of neurons in the hidden layer depends on the number of neurons in the input layer, which in turn is determined by the feature selection, this number can be specified after the data pre-processing. In order to compare the accuracy of the single hidden layer network with the multiple hidden layers network, the same number of neurons will be used for the multiple hidden layers network.

- The hyperbolic sigmoid function will be used as the activation function for the MLP network.

- Different learning algorithms are tested for accuracy, speed and consistency. The *Bayesian Regularization* training algorithm has shown the most accurate and consistent results and relatively fast. For most network topologies, the training time was less than a second.

- Four stopping criteria will be applied for training the network:

  - A target MSE of ≤ 0.1;
  - A maximum of six consecutive increases of the error (validation failures);
  - Maximum number of epochs is 200;
  - A time constraint of 20 minutes.

- Network initializing is done in Matlab automatically when creating the network.

- Normalization of in- and output is done by the 'mapminmax' function according to the Thales theorem (formula 6.13).

7.6. Post-processing

The accuracy of the model will be evaluated by calculating the mean relative error ($\overline{RE_K}$) of all K relative errors of each kth training subset, with all N noon reports in the test sub set (see formula 7.3). Here, $\hat{Y}$ is the estimated output value and Y is the actual output value known from the nth noon report.

$$\overline{RE} = \frac{1}{K} \frac{1}{N} \sum_{k=1}^{K} \sum_{n=1}^{N} \frac{\hat{Y}_n - Y_n}{Y_n} \tag{7.3}$$

The output variable of the fuel model is the shaft power P_S. The average value of all k estimation of the model is taken as the final reference value.

Formula 4.14 is used to determine the fuel consumption. The gearbox efficiency (η_{GB}) has to be estimated, while the specific fuel consumption (sfc) is known from the engine manufacturer, sea trial results or from (inhouse available) engine performance audits. The result is formula 7.4, which is shown in figure 7.3 as well.

$$FC = \frac{P_S}{k_e \cdot \eta_{GB}} \cdot sfc \tag{7.4}$$

7.7. Validation

Both the fuel model and the generated trim tables are validated. Validation of the fuel model is done by comparing the estimated power of the fuel model with the actual shaft power requirement from a test subset of the noon report data. Also, the effects of other input variables on shaft power are considered in a qualitative way, by fixing all input variables except the one of interest.

Delivered power P_D

(Output of existing trim tables)

$P_D = P_S \cdot \eta_S$

Shaft power P_S

(Output of fuel model and noon reports)

$FC = \dfrac{P_S}{k_e \cdot \eta_{GB}} \cdot sfc$

Fuel consumption FC

(Output of fuel model)
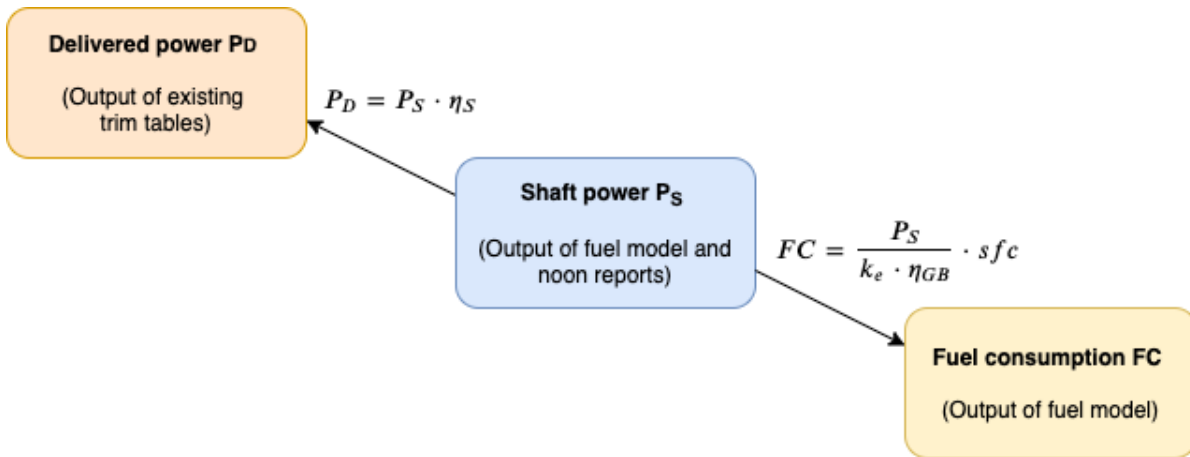
Figure 7.3: Overview of transforming shaft power P_S to delivered power P_D and fuel consumption.

Validation of the generated trim tables is done with additional sea trial data. These sea trials are performed for vessels of the C38 ship class in calm water conditions, as defined in paragraph 7.3.8 for trim conditions between -0.5 to +2.0 meter and for speeds through water of 11, 12, 13 and 14 knots. Depending on the available time for the ships to perform the sea trials and the local weather conditions, multiple sea trials are conducted for a range of mean drafts and trim conditions. Instructions to the ship's crew for conducting sea trials are included in appendix G.

During the sea trials, more parameters than trim will change. For example, the ship's heading, the displacement due to additional ballast water or a change in wind and sea conditions. The generated trim tables however, are valid for only one specific condition at a time. To cope with the change in operational and weather conditions during the sea trials, the model is evaluated in two ways.

The first way is to mimic each sea trial condition one by one, as close as possible. The main advantage of this approach is that it validates all effects of the model, including the effect of (change in) weather conditions on the required shaft power. A peak in shaft power because of an increase in sea state, will be made visible. However, the shaft powers are a result of more than trim only.

The second approach is to take the average sea trial conditions, and generate the complete trim table for a certain speed at once. The advantage of this approach is that the isolated effect on trim on shaft power is extracted in a clear way, but effects of changes in weather conditions are not accounted for.

Sea trials

1. Validation of generated trim tables

2. Evaluation of existing trim tables

Generated trim tables

Trim tables from model scale towing tests
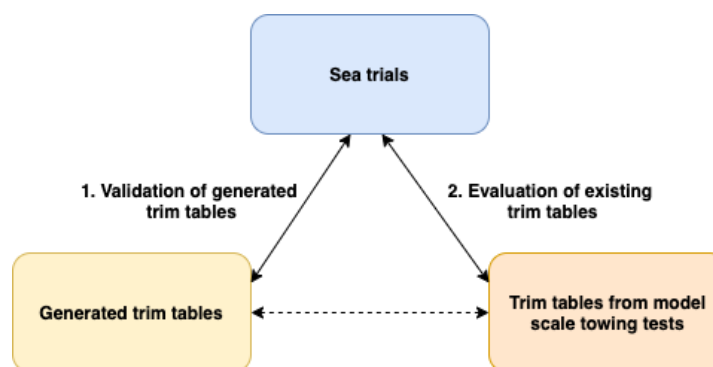
Figure 7.4: Different steps of validation of the generated trim tables.

7.8. Evaluation of trim tables based on model scale towing tests

The accuracy of the trim tables based on model scale towing tests are evaluated in a similar way of the generated trim tables. The shaft power for the given mean draft, trim and ship speed is compared to the matching

averaged sailing condition of the sea trial. This evaluation will answer research question 4 (*How accurate are trim tables based on model scale towing tests?*).

7.9. Integration of trim model in voyage management system

The voyage management will consist of a sequence of tasks, to be performed by a number of actors. This process will be modelled for both the current process of voyage management, as well as the potential process in which trim optimization is integrated. This acts as a tool to decide when, how and by whom trim optimization should be used in this process. The result will be a process description in which trim optimization is part of the voyage management process.

The process modelling is based on observations and validated with interviews within Stolt Tankers[1].

Business process modelling is done according to the instructions of business modelling of Bridgeland and Zahavi (2009), using the structure as summarized in figure 7.5.
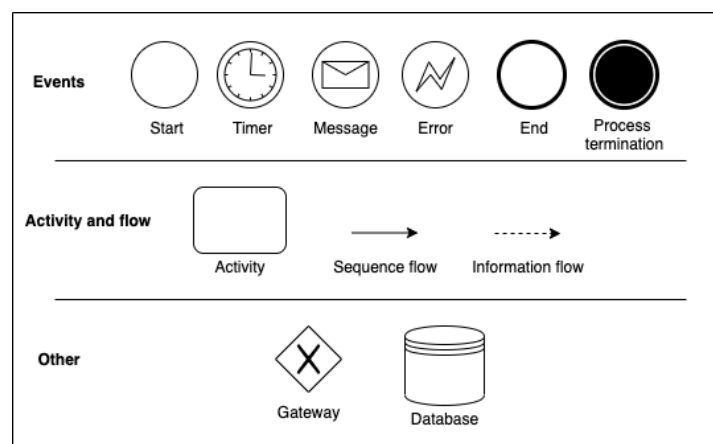
Figure 7.5: Rules of business process modeling.

---

[1] Meeting with W. de Vries, operations manager within Stolt Tankers, on 04-05-2020. and with J. Bogaard, project manager within Stolt Tankers, on 12-05-2020.

8
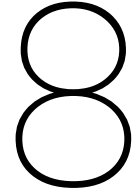
Case study model

In this chapter, a case study will be performed. The purpose of this chapter is to show the ability of the method (described in chapter 7) to generate trim tables in a dynamic way.

8.1. Case study description

The C-38 *Pride* ship class, shortly *the C-38*, is used for the case study. The C-38 is a 38 000 + DWT single screw ocean going parcel tanker for transporting chemicals, oil products and vegetable oils. Figure 8.1 shows the *M/T Stolt Pride*, which is one of the ships of the C-38 ship class. Paragraph 8.1.1 briefly explains why the C-38 is chosen for the case study. Next, relevant ship specifications considering the design, engine, propulsion and cargo holds are described in paragraph 8.1.2.

Figure 8.1: Stolt Pride, one of the ships used in the case study (picture from offshore-energy.biz).

8.1.1. Choice of ship class

From the range of ship classes within Stolt Tankers, this ship class is the most suitable for two reasons. First of all, trim tables have been developed for this ship class, so these can be compared with the actual performance known from noon report data and with the trim tables constructed from the fuel model. This means that research question about the accuracy of the available trim tables can be answered.

The second reason is that both the data quality and quantity is expected to be sufficient. The C-38 has shaft power meters which can be used to document the shaft power in the noon reports in an accurate way. Furthermore, 6 sister vessels exist in this ship class. The available data from these 6 ships can be accumulated. The age of the ships vary between 1.5 and 3.5 years, counted from January 2020.

8.1.2. Ship design and propulsive specifications

Table 8.1 presents the ship design parameters. The ship has a U-shaped stern section. No bulb is attached to the bow section. The displacement is an average over the actual displacements of all 6 ships.

Table 8.1: **Ship design parameters of C-38 ship class.**

Ship design parameter		Value	Unit
Length overall	L_{OA}	185.04	m
Length between perpendiculars	L_{PP}	181.8	m
Breadth moulded	B_m	32.25	m
Draft moulded	D_m	14.96	m
Draft at summer loadline	T_s	10.35	m
Service speed	V_{des}	14.0	knots
Displacement	Δ_{des}	38873	t
Tonnes per centimeter	TPC	57.2	$\frac{t}{cm}$

The C-38 ship class has one single engine for propulsion, and is coupled with a shaft generator. The engine is a slow-speed 6 cylinder 2-stroke Wärtsilä engine. The engine delivers a brake power P_B of 7 900 kW at an engine speed of n_e of 100 rpm.

The engine is directly coupled to a 4-bladed controllable pitch propeller with a diameter (D) of 6.30 m.

The cargo section is divided into 39 cargo tanks, with a port, center and starboard section. In addition, 4 deck tanks are available on deck. All cargo tanks made from duplex stainless steel.

8.2. Data pre-processing and description

The steps as described by figure 7.2 are performed in the next paragraphs.

8.2.1. Data integration, transformation and raw data description

Voyage data from the C38 has been downloaded of the period between 01-06-2016 and 01-02-2020, providing noon reports with record periods between 1 and 3.5 years, depending on the age of the ship. Information of the lightweight of the ship, the admiralty coefficient from sea trial results and the history record of hull cleaning and propeller polishing has been integrated with the noon report data. In total, 2923 raw noon reports have been collected from 6 ships.

Data transformation is performed to obtain the required parameters. This includes the steps and formulas 8.1 to 8.10.

$$\nabla[t] = \frac{\text{DWT} + \text{lightweight}}{\rho \times 1000} \tag{8.1}$$

$$V_S = \frac{\text{log distance}}{\text{sailing period}} \tag{8.2}$$

$$T_{mean} = \frac{T_{aft} + T_{fwd}}{2} \tag{8.3}$$

Formulas 8.4 to 8.6 show the transformation from absolute wind, sea and swell direction in compass directions (N-NNE-NE etc.) to the direction relative to the ship in degrees, with a range of 0.1 to 360. It is assumed that the effect of wind, sea and swell from portside is equal to that of starboard side. Therefore, the directions with an angle greater than 180 degrees, are mirrored to an equivalent direction.

$$\text{Wind, sea or swell direction [deg]} = \begin{cases} 0, \text{ if direction} = \text{N} \\ 22.5, \text{ if direction} = \text{NNE} \\ (...) \\ 337.5, \text{ if direction} = \text{NNW} \end{cases} \tag{8.4}$$

$$\alpha_{360}[deg] = \text{Wind direction} - \text{Heading} \tag{8.5}$$

$$\alpha, \mu, \beta[deg] = \chi[deg] = \begin{cases} \chi_{360} + 360, \text{ if } -360 \leq \chi_{360} < -180 \\ \chi_{360} - 2 \times \chi_{360}, \text{ if } -180 \leq \chi_{360} < 0 \\ \chi_{360}, \text{ if } 0 \leq \chi_{360} < 180 \\ \chi_{360} - 2 \times (\chi_{360} - 180), \text{ if } 180 \leq \chi_{360} < 360 \end{cases} \tag{8.6}$$

$$\text{Days from propeller polishing } N = \text{Current date} - \text{Date propeller polishing} \tag{8.7}$$

$$\text{Days from last propeller polishing} = \begin{cases} \infty, \text{ if days from propeller polishing} < 0 \text{ (penalty function)} \\ \text{MIN(Days from propeller polishing } N), \text{ if days from propeller polishing} \geq 0 \end{cases} \tag{8.8}$$

A similar procedure can be followed to determine the days since last hull cleaning. However, for all C-38 vessels no hull cleaning has been performed yet. Therefore the date of last hull cleaning is equal to the delivery date from the yard. Then formula 8.9 is used.

$$\text{Days from last hull cleaning} = \text{Current date} - \text{Date last hull cleaning} \tag{8.9}$$

Furthermore, trim is calculated using formula 1.1, the propulsive power according to the Admiralty (P_{adm}) coefficient using formula 3.1.

To calculate the displacement, the water density is required as well, which is not recorded in the noon report data. The sea water density is approximated by a regression formula as a function of sea temperature, based on data from 26th ITTC Specialist Committee on Uncertainty Analysis (2011) (see figure C.1 in the appendix) as shown in formula 8.10.

$$\rho = -0.0047 \times Temp_{sea}^2 - 0.0752 \times Temp_{sea} + 1028.2 \tag{8.10}$$

The quality of the raw data can be described with table 8.2, which shows the number of zeros and blank fields, and the number of unrealistic values. The following remarks can be made:

- The reported speed over ground is not recorded in 66% of the noon reports. However, this should be the same as the speed over ground calculated with the observed distance and the sailing period. Both parameters are considered accurate: the observed distance is determined by GPS and the sailing period is 23, 24 or 25 hours in most of the times (23 or 25 when the ship crosses a longitudinal). Sailing hours exceeding 25 hours or less than 23 hours correspond to noon reports which include a few hours of port departure or arrival, or activities such as maintenance, where the sailing period are rounded to 0.5 or 1 hours. Since these reports correspond to unusual operations and may introduce noise due to rounding, these reports are not included. This approach is preferred since it represents an average speed over ground, while the reported speed over ground can be perceived by the crew as the on-the-spot speed over ground.

- The current velocity is recorded as "0" for roughly half of the noon reports. It is difficult to evaluate in which case there was no current present and in which case the current is not recorded. An alternative is to use the logged distance through the water and the reporting period, to calculate the ship speed through the water. The log instrument provides the distance and speed through the water based on the Doppler effect, with an accuracy of 0.01 $\frac{m}{s}$ (Furuno, 2010).

- The sea temperature is not recorded in 385 cases, corresponding to 13% of the noon reports. Sea temperature is required in both WBMs, to approximate the water density and kinematic viscosity.

- The sea condition is recorded in two ways: sea state and sea height. It is found that sea state is recorded in most cases, while sea height is often left blank or zero. Therefore, it is chosen to use the sea state as the parameter to describe the sea condition.

- Similar to the sea condition, the swell condition is usually recorded by swell state, rather than swell height. It is chosen to use sea swell as the parameter to describe the swell condition.

- Taking into account the above mentioned approaches, 414 noon reports contain unreported data entries, of which in 385 cases the water temperature is missing.

- Taking into account the above mentioned approaches, 658 noon reports contain unrealistic data entries, of which in 376 cases the reporting period is less than 23 hours.

8.2.2. Noise identification, data imputation and data cleaning

Noise identification is performed by using table 8.2, considering the remarks in the noon reports and by comparing the power with the estimated power according to the Admiralty coefficient.

When possible, empty data fields in the noon reports are imputed. Data imputation is performed for:

- Sea temperature: Missing temperatures have been interpolated for 116 noon reports;

- Air temperature: For 1 noon report, air temperature was missing, but could be imputed by interpolating the air temperatures of the day before and after;

- If the entry of wind, sea or swell direction is empty or "NA", while the wind force, sea state or swell state is zero as well, respectively, north direction "N" is assigned. This is done for 5 noon reports.

Remaining data is cleaned by deleting complete noon report entries with empty fields or unrealistic data, as defined by table 8.2. In this step, 913 noon reports are deleted. Additionally, remarks of the noon reports are considered. When a cause for noise in the report is observed, for example a man overboard drills, testing, main engine maintenance or a mismatch in described sea conditions and reported sea conditions. This resulted in deleting 8 more noon reports.

Table 8.2: **Quality of raw noon report data.**

Noon report entry	Zero/blank	Unrealistic value	Specification
Actual DWT	56	150	97% of actual DWT should be less than max DWT
Ordered speed	0	0	More than 16 kn
Reported speed	1929	0	More than 16 kn
Observed distance	0	0	More than 384 nm (more than 16 kn on average for 24 h)
Log distance	1	0	More than 384 nm (more than 16 kn on average for 24 h)
Sailing period	0	376	Less than 23 h or more than 31 h (noon report boundaries)
Forward draft	0	0	More than 12 m
Aft draft	3	0	Less than 6.5 m (propeller immergence)
Engine speed	0	2	More than 100 rpm (max engine speed)
Shaft power	0	8	Engine power for propulsion and shaft generator power more than 7900 kW (total installed engine power)
Heading	0	0	More than 360 degrees
Current velocity	1423	2	More than 4 kn
Current direction	-	7	Zero while current speed is not zero
Air temperature	1	1	More than 45 degrees Celsius
Sea temperature	385	2	More than 35 degrees Celsius
Wind force	5	0	More than 12 Bf
Wind direction	-	19	Blank or "NA" while wind force is not zero
Sea state	0	1	Sea state zero while sea height is not zero
Sea height	-	1286	Sea height zero while sea state is not zero
Sea direction	-	55	Blank or "NA" while sea state is not zero
Swell state	0	12	Sea swell state zero while swell height is not zero
Swell height	0	952	Swell height zero while sea swell state is not zero
Swell direction	-	23	Zero while sea swell is not zero

Furthermore, outliers are identified by comparing the actual (recorded) shaft power with the estimated shaft power using the Admiralty coefficient, as can be seen in figure D.1 for all weather conditions and in figure D.2 for calm water conditions. The outliers indicate impossible data entries, possibly by entering wrong shaft power recordings or wrong weather conditions. Twelve noon reports are deleted in total in this step.

Also, a scatter plot is made, showing the displacement for each mean draft. These two variables are closely related, and will only vary a little as an effect of trim and water density. Therefore outliers indicate that either the draft of the load (and hence displacement) is wrongly entered. Inspection of the individual noon reports showed that a missing final number could be a reason. As can be seen in figure D.3, five noon reports are deleted.

The result is a cleaned dataset, consisting of 1988 noon reports. In total, 935 noon reports have been deleted. Based on this cleaned data, histograms and boxplots are made, which show the operational profile of the ship class as a whole, which is used to determine the boundaries of the fuel model. The frequency histogram of the trim conditions is shown in figure 8.2. This figure shows that in most cases (58%) the ship sails at a (near) fully loaded condition, while other load conditions are sailed less frequently. At this condition, most trim conditions have been sailed, but noon reports with trim by bow are scarce. At other draft conditions, the ship is trimmed to the stern more often, which can be explained by the weight distribution of the ship. The remaining variables in appendix B. Outside these boundaries, the results are based on a small number of data points and extracted using extrapolation. The combination of the WBM with the neural network improves the extrapolation qualities, but should be considered carefully. The boundaries of the GBM are defined as following:

- $11.5 \le V_S \le 14.5$;

- $1 \le$ wind force ≤ 7;

- $1 \le$ sea state ≤ 6;

- swell state ≤ 6;

- $-0.375 <$ trim ≤ 2.0, for $T_{mean} > 9.5$;

- $0.375 <$ trim ≤ 1.875, for $8.5 < T_{mean} \le 9.5$;

- trim > 0.625, for $7.5 < T_{mean} \le 8.5$;

- trim > 0.375, for $6.5 < T_{mean} \le 7.5$;

- for $T_{mean} > 9.5$ represents 58% of the noon reports, while other mean draft conditions are less represented.
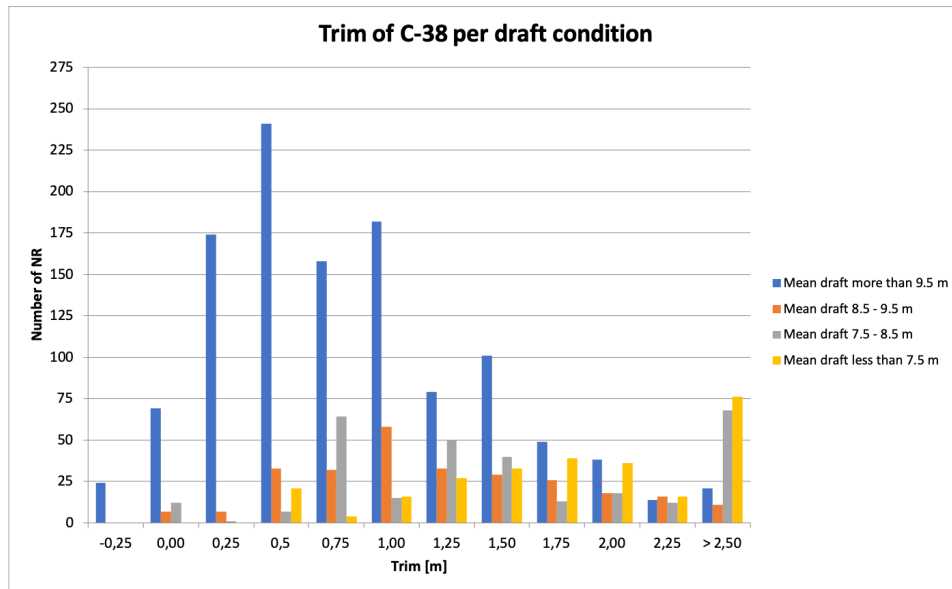
Figure 8.2: Frequency histogram of trim in metres for relevant draft conditions.

8.2.3. Data selection, feature selection and data normalization

Two datasets have been made, as defined in paragraph 7.3.8. For the all weather dataset, the boundaries as defined in paragraph 8.2.2 are valid without further limitations. The boundaries of the calm water dateset is smaller, as can be seen with figure 8.3 and 8.4.

Figure 8.5 illustrates how many noon reports are within a combination of sea- and swell states. Noon reports that comply with the calm water conditions, are shown in the upper-left box.

	Trim	≤ 2,00	1,75	1,50	1,25	1,00	0,75	0,50	0,25	0,00	-0,25	-0,50
Mean draft		303	126	198	224	273	260	302	367	88	14	11
6,5	42	16	2	3	12	7	2	0	0	0	0	0
7,0	127	56	24	19	5	5	0	18	0	0	0	0
7,5	180	67	12	15	43	3	35	4	1	0	0	0
8,0	266	25	4	23	9	9	8	5	183	0	0	0
8,5	207	46	13	35	45	24	24	1	7	12	0	0
9,0	140	20	21	1	30	31	22	14	0	1	0	0
9,5	135	1	10	25	5	12	13	50	11	8	0	0
10,0	406	49	16	35	54	78	14	88	51	10	3	8
10,5	662	22	24	42	21	104	142	122	114	57	11	3
11,0	1	1	0	0	0	0	0	0	0	0	0	0

Figure 8.3: Surface plot of trim occurrences per mean draft of the dataset for all weather conditions.

Besides filtering on sea- and swell state for the calm water dataset, both datasets are filtered on reporting time. The sailing time should not be more than 25 hours ($T_{sail} \ge 25$). This way, all noon reports that reflect a beginning of a voyage are filtered out, since it is likely that a number of reported parameters have been

Trim		2,00 or less	1,75	1,50	1,25	1,00	0,75	0,50	0,25	0,00	-0,25	-0,50
Mean draft		118	37	70	53	89	86	97	111	44	2	5
6,5	12	5	1	0	3	3	0	0	0	0	0	0
7	36	18	4	7	1	1	0	5	0	0	0	0
7,5	60	16	2	4	14	3	20	0	1	0	0	0
8	86	9	2	6	2	5	2	5	55	0	0	0
8,5	62	15	6	16	7	6	10	0	2	0	0	0
9	43	10	10	1	6	9	6	1	0	0	0	0
9,5	49	1	0	9	1	2	4	23	8	1	0	0
10	141	28	10	12	13	24	4	34	8	4	1	3
10,5	222	15	2	15	6	36	40	29	37	39	1	2
11	1	1	0	0	0	0	0	0	0	0	0	0

Figure 8.4: Surface plot of trim occurrences per mean draft of the dataset for the calm water conditions.

varying more than usual. Together with the sailing time constraint, the calm water dataset contains 674 noon reports, while the dataset representing all weather- and sea conditions contains 1954 noon reports.

Swell state		0	1	2	3	4	5	6	7	8	9
Sea state	1988	351	290	259	420	398	189	51	20	10	0
0	4	1	1	0	1	1	0	0	0	0	0
1	12	7	3	2	0	0	0	0	0	0	0
2	232	82	63	68	11	4	2	1	1	0	0
3	769	176	158	136	233	51	14	0	0	1	0
4	624	65	60	40	136	250	65	6	0	2	0
5	263	14	5	13	38	76	89	19	7	2	0
6	69	5	0	0	1	13	16	23	8	3	0
7	14	1	0	0	0	3	3	2	4	1	0
8	1	0	0	0	0	0	0	0	0	1	0
9	0	0	0	0	0	0	0	0	0	0	0

Figure 8.5: Cleaned dataset divided into groups of sea- and swell states. The upper-left box highlights the selected group of noon reports, which corresponds to a sea state up to and including 3 and a swell state up to and including 2 on the scale of Douglass.

The results of the Spearman rank correlation can be found for both data sets in figure 8.6 and 8.7. Besides for the feature selection, the correlation matrix can be used to investigate data quality and provide an indication of the effect of the variables on shaft power. The correlation matrix is analysed for expected and unexpected correlations. However, as described in paragraph 3.2, this method is not sufficient to make conclusions regarding the effect of the variables on required shaft power, since the effect of the variables can not be isolated from each other. A number of correlations and both expected and unexpected results are considered.

- A third order relation between ship speed and required power may be expected, and therefore also a correlation between these factors. For calm water conditions, such a correlation is actually found between ship speed and shaft power. For the all weather data set however, this relation is not found. The ship is operated using an engine power that does not significantly vary within a small range. The speed that is reached, is not only a result of this engine setting, but of weather and sea conditions as well. In rough conditions, speed will vary more than in calm water conditions, which explains the difference between the correlation found in both data sets.

- The correlation between trim and shaft power in calm water conditions is -0.020, indicating that no real correlation exists. It is known that the effect on trim on shaft power will be in the order of a few percents, as described in paragraph 1.2, therefore this small number is in line with the expectation. Moreover, it illustrates why it is hard to quantify the effect of trim on required power by simple regression methods, as was investigated in paragraph 3.2.

- Days from last hull cleaning and propeller polishing has a positive correlation with shaft power, as expected.

	Shaft power	Displacement	Ship speed	Draft	Trim	Air temp	Sea temp	Windforce	Sea state	Swell state	Wind direction	Sea direction	Swell direction	Hull fouling	Propeller polishing
Shaft power	1,000	0,119	0,072	0,110	-0,072	-0,217	-0,199	0,202	0,192	0,129	-0,125	-0,108	-0,117	0,206	0,211
Displacement	0,119	1,000	-0,236	0,958	-0,509	0,068	0,026	-0,009	-0,018	0,006	-0,005	0,021	-0,014	0,095	0,099
Ship speed	0,072	-0,236	1,000	-0,225	0,044	0,263	0,233	-0,337	-0,403	-0,397	0,270	0,183	0,189	-0,099	-0,053
Draft	0,110	0,958	-0,225	1,000	-0,485	0,047	-0,005	-0,022	-0,031	-0,003	0,003	0,021	-0,018	0,062	0,099
Trim	-0,072	-0,509	0,044	-0,485	1,000	-0,037	-0,031	-0,031	-0,004	-0,028	0,009	-0,004	0,040	-0,147	-0,028
Air temp	-0,217	0,068	0,263	0,047	-0,037	1,000	0,903	-0,323	-0,335	-0,258	0,033	0,047	0,001	-0,068	-0,101
Sea temp	-0,199	0,026	0,233	-0,005	-0,031	0,903	1,000	-0,270	-0,290	-0,234	-0,004	0,015	-0,001	-0,027	-0,054
Windforce	0,202	-0,009	-0,337	-0,022	-0,031	-0,323	-0,270	1,000	0,811	0,476	-0,076	-0,063	-0,058	0,073	0,078
Sea state	0,192	-0,018	-0,403	-0,031	-0,004	-0,335	-0,290	0,811	1,000	0,589	-0,107	-0,088	-0,093	0,038	0,037
Swell state	0,129	0,006	-0,397	-0,003	-0,028	-0,258	-0,234	0,476	0,589	1,000	-0,055	-0,045	-0,068	-0,011	-0,011
Wind direction	-0,125	-0,005	0,270	0,003	0,009	0,033	-0,004	-0,076	-0,107	-0,055	1,000	0,674	0,485	-0,020	0,043
Sea direction	-0,108	0,021	0,183	0,021	-0,004	0,047	0,015	-0,063	-0,088	-0,045	0,674	1,000	0,624	-0,010	0,061
Swell direction	-0,117	-0,014	0,189	-0,018	0,040	0,001	-0,001	-0,058	-0,093	-0,068	0,485	0,624	1,000	-0,047	0,025
Hull fouling	0,206	0,095	-0,099	0,062	-0,147	-0,068	-0,027	0,073	0,038	-0,011	-0,020	-0,010	-0,047	1,000	0,343
Propeller polishing	0,211	0,099	-0,053	0,099	-0,028	-0,101	-0,054	0,078	0,037	-0,011	0,043	0,061	0,025	0,343	1,000

Figure 8.6: Spearman rank correlation for all weather conditions.

	Shaft power	Displacement	Ship speed	Draft	Trim	Air temp	Sea temp	Windforce	Sea state	Swell state	Wind direction	Sea direction	Swell direction	Hull fouling	Propeller polishing
Shaft power	1,000	0,097	0,354	0,102	-0,020	-0,176	-0,173	0,114	0,082	-0,007	-0,088	-0,043	-0,075	0,170	0,197
Displacement	0,097	1,000	-0,291	0,960	-0,468	0,055	-0,022	0,088	0,111	0,112	-0,037	0,061	-0,003	0,111	0,012
Ship speed	0,354	-0,291	1,000	-0,291	-0,027	0,120	0,117	-0,013	-0,054	-0,153	0,145	0,054	0,007	0,015	0,038
Draft	0,102	0,960	-0,291	1,000	-0,478	0,030	-0,065	0,064	0,084	0,111	-0,030	0,084	-0,010	0,070	0,011
Trim	-0,020	-0,468	-0,027	-0,478	1,000	-0,094	-0,046	-0,092	-0,040	-0,033	0,091	0,010	0,060	-0,161	0,029
Air temp	-0,176	0,055	0,120	0,030	-0,094	1,000	0,878	-0,175	-0,212	-0,054	0,022	-0,026	-0,057	0,026	-0,035
Sea temp	-0,173	-0,022	0,117	-0,065	-0,046	0,878	1,000	-0,150	-0,174	-0,050	-0,040	-0,071	-0,045	0,040	0,011
Windforce	0,114	0,088	-0,013	0,064	-0,092	-0,175	-0,150	1,000	0,518	0,003	-0,029	-0,039	0,026	0,060	0,029
Sea state	0,082	0,111	-0,054	0,084	-0,040	-0,212	-0,174	0,518	1,000	0,007	-0,056	-0,040	0,040	0,024	0,034
Swell state	-0,007	0,112	-0,153	0,111	-0,033	-0,054	-0,050	0,003	0,007	1,000	0,071	0,076	0,080	0,063	-0,019
Wind direction	-0,088	-0,037	0,145	-0,030	0,091	0,022	-0,040	-0,029	-0,056	0,071	1,000	0,607	0,329	-0,029	0,005
Sea direction	-0,043	0,061	0,054	0,084	0,010	-0,026	-0,071	-0,039	-0,040	0,076	0,607	1,000	0,472	-0,019	0,040
Swell direction	-0,075	-0,003	0,007	-0,010	0,060	-0,057	-0,045	0,026	0,040	0,080	0,329	0,472	1,000	-0,012	0,004
Hull fouling	0,170	0,111	0,015	0,070	-0,161	0,026	0,040	0,060	0,024	0,063	-0,029	-0,019	-0,012	1,000	0,293
Propeller polishing	0,197	0,012	0,038	0,011	0,029	-0,035	0,011	0,029	0,034	-0,019	0,005	0,040	0,004	0,293	1,000

Figure 8.7: Spearman rank correlation for calm water conditions.

- Wind force, sea- and swell state have a negative correlation on speed.

Regarding feature selection, the following is observed:

- Displacement and (mean) draft are strongly correlated to each other (+0.958), as may be expected. Draft is what is directly reported, whereas displacement is based on an estimation using the load, lightweight of the ship and water density (approximated using sea water temperature). Draft is therefore preferred as input for the neural network. The (estimation of) displacement will be used as well, since this is a required variable for the WBMs.

- Air temperature and sea water temperature are strongly correlated as well (+0.903). Moreover, a negative correlation is found between air and sea water temperature and wind force, sea- and swell state, being a bit stronger for the air temperature. This indicates that an increase in (air or sea) temperature is correlated to a decrease in wind force and sea- and swell state. Air temperature is considered as the most redundant variable between the two and not used in training the ANN. Although sea temperature is a redundant variable as well, this variable was selected initially. A trained fuel model was used to evaluate the effect of sea water temperature on shaft power. The effect of sea water temperature was extracted by keeping all variables constant, except for the sea water temperature. The result is shown in

figure 8.8. It is found that the effect of sea water temperature on shaft power is much bigger than may be expected. The exaggerated effect can be explained by the found correlation between colder sea water temperatures with more severe weather conditions. This verifies that sea water temperature is a redundant variable. However, a trained network without sea water temperature as input, is at least 0.19 % less accurate, consistently for multiple network topologies, as can be seen in table 8.3, in which the network performance of a number of network topologies is shown, with and without sea water temperature as input variable. It is concluded that sea water temperature is a redundant variable with wind force, sea- and swell state, but does provide the network additional information that improves the accuracy. Sea water temperature is therefore included in the input variables.

- Wind force and sea state are strongly positively correlated as well (+0.811). However, looking to the correlation between the direction of wind and sea, the correlation is less strong (+0.674). Moreover, the effect of direction will be different as well. Following wind will be favourable, while this may not be necessarily true for waves. Since the combined effect of magnitude and direction will be different, both wind and waves are considered in training the ANN.

Based on the data quality and Spearman rank analysis, the following features are selected: mean draft, ship speed (through water), trim, wind force, sea state, swell state, wind direction, sea direction, swell direction, days since last hull cleaning and days since last propeller cleaning.

Data normalization is performed by Matlab with the 'mapminmax' function similar to the Thales theorem of 6.13.
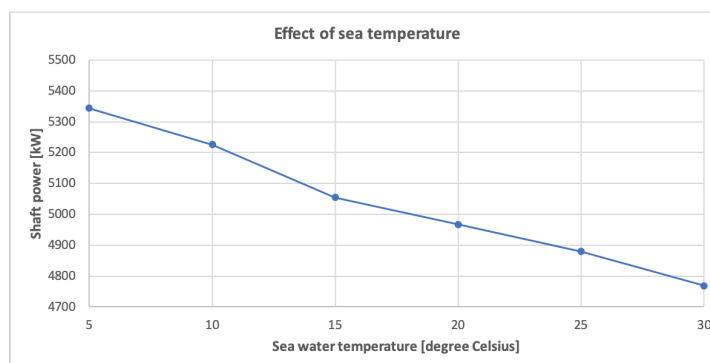
Figure 8.8: Effect of sea water temperature in shaft power.

Table 8.3: **network performance of a number of network topologies, with and without sea water temperature as input variable.**

	With sea water temperature		Without sea water temperature	
nr. of neurons	Relative error [%]	Standard deviation	Relative error [%]	Standard deviation
9	6.65	0.462	6.84	0.413
12	6.60	0.444	6.84	0.516
15	6.66	0.425	6.86	0.486

8.3. Speed-power curves of WBMs

Speed-power plots of the noon report data of the final two data sets and the estimations using both PLK and PHM as WBM, are shown in figure 8.9 and figure 8.10. It is clear that both WBMs assume an exponential relationship between speed and power, while the actual noon report data show that the speed is more a result of engine setting and weather conditions, as was concluded from the results of the correlation between speed and shaft power in the Spearman Rank analysis as well.

The goal of the WBM is to estimate the calm water power requirement; the increase in required shaft power due to added resistance is considered by the BBM. It is observed that the PHM model over-estimates the required power for calm water conditions significantly, and to a lesser extent the PLK model as well, especially for the higher speed region above 13 knots. A correction factor to tune the power estimation of the PLK model can provide more realistic results. The effect of such a factor on the accuracy of the GBM will be investigated. However, first the optimal network topology using the initial estimation of the PHM model is found in section 8.4.
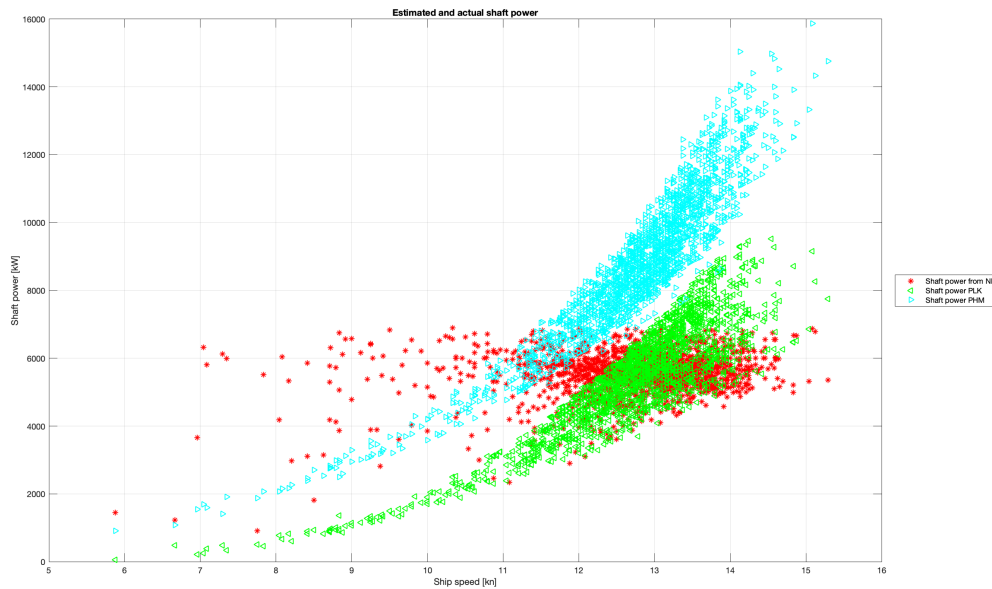
Figure 8.9: Speed-power curves using the all weather data set, showing the actual shaft power from the noon reports and the estimated shaft power using the both WBMs.

Figure 8.10: Speed-power curves using the calm water data set, showing the actual shaft power from the noon reports and the estimated shaft power using the both WBMs.

8.4. Network topology

The total number of input parameters of the neural network is 13, with one output. The Fletcher-Gloss method of formula 6.1 is used as a guideline, which results in a range of number of neurons n_1 of $9 \leq n_1 \leq 27$. For the pure BBM, where the result of the WBM is excluded, the range is $8 \leq n_1 \leq 25$. The performance of the three variants of fuel models 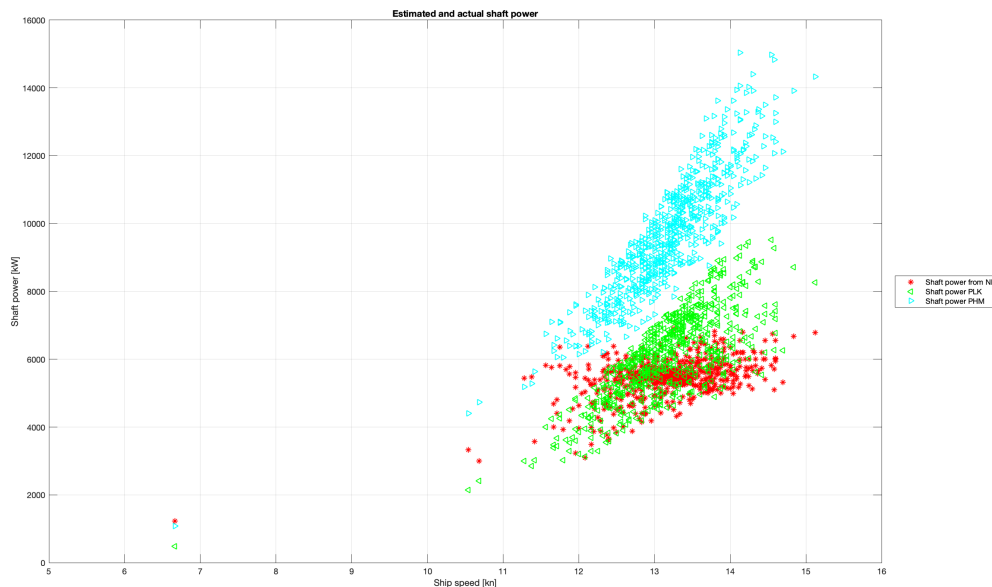are investigated for a range of number of hidden layers and a range of neurons on each layer, both within and outside the range of the Fletcher-Gloss method. The performance of these different topologies are tested on:

- Accuracy, by means of the relative error between the estimated and actual shaft power (formula 7.3);

- Stability, by means of the standard deviation between the relative errors of all k trained neural networks.

The results are shown in figure 8.11a, 8.11b and 8.11c. Full tables of the model performance is presented in appendix E. The best performing topology considering both the accuracy and the stability, is shown in table 8.4. The performance is also determined when using the calm water data set. Speed-power plots on a fixed test set is shown in figure 8.12 for the all weather and calm water data set for the three variants of the fuel model.

Table 8.4: **Performance of fuel model, for the calm water and all weather conditions dataset, using the optimal network topology.**

Model variant	Best topology	All weather data set		Calm water data set	
		RE %	STD	RE %	STD
GBM - PHM	1 x 18	6.62	0.431	5.74	0.486
GBM - PLK	1 x 15	6.58	0.452	5.86	0.581
BBM	1 x 27	6.63	0.417	5.83	0.507

Based on the results of the topologies for the different models, the following is concluded:

- In most cases, the use of one hidden layer provides a more accurate and more stable networks than a network with two hidden layers. Both the average relative error and the standard deviation of the relative errors of each training iteration is generally smaller.

- Considering the speed-power curves, multiple hidden layers tend to limit the variability in estimated shaft power. Network topologies with three of four hidden layers tend to saturate and cluster estimations to an average value and sometimes even provides one single value.

- For GBM - PHM, the network topology with one hidden layer with 18 neurons, performs best when considering both the average relative error and the standard deviation. For GBM - PLK, a network topology of one hidden layer with 15 neurons in it performs the most accurate. The pure BBM performs best with a network topology of one hidden layer with 27 neurons. However, the exact number of neurons is not critical for performance.

- The differences in performance between the three models are very small. A significant difference is only observed for the calm water dataset, where the GBM - PHM model performs slightly more accurate compared to the GBM - PLK and the pure BBM.

- All three graphs in figure 8.11 have the same trend in average relative performance. The range of the Fletcher-Gloss method generally includes or the best performing topologies. The optimal number of neurons for the topology of the pure BBM is an exception, which should have a few more nuerons than approximated.
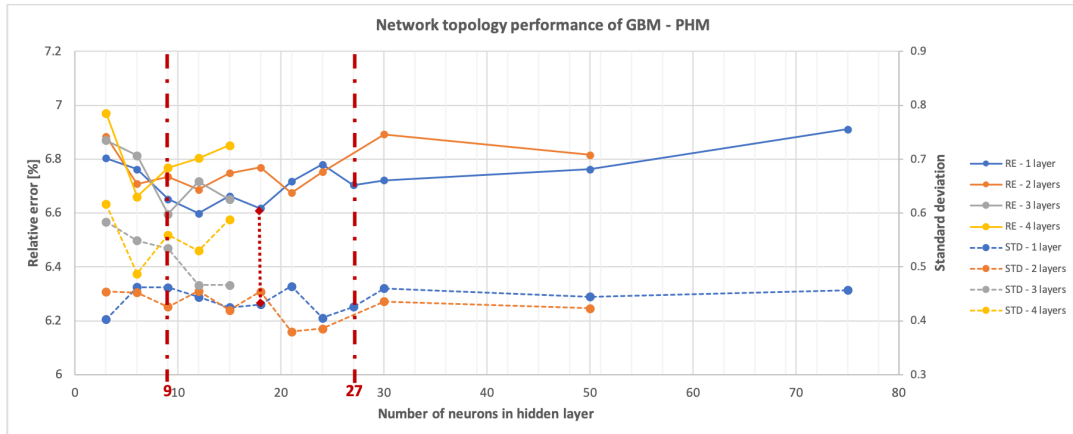
(a) Topology performance of GBM - PHM.
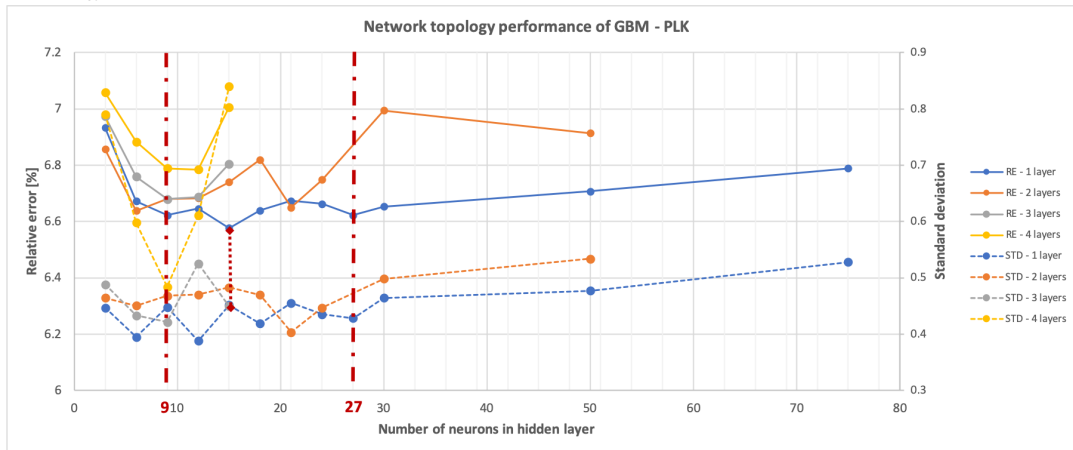
(b) Topology performance of GBM - PLK.
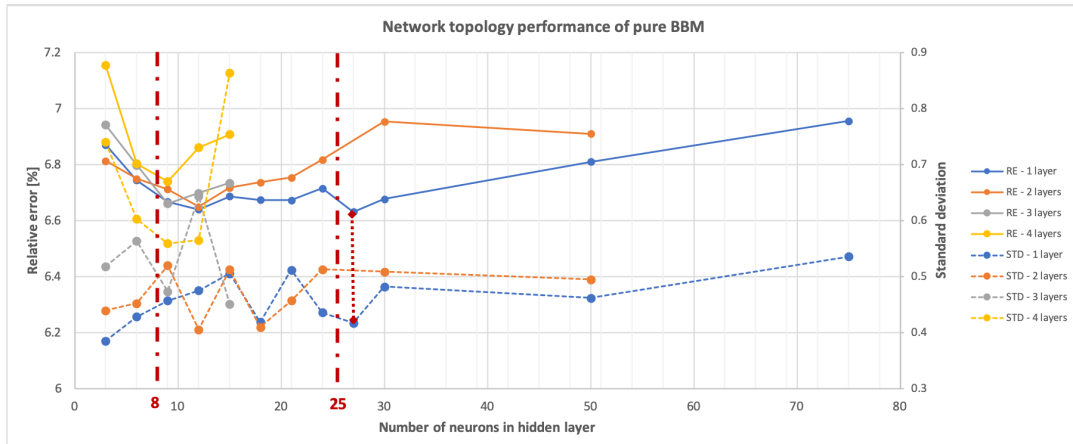
(c) Topology performance of BBM.

Figure 8.11: Performance of different network topologies of the (a) GBM using PHM as WBM, (b) GBM using PLK as WBM and (c) a pure BBM. The x-axis shows the number of neurons in the hidden layer(s). The left y-axis shows the relative error (RE) between the estimated and actual required shaft power in %, the right axis shows the standard deviation of the relative error over all k training repetitions.

8.5. Effect of tuning PHM

The power estimation using the PHM model is tuned with static and speed-dependant factors (speed through water, measured in knots). The result is shown in table 8.5. It is found that tuning the model has a negligible to no effect, even when the correction factor is exaggerated. This can be explained with the working principle of the neural network. During the training of the neural network, a weight factor is attributed to the input, as well as the (complex) relationship with other nodes in the neural network.

Table 8.5: **Effect of tuning PHM on the accuracy of GBM - PHM on estimating shaft power.**

PHM · factor	RE of GBM - PHM [%]	Standard deviation
PHM · 1.0 (benchmark)	6.62	0.431
PHM · 0.4	6.69	0.465
PHM · 0.5	6.69	0.452
PHM · 0.6	6.60	0.452
PHM · 0.7	6.65	0.465
PHM $\cdot speed^{1/4}$	6.65	0.459
PHM · 0.01	6.68	0.460
PHM · 100	6.65	0.483
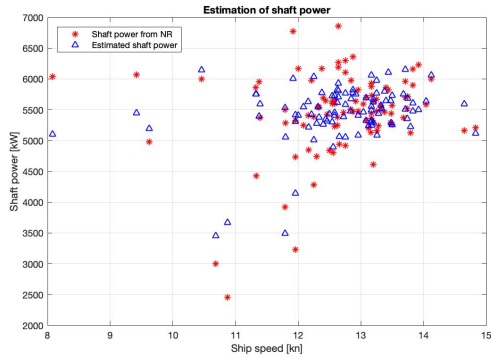
(a) All weather conditions, GBM-PHM.
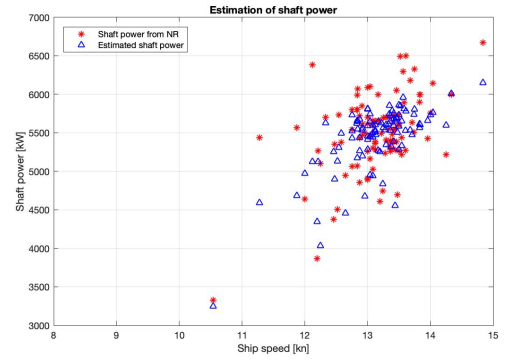
(b) Calm water conditions, GBM-PHM.
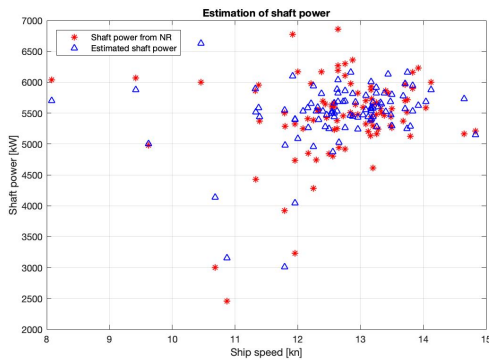
(c) All weather conditions, GBM-PLK.
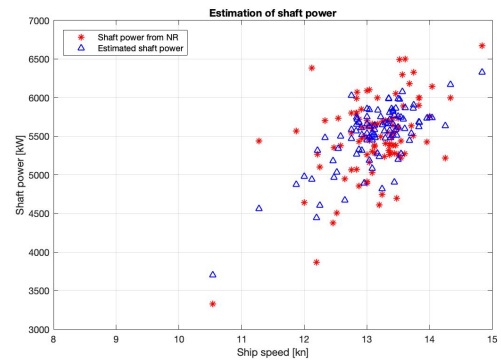
(d) Calm water conditions, GBM-PLK.
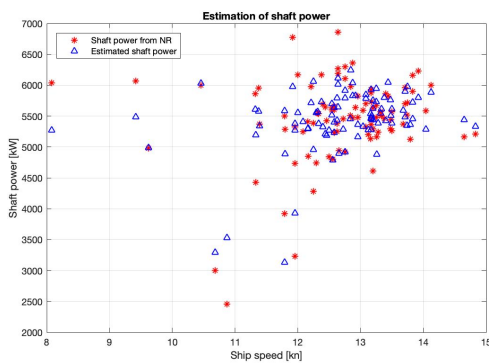
(e) All weather conditions, pure BBM.
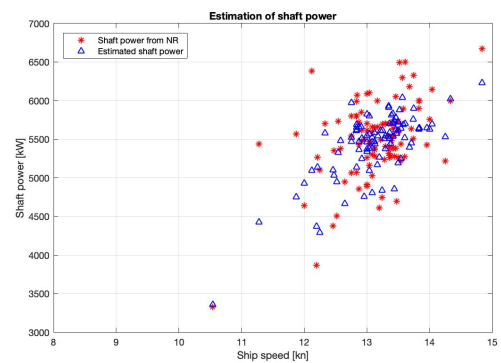
(f) Calm water conditions, pure BBM.

Figure 8.12: Speed power curves of three variants of the fuel model (GBM-PHM, GBM-PLK and the pure BBM), using a fixed test set of both the all weather dataset (left) and calm water dataset (right). The x-axis shows the speed in knots, the y-axis shows the shaft power in kW.

9

Case study results

Results of the fuel model for the C38 ship class are analyzed and validated in this chapter.

9.1. Effect of trim on required shaft power

Three variants of the fuel model (GBM - PHM, GBM - PLK and a pure BBM) have been constructed and can estimate the required shaft power for a given set of operational parameters and weather conditions. Trim tables can be generated by varying trim and keeping other parameters constant. An example trim table is generated in figure 9.1, for a voyage condition with the input parameters of table 9.1.

Table 9.1: **Input parameters for generated trim table.**

Stolt Loyalty			
Speed	13 knots	**Sea condition**	3 Douglas - head direction
Load (DWT)	35000 t	**Swell condition**	2 Douglas - beam direction
Water temperature	25 $^\circ C$	**Last hull cleaning**	892 days (3.3 years)
Wind condition	4 Bf - head direction	**Last propeller cleaning**	54 days

Considering the boundaries of the model based on the operational profile of the ship class (see paragraph 8.2.2, the lower part of the trim table of figure 9.1 (mean draft of 9.5 m and more) is represented by the most significant part of the historical noon report data. The results for these mean draft conditions are therefore considered to be the most reliable. Trim conditions on the upper right part of the table (boundary is marked with dotted line) are never recorded in the noon report data, causing the model to extrapolate. In the grey area 100% propeller immersion cannot be ensured in calm water. To avoid severe impact loads on the propeller blades due to propeller emmergence, these conditions should be avoided. Due to ship motion and waves, draft conditions around this region is and should be avoided as well.

The optimal trim condition for a range of load conditions and speeds is found by figure 9.2. In this figure, trim from -0.5 m to +2.0 m, draft from 6.50 m to 10.60 m and speed from 11 knots (bottom) to 14 knots (top) are considered. The moderate weather conditions are represented by wind force 4 Beaufort and sea- and swell state 4 on the scale of Douglas, in this case all in opposite direction of the ship's heading. In general, trim by bow decreases the required shaft power for all conditions. Increase in weather conditions has no effect on the location of the optimal trim.

Draft [m]	Trim (Ta-Tf) [m]											PD [kW]
	2,00	1,75	1,50	1,25	1,00	0,75	0,50	0,25	0,00	-0,25	-0,50	
(even keel)												(even keel)
6,50	199	174	150	125	100	75	50	25	0			4807
6,60	198	174	149	125	100	75	50	25	0			4827
6,70	196	172	148	123	99	74	50	25	0			4865
6,80	196	172	148	123	99	74	50	25	0	-25		4884
6,90	195	171	147	123	99	74	50	25	0	-25		4903
7,00	195	171	147	123	99	74	50	25	0	-25		4921
7,10	195	171	147	123	99	74	50	25	0	-25	-50	4939
7,20	195	171	147	123	99	74	50	25	0	-25	-50	4957
7,30	195	171	147	123	99	74	50	25	0	-25	-50	4974
7,40	195	171	147	123	99	74	50	25	0	-25	-50	4991
7,50	195	171	147	123	99	74	50	25	0	-25	-50	5008
7,60	195	171	147	123	99	74	50	25	0	-25	-50	5024
7,70	195	171	147	123	99	74	50	25	0	-25	-50	5040
7,80	195	171	147	123	99	74	50	25	0	-25	-51	5055
7,90	195	171	148	123	99	75	50	25	0	-25	-51	5070
8,00	195	172	148	124	99	75	50	25	0	-25	-51	5085
8,10	196	172	148	124	99	75	50	25	0	-25	-51	5100
8,20	196	172	148	124	100	75	50	25	0	-25	-51	5114
8,30	197	173	149	124	100	75	50	25	0	-25	-51	5127
8,40	197	173	149	125	100	75	50	25	0	-25	-51	5141
8,50	198	174	150	125	101	76	51	25	0	-26	-51	5154
8,60	198	174	150	126	101	76	51	25	0	-26	-51	5166
8,70	199	175	151	126	101	76	51	26	0	-26	-52	5179
8,80	197	174	150	125	101	76	51	26	0	-26	-52	5236
8,90	198	174	150	126	101	76	51	26	0	-26	-52	5248
9,00	199	175	151	127	102	77	51	26	0	-26	-52	5259
9,10	200	176	152	127	102	77	52	26	0	-26	-53	5270
9,20	201	177	153	128	103	77	52	26	0	-26	-53	5280
9,30	202	178	153	128	103	78	52	26	0	-26	-53	5290
9,40	203	179	154	129	104	78	52	26	0	-27	-53	5299
9,50	204	180	155	130	104	79	53	26	0	-27	-53	5309
9,60	205	181	156	131	105	79	53	27	0	-27	-54	5318
9,70	207	182	157	131	105	79	53	27	0	-27	-54	5326
9,80	208	183	158	132	106	80	53	27	0	-27	-54	5335
9,90	209	184	159	133	107	80	54	27	0	-27	-54	5343
10,00	210	185	159	134	107	81	54	27	0	-27	-55	5350
10,10	212	186	160	134	108	81	54	27	0	-27	-55	5358
10,20	213	187	161	135	109	82	55	27	0	-28	-55	5365
10,30	214	189	162	136	109	82	55	28	0	-28	-55	5371
10,40	216	190	163	137	110	83	55	28	0	-28	-56	5378
10,50	217	191	164	138	111	83	56	28	0	-28	-56	5384
10,60	219	192	166	138	111	84	56	28	0	-28	-56	5390
								stern trim		bow trim		

Figure 9.1: Example of a generated trim table for a speed of 13 knots, considering dynamic factors as weather and fouling of hull and propeller. The marked region in the upper left of the table, indicates that the results are extrapolated. In the grey area 100% propeller immersion cannot be ensured in calm water.

The effect of trim on shaft power, the optimum trim value and the potential on shaft power reduction by trim for calm water conditions, as indicated by the fuel model, is shown in figure 9.3 for two mean draft conditions and speeds of 12, 13 and 14 knots. These model results show that the required shaft power is minimized by bow trim, with a linear effect between trim and shaft power. Depending on the speed and load condition, between 1% and 2% in shaft power can be saved with a change in trim of 0.50 m.
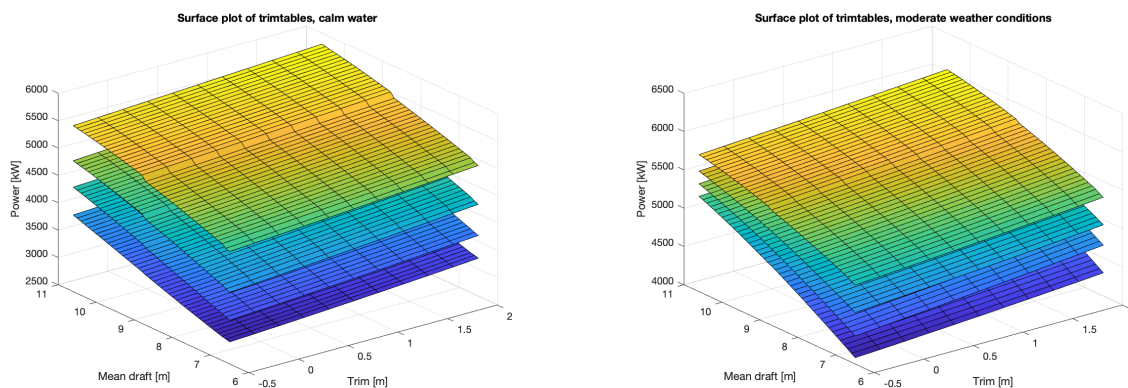
(a) Surface plot of trim tables for calm water.

(b) Surface plot of trim tables for moderate weather conditions.

Figure 9.2: Surface plot of trim tables for two different weather conditions, for a speed of 11 knots (bottom) to 14 knots (top), showing the location of optimal trim for draft conditions between 6.50 m and 10.60 m.
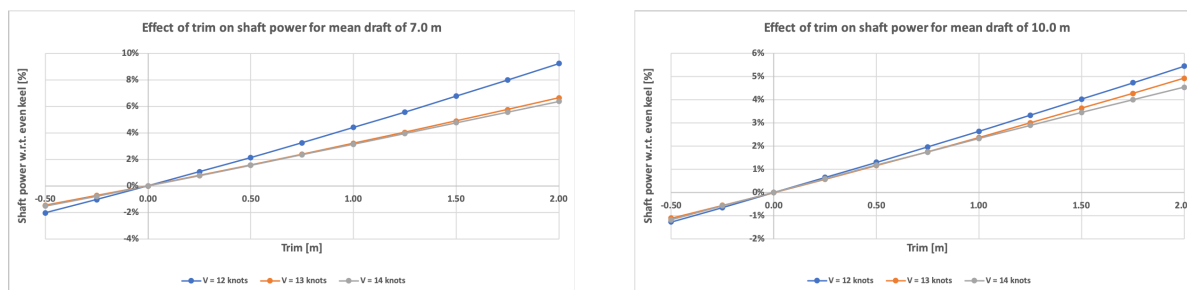
(a) Effect of trim on shaft power for a mean draft of 7.0 m.

(b) Effect of trim on shaft power for a mean draft of 10.0 m.

Figure 9.3: Effect of trim on shaft power for two mean draft conditions. A linear effect between trim and shaft power is found. Trim by bow reduces the required shaft power.

9.2. Effect of other variables on shaft power

One of the drawbacks of using a black- or grey box modelling approach, is the limited model interpretability. This can be improved by considering the effect of other input parameters one-by-one and remain other parameters fixed.

The effects of other input parameters than trim on shaft power as extracted by the fuel model, are shown in figure 9.4, 9.5 and 9.6. The extracted effects are valid for a speed of 13 knots, a mean draft of 10.0 m, a seawater temperature of 25 $°C$ and no effects of weather and fouling.

For calm water conditions, an exponential function between speed and power exists, as may be expected. An increase in weather conditions has a significant effect on the power demand for all speeds, consistent with the correlation as found in the Spearman rank analysis. However, the trend of the effect of speed in moderate weather conditions causes problems. The higher speed region (of ca. 8 knots and more) in moderate weather conditions, deviates from what would be expected. In off-design conditions, the slope of the speed-power curve would increase for all speeds. The fuel model results show differently: increasing the speed with one knot, would require only a little bit more power. It is concluded that the power and fuel consumption estimations in non-calm water conditions provide wrong results.

The effect of draft on required shaft power shows a realistic effect. For drafts more than 6.5 m and for a fixed speed, an increase in draft will result in a near linear increase in wetted surface and displaced volume.

The effect of days since last hull cleaning is smaller than expected, when compared to described effect
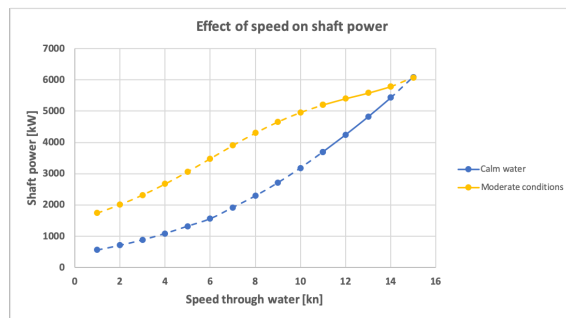
(a) Effect of speed on shaft power. The dotted line represent results based on model extrapolation.
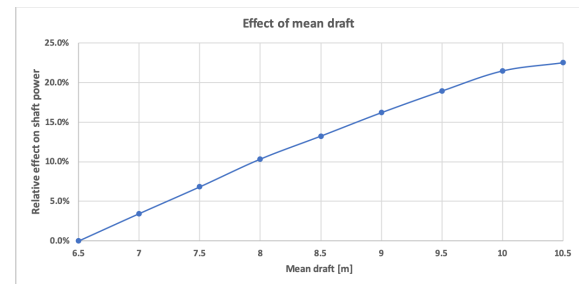
(b) Effect of mean draft on shaft power.

Figure 9.4: Effect of speed and draft on shaft power.
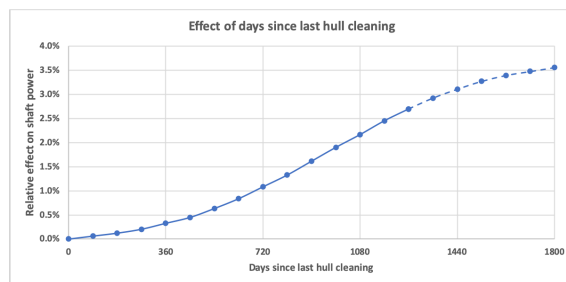
(a) Effect of days since last hull cleaning on shaft power. The dotted line represent results based on model extrapolation, since noon report data is collected up to 3.5 years from last hull cleaning.
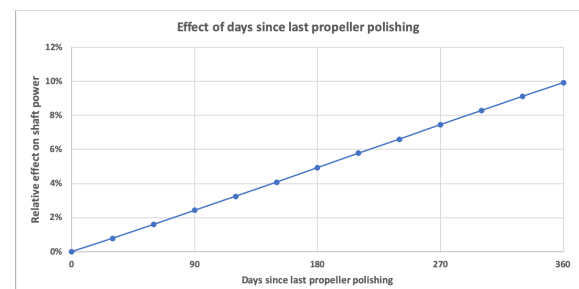
(b) Effect of days since last propeller polishing on shaft power.

Figure 9.5: Effect of fouling factors on shaft power.

of Uzun et al. (2019). A possible reason can be that hull fouling can not be modelled by days since last hull cleaning only, meaning that this parameter only contributes partly to hull fouling. According to Uzun et al. (2019), the rate of different types of hull fouling is depending on the geographical location as well. That would mean that the fouling degree of particular ships in the fleet deviates from the curve of figure 9.5a, while the curve shows the average effect among all six ships. Also, it could be that the anti-fouling on the ship's hull is more effective than average.

The effect of days since last propeller cleaning on required power is significant. Due to the high tangential speeds of the propeller blades, a small degree of propeller fouling may already cause undesired cavitation and a significant loss in propulsion efficiency.

The effects of weather conditions are counter-intuitive in some aspects. Generally, an increase in wind force or sea- or swell state increases the required shaft power. However, a following strong wind is expected to be more beneficial than a weaker wind. An explanation can be found in the Spearman rank correlation analysis of figure 8.6. Wind force is correlated to sea- and swell state, meaning that a stronger wind will come together, to a limited degree, with higher sea and swell conditions. The results therefore show that the model attributes no increase in power due to the combined effects represented by a following wind with wind force 6 Bf.

The effect of sea- and swell conditions from different relative directions are counter-intuitive as well. Every time a wave is encountered, the ship's speed will drop, causing an additional power demand to maintain a certain speed. In following waves, the wave encounter frequency is likely to drop, therefore the additional power demand is expected to be less than in head seas. A potential reason could be that the steering pilot has difficulties keeping a steady course in following sea conditions, causing an increase in rudder actions and rudder angle. Following waves are defined as waves with an angle within 22.5 degrees relative to the ship's heading, so a lateral component exists as well. This potential reason can be validated in further research by
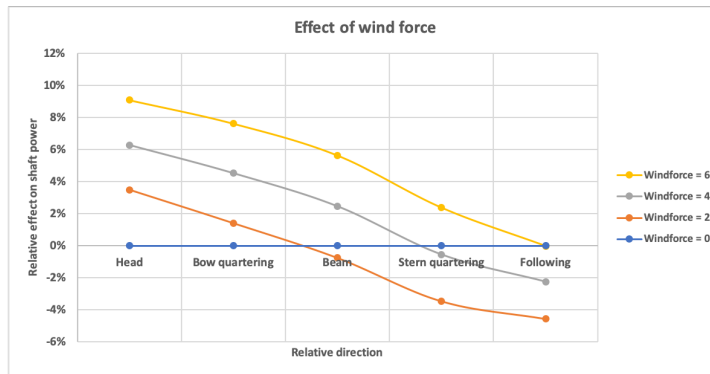
(a) Effect of wind force and direction on shaft power.
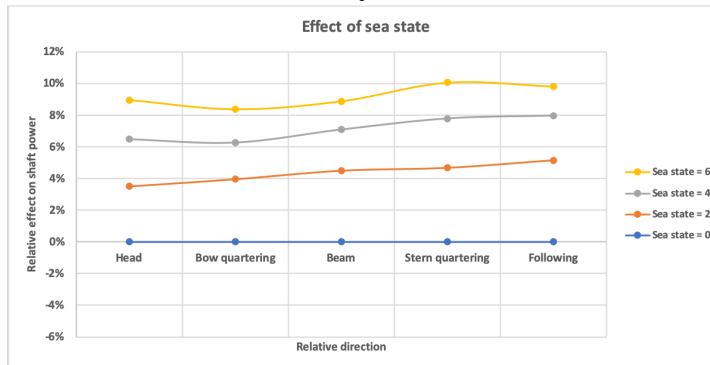
(b) Effect of sea state and direction on shaft power.
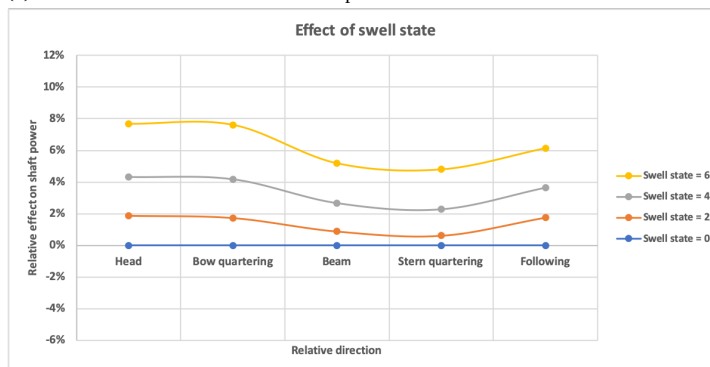
(c) Effect of swell state and direction on shaft power.

Figure 9.6: Effect of weather factors on shaft power.

crew experience or by measuring the rudder actions in various sea conditions.

Besides the effect of trim, these other effects can be validated by sea trials.

9.3. Model validation

9.3.1. Description of performed sea trials for validation

Three sea trials are performed by three different ships. The sea trial results are included in appendix H.

The first sea trial is performed at a (near) full load condition, with a mean draft of about 10.45 m and with trim conditions in the range of -0.50 m to +0.50 m, with steps of 0.25 m. Trimming is done by adding ballast water, therefore each mean draft condition and displacement is different for each tested trim condition. Next to that, trim conditions of +0.25 m and +0.50 are done in slightly stronger winds and slightly higher sea state.

The second sea trial is performed in part load condition, with a mean draft of 7.0 m. Measured trim conditions vary from -0.50 m to +2.0 m, in steps of 0.50 m. The ship is trimmed by shifting ballast water, therefore keeping the displacement similar. Overall weather conditions are on the limit of preset boundaries in which the experiment should be performed.

Another sea trial is performed at full load condition, with a mean draft of 10.55 m, but for a stern trim of +0.50 m only. Therefore the effect of trim can not be extracted, but the results show a similar relationship between speed and power compared to the other sea trials for a trim condition of +0.50 m.

9.3.2. Initial results of the fuel model for sea trial conditions

The fuel model is used to estimate the required shaft power for each test condition in the sea trials in which multiple trim conditions are tested. The results are shown in figure 9.7 for the first sea trial and in figure 9.8 for the second sea trial. Model results are shown in two ways as defined in section 7.7. The averaged conditions used as input for the fuel model is shown in table 9.2.

Table 9.2: **Averaged fixed parameters of both sea trials, used for model input to generate trim tables.**

	Stolt Loyalty	**Stolt Integrity**
Local date	19/04/2020	01/05/2020
Heading [deg]	300	58
Sea temperature [deg Celsius]	30	22
Wind force [Beaufort]	2	4
Wind direction	NW	SE
Sea state [Douglas]	2	3
Sea direction	NW	SE
Swell state [Douglas]	2	2
Swell direction	SW	E

9.3.3. Observations of sea trial results

Performance of model variants

The results of the model variant GBM-PLK and the pure BBM perform very similar in both sea trial conditions. On a marginal level, the GBM-PLK shows a trend with a steeper slope for the first sea trial conditions, which is closer to the sea trial results than the trend of the BBM. Results of the GBM-PHM for the first sea trial, shows a weaker relationship between trim and power and for speeds of 11, 12 and 14 knots, an opposite trend is observed for the first sea trial.

Trend in trim on power

A clear trend is found in the results of the first sea trial, showing that an increase in trim cause an increase in required shaft power, despite the additional ballast water to achieve forward trim. Fuel model results show as well that the effect of trim is bigger than the effect of the small increase of mean draft due to additional ballast water (see figure 9.7b). A similar trend with smaller magnitude is found between trim and power by the fuel model. Regarding the first sea trial, on average a decrease in power of 64 kW is found when the ship is trimmed from even keel to 0.5 m bow trim, which corresponds to 1.3 %. Sea trial results confirm that bow trim is optimal, with a similar trend, but with a much bigger magnitude. Depending on speed, between approximately 6% and 8% in required shaft power can be saved with a change in trim of 0.50 m. More specifically, the sea trial results for a speed of 13 knots, show that trimming from even keel to 0.5 m forward trim results in a decrease of 423 kW, which corresponds to a decrease of 8.2 %. The difference in power for stern trim conditions (stern trim of 0.25 m and 0.50 m) may be exaggerated, due to an increase in weather parameters. This increase is visible in the model output as well.

A much smaller effect of trim in power is found in the second sea trial for a mean draft of 7.0 m. In zero
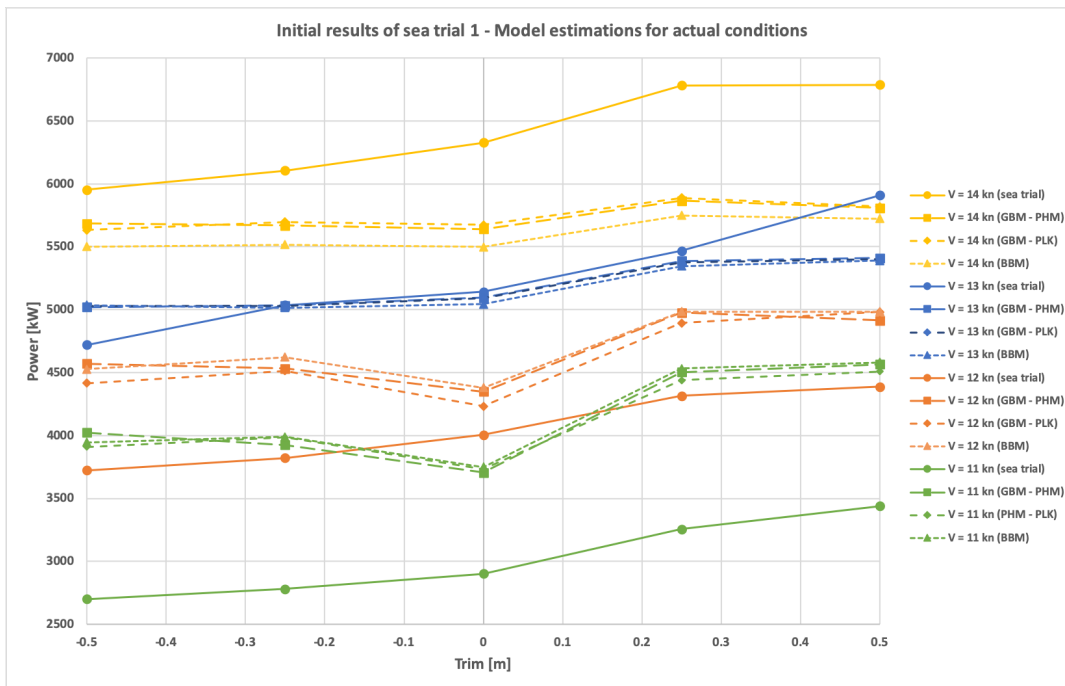
(a) First sea trial. Results of the fuel model with estimations of shaft power for every trial condition, compared with sea trial results.
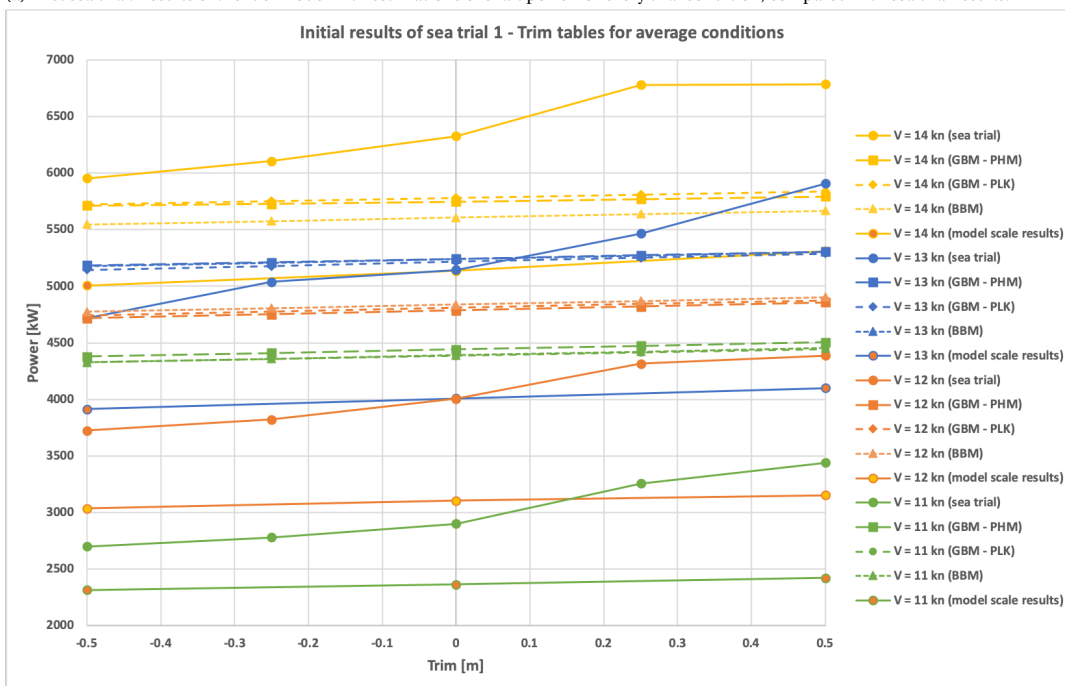
(b) First sea trial. Results of generated trim tables for averaged conditions, compared with sea trial results and the results known from model scale towing tests.

Figure 9.7: Initial results for the first sea trial with a mean draft of about 10.45 m (varies per trim condition).

noon reports, a stern trim of 0.25 m, even keel or bow trim for a mean draft of 7.0 m is recorded, meaning that the model is extrapolating for the data points of even keel and 0.5 m bow trim for this sea trial. As can be seen in figure 9.1, propeller immergence cannot be ensured for these trim conditions. The model nevertheless performs consistent with the sea trial results. Although less historical noon reports are available for this draft condition, it should be sufficient to represent the effect of trim on power for the stern trim conditions. However, the model performs worse compared to the first sea trial. A maximum is found for 1.0 m stern trim for speeds of 11, 12 and 13 knots and for 1.0 m and 1.5 m stern trim for a speed of 11 knots. In the
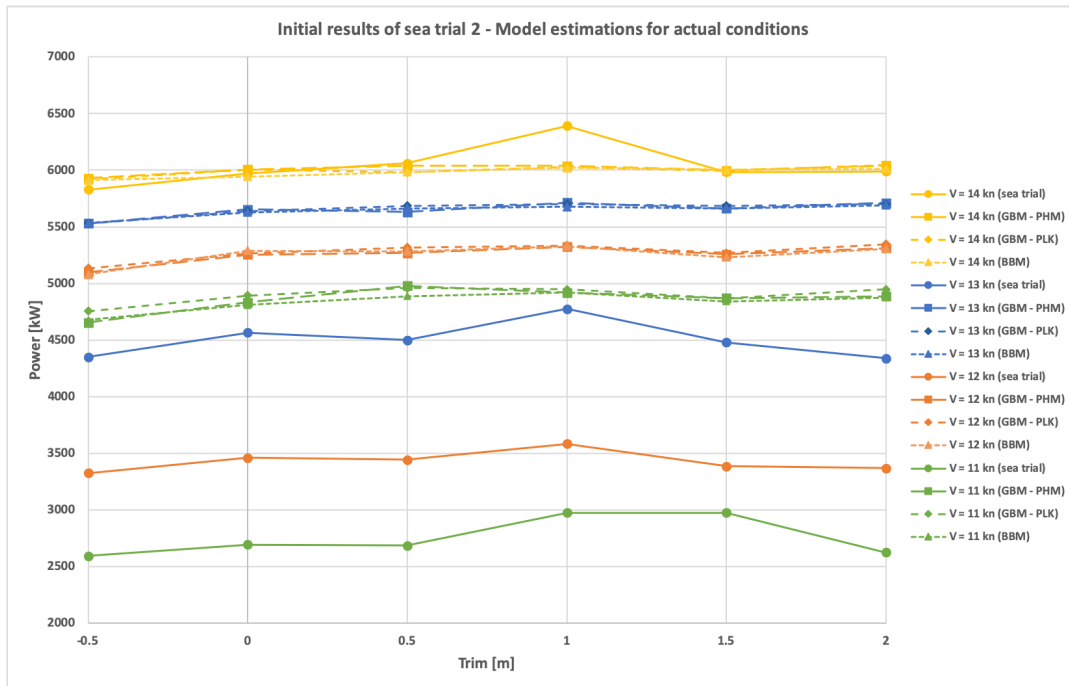
(a) Second sea trial. Results of the fuel model with estimations of shaft power for every trial condition, compared with sea trial results.
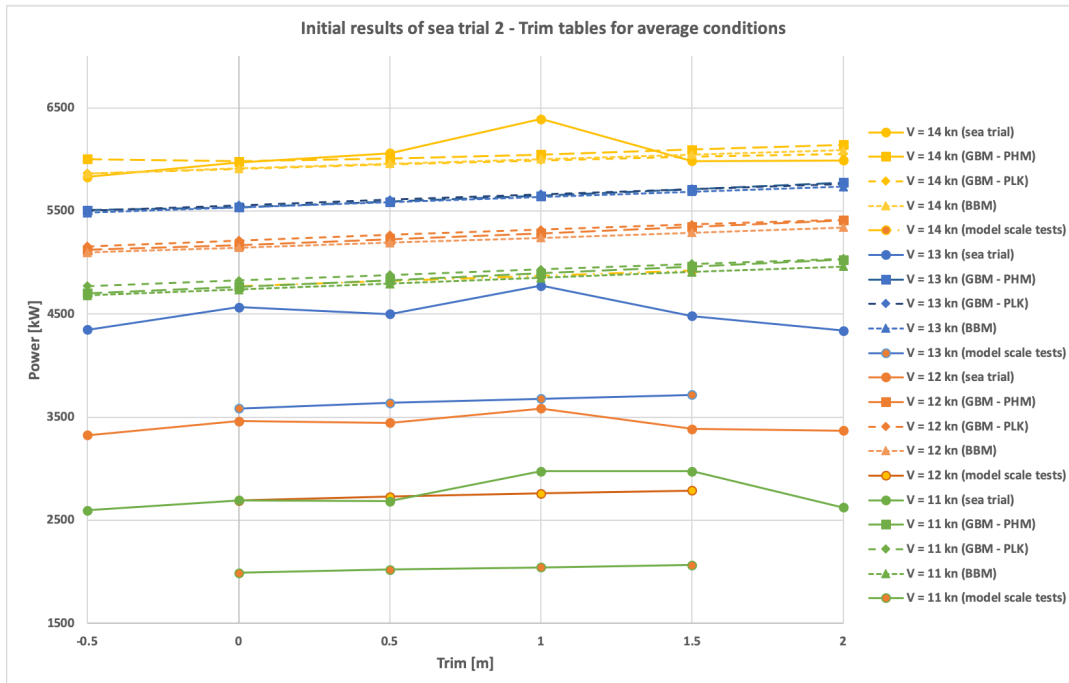
(b) Second sea trial. Results of generated trim tables for averaged conditions, compared with sea trial results and the results known from model scale towing tests.

Figure 9.8: Initial results for the second sea trial with a mean draft of 7.0 m.

sea trial conditions, it is seen that the wind force was 5 Beaufort for this condition, instead of 3 or 4 Beaufort for other trim conditions. This peak in power is not as clearly visible in the model results. Also, the decrease in power visible in the sea trial results for a trim of 2.0 m, is not seen in the model output. This local minimum is not visible in the trim tables based on model scale towing tests. A second sea trial can confirm if this local minimum is due to trim effects or other effects.

Structural deviations between fuel model and sea trial results

In the first sea trial, a local minimum in power is clearly observed at even keel for speeds of 11 and 12 knots, which is not present in the sea trial results. This condition is specified with very calm water conditions with less displacement compared to the bow trim conditions, which could be a reason for this local minimum. Also, the clear drop of the power observed in the sea trial results for a speed of 13 knots and for a trim of -0.5 m in respect to -0.25 m, is not visible in the model results.

The trend between trim and power from the fuel model is similar for all mean drafts, whereas sea trial results and model scale towing tests show different magnitudes of the trend and a possible different trend for a mean draft of around 8.50 m. This indicates that the fuel model trend is averaged for all draft conditions, instead of a unique trend per draft condition. Since the majority of recorded draft conditions are for 9.5 m and more, it could be that the trend for this draft condition is (partly) extrapolated to other draft conditions. A solution could be to perform a model experiment, by training the neural network with noon reports for a limited range of draft conditions, for example ballast load, part load and full load. Additionally, sea trials at a mean draft condition of 8.50 m help to understand the effect of trim on power for this draft region.

Only a small difference in shaft power is seen between the trendlines for different speeds. As was expected based on figure 9.4a, weather factors dominate the power estimation, causing that the effect of speed on shaft power is unrealistically embedded by the model. For a full load condition, the model estimates the power correctly for a speed of 13 knots. For the part load condition in the second sea trial, the model estimates the power correctly for a speed of 14 knots.

In the noon report data, a significant part of the lower speed recordings still have a high shaft power, as can be seen in figure 8.9. Moreover, a weak correlation between speed and power was found in the Spearman rank correlation analysis (see figure 8.6). The speed that is reached, is a result of the engine speed and propeller pitch ratio and of the weather and sea conditions, causing some relatively high power recordings in the noon reports at lower speeds.

The effect of the engine and propeller settings on shaft power and speed is specified as follows. The C38 ship class has a CPP and a shaft generator. A prerequisite for the shaft generator to provide power for auxiliary systems, is a fixed shaft frequency (fixed RPM). As a consequence, when the ship is to sail at a lower speed while using the shaft generator, the P/D ratio of the CPP is decreased to decrease the delivered thrust, while remaining the same sailing speed. This may have an effect on the propeller efficiency, causing a lower speed for equal required shaft power. This effect can be approximated by considering a typical open water diagram, as shown in figure 9.9a. From this figure, it can be observed that when the P/D ratio decreased, the K_T curve shift vertically downwards and the curve of the open water propeller efficiency significantly changes. Additionally, the propeller curve is plotted as well, following formula 9.1 of Kuiper and Bernaert (2002). Considering that the ship sailing speed will decrease, the delivered thrust T and the advance velocity V_A will decrease, causing the advance ratio J (see formula 4.12) to decrease, since the propeller speed n and diameter will remain fixed. The slope of the propeller curve will change, as both T and V will decrease. Considering that $T \sim R$ and $R \sim V^2$, while ρ and the n remain fixed, it is likely that the slope of the propeller curve will increase. Two different scenarios are considered in figure 9.9b. The curves in red represent the reference curves for an example speed of 13 knots. The blue curves represent a sailing condition with a reduced P/D ratio, decreased sailing speed but with the fixed propeller speed. As described, the K_T curve shifts downwards, the curve of the open water efficiency changes, the slope of the propeller curve increases and J decreases. The results show that the hypothetical open water propeller efficiency can drop from 65% to 55%. This illustration explains that the decrease in propeller efficiency can be significant when the ship is sailing at reduced speed by reducing the P/D ratio and remain a fixed shaft speed in order to use the shaft generator. This explains that in some cases, the recorded shaft power at lower speeds are still higher than may be expected by just the propeller law. It furthermore shows that recording the P/D setting of the CPP, and using it as an input variable of the fuel model, may increase the accuracy.

Although this report focuses on shaft power estimation and assumes a fixed specific fuel consumption of the engine to approximate the fuel consumption, decreasing sailing speed by decreases the P/D ratio only, cause to increase the specific fuel consumption. This effect is illustrated in figure 9.10. Assuming point *1* as reference point, the operating point will shift to point *2* when using the combinator mode, meaning that both the shaft speed and the P/D ratio is changed. When the same speed is to be obtained with fixed shaft speed as

required to run the shaft generator, the operating point will shift to point *3*. The specific fuel consumption in point *3* is higher than in point *2*, illustrating the additional adverse affect on fuel consumption when reducing speed with fixed shaft speed.

$$\frac{K_T}{J^4} = \frac{T n^2}{\rho V^4} \tag{9.1}$$
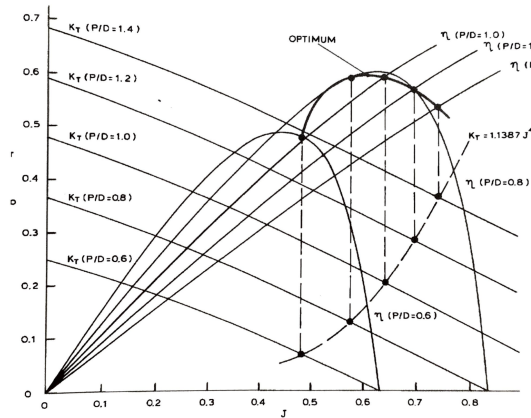
(a) Typical open water propeller diagram, showing the open water propeller efficiency for two different P/D ratios (Kuiper and Bernaert, 2002). The x-axis represents the advance velocity J and the y-axis represents the values of K_T, $10 K_Q$ and η_O.
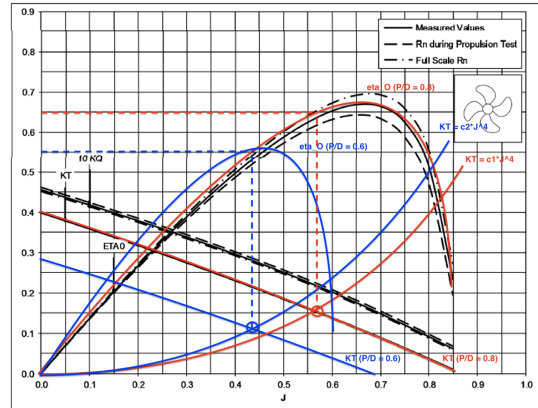
(b) Actual open water propeller diagram of the C-38 ship class. The reference condition is shown in red, the sailing condition at reduced sailing speed at fixed propeller speed and lower P/D ratio is shown in blue. Coloured lines represent examples only.

Figure 9.9: Possible effect of decreasing the sailing speed by decreasing the P/D ratio on the propulsion efficiency.
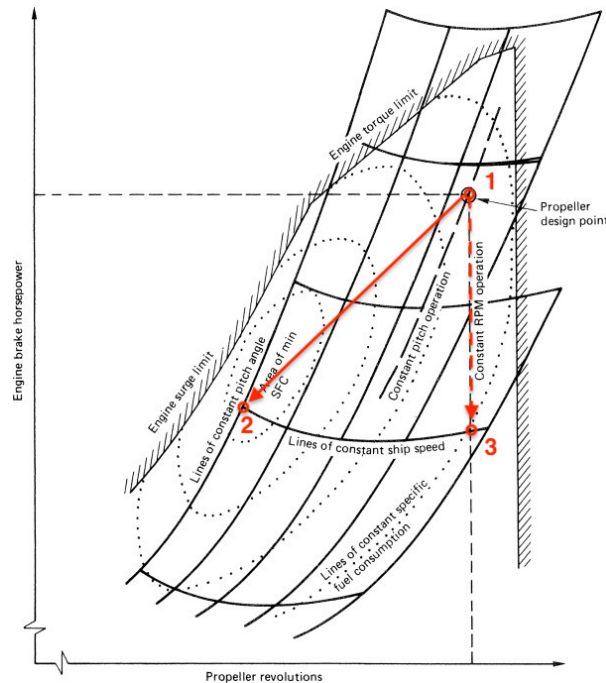
Figure 9.10: Typical controllable pitch propeller characteristic curve. Based on Carlton (2018).

Additionally, draft and trim conditions are not always updated daily in the noon reports. This is illustrated in figure 3.8 for two consecutive voyages and concluded from contact with ship's crew in the survey (see appendix F). This causes multiple (different) power recordings for the same draft and trim condition. Therefore, the effect of trim on power as extracted by the fuel model, may show an averaged trend between trim and power.

Other errors in the noon report or sea trial data may cause errors in the model performance. These errors include: (i) the mismatch between average shaft power and snapshot of weather conditions, heading; and (ii) the human error in estimating and recording weather conditions and operational parameters (for example actual shaft power instead of day-average shaft power).

Another reason for differences between model and sea trial results can be that the model does not include a parameter, which has a significant effect on shaft power or other input parameters.

9.3.4. Suggested calibration of model

It is observed that the model systematically underestimates the effect of speed on power for 11 to 14 knots, especially in non-calm water conditions. Model calibration can be done by translating the power estimations vertically, without changing the shape of the trends between trim and power. The result of this calibration will be a more realistic model output, which improves the ability to compare model and sea trial results.

A requirement to calibrate the model results to more realistic results, will be sea trials. These sea trials should conduct power measurements for a range of speeds, without the need of varying trim conditions.

To illustrate the effect of model calibration, the sea trial results of all three sea trials are used. All three sea trials have conducted power measurements at a trim condition of 0.5 m stern trim. The difference between the effect between speed and power of the sea trials and of the model is determined in figure 9.11. The speed calibration is done for both draft conditions, as it was observed in full load condition the model results were realistic for a speed of 13 knots, whereas for small mean draft conditions the model results were realistic for 14 knots. The resulting trend lines are the basis for the calibration table (see table I.1) which can be used to translate the model results for a range of speed and mean draft conditions. Mean draft conditions of 7.0 and 10.5 m has been used as references, linear interpolation is used to generate the table values for other mean draft conditions.
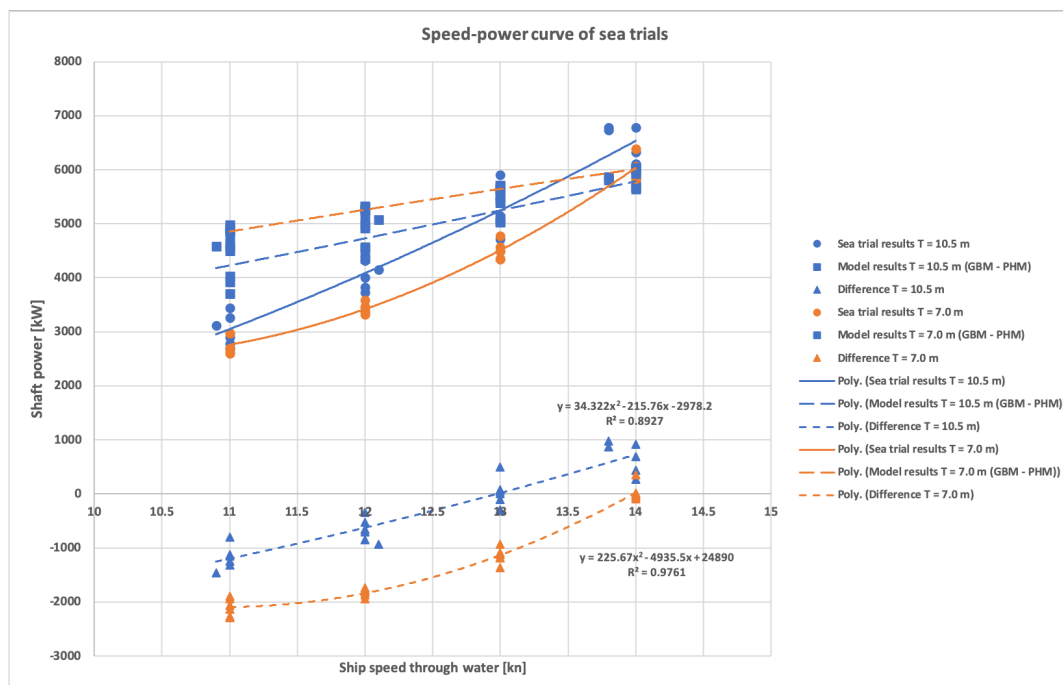
Figure 9.11: Speed-power curves of both the model and sea trial results. The difference is used to calibrate the model results to more realistic values, without changing the shape of the trend.

9.3.5. Final results (to be validated)

Results of the fuel model and generated trim tables compared to the sea trial results are shown in figure 9.12. Model output now shows more realistic values, however the trend as found in the initial results remain unchanged.

The calibration from initial model results to realistic values is to be validated with more sea trials. However, the goal of this calibration is to improve the practical use of the model output by calibrating the model output to more realistic values.
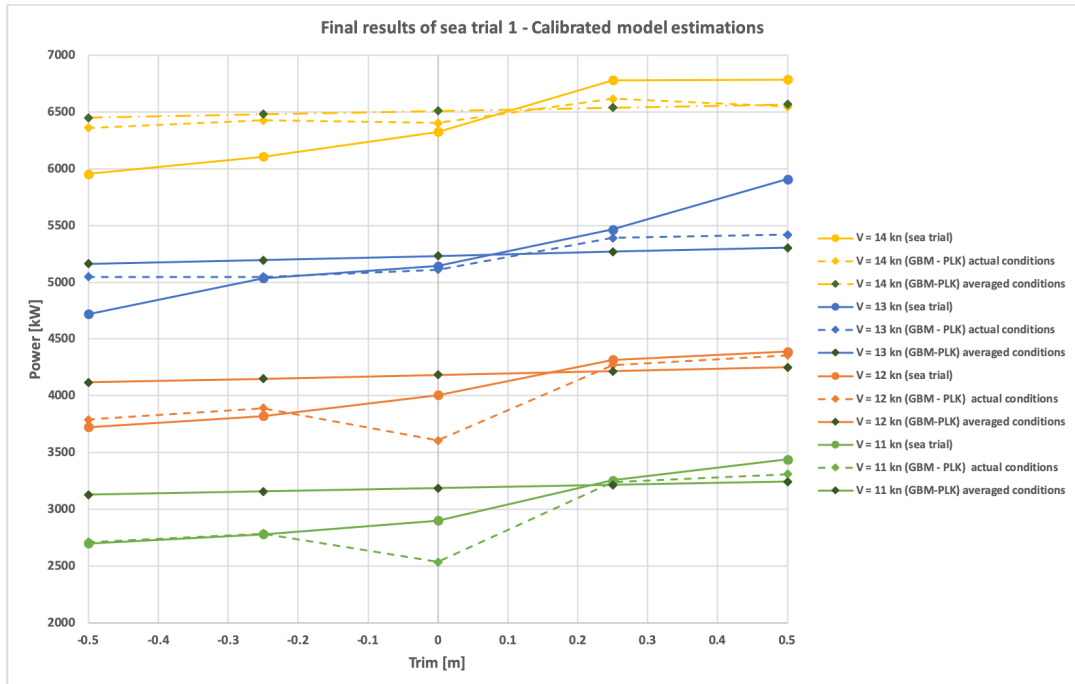
(a) Results for the first sea trial.
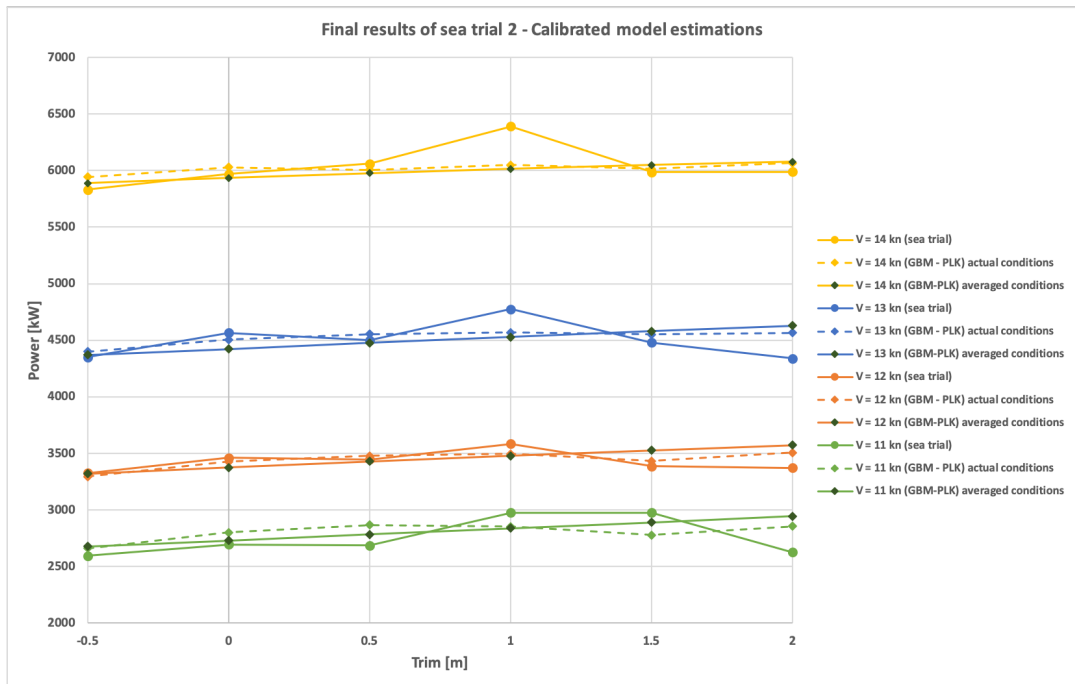
(b) Results for the second sea trial.

Figure 9.12: Calibrated model results and sea trial results for both sea trials.

9.4. Performance of trim tables based on model scale towing tests

Research question 4 (*How accurate are trim tables based on model scale towing tests?*) is answered in this section.

Model scale tests results are available for a mean draft between 6.50 m and 10.0 m. The test results of a mean draft of 10.0 m are compared with the sea trial results and fuel model results for a mean draft condition of around 10.5 m are presented in figure 9.7. Figure 9.8 includes the results for a mean draft of 7.0 m. For this mean draft condition, the range of trim in the model scale test results in limited from 1.5 m stern trim to even keel.

Model scale towing test results show a linear trend between trim and shaft power for the measured draft conditions, indicating that trim by stern increases the required shaft power. The trend is similar for speeds between 11 and 14 knots. These results comply with the results of the first sea trial and are very similar to the fuel model results. For the second sea trial, the trend show no indication of a decrease in required shaft power from 1.0 m to 2.0 m stern trim, which is observed in the sea trial results.

The model scale results deviate in terms of the magnitude of the effect of trim for the first sea trial and the absolute power predictions for different speeds for both sea trials. The trend of the model scale results is an estimated factor of 2 smaller than the sea trial results, and the required shaft power is underestimated by more than 20% for speeds between 12 and 14 knots.

In addition, it should be noted that the results of the model scale towing test for other drafts (see appendix J) show that for a mean draft condition between approximately 8.0 m to 9.0 m, the effect of trim in shaft power is different than the fuel model results. For this draft condition, the required shaft power decreases for both bow trim and, to a smaller extent, for stern trim as well. Sea trials should be performed at a mean draft at around 8.50 m to validate this trend.

9.5. Overall model performance

The GBM-PHM variant has shown to result in opposite relations between trim and power compared to the results of the sea trials in multiple cases. Because of the (marginal) steeper slope in the resulting trend of the GBM-PLK compared to the results of the BBM, the GBM-PLK variant is considered to perform superior to the other model variants. Moreover, it was found in table 8.4 that the GBM-PLK variant has a marginal advantage of accuracy over the other variants. Further analysis are performed using the GBM-PLK model. The accuracy of the GBM-PLK fuel model is 6.6% for a random test subset from the noon report data. Due to the cluster of recordings around a speed of 13 knots, the accuracy will be optimal at around this speed, and gets worse for speeds below 12 knots. A linear trend is found between trim and power for all mean drafts, showing a potential in fuel savings between 1 and 2 % for a change in trim of 0.5 m. Validation with sea trials show that the trend is fairly accurate for a mean draft of 10.5 m. However, the magnitude of the trend is too small and the effect of speed on power is unrealistically embedded. Sea trials at 7.0 m mean draft deviate for 1.0 m and more stern trim conditions with fuel model results.

The model applicability is limited for draft conditions of 9.5 m and more, meaning that only part of the generated trim table should be used for trim optimization for the current state of model performance and validation. Despite the partially good performance of the fuel model for the mean draft condition of 7.0 m, no sufficient evidence is provided yet that the fuel model should be used in practice for drafts below 9.5 m. This limited applicability is based on a few indications of the model performance. Firstly, the significant part of the noon report data represents draft conditions of 9.5 m or more, while other draft conditions are less frequently met. The model might be overtrained for draft conditions most frequently recorded, which affects the accuracy for other draft conditions. Secondly, a very similar trend in the effect of trim on shaft power is extracted by the model for all drafts, while sea trial results show a different magnitude of the effect for different draft conditions. Lastly, results from the model scale towing tests show that the effect of trim on shaft power is very different for drafts between 8 and 9 m, which is not seen in the fuel model results.

Figure 9.13 shows an overview of the performance of the fuel model compared to the sea trial results, only

considering the trend of trim on shaft power as presented in figure 9.12. Speeds around 13 knots (± 1 knot) represent a large part of the operational profile of the ship class of the case study.

No indication is observed showing that the GBM approach increases the extrapolation qualities of the BBM, nor decreases it. The most significant limitation in input data are the relatively small forward draft conditions (small mean draft with forward or even keel trim condition) and low speed (up to 10 knots) recordings. The effect of speed on power is not realistic for both types of variants and no difference is observed between the model variants in low forward draft conditions. Other advantages of a GBM over a pure BBM may still hold, which has not been proven in this analysis. These advantages include the prevention of unreasonable results, and the possibility to use less historical data than a pure BBM.
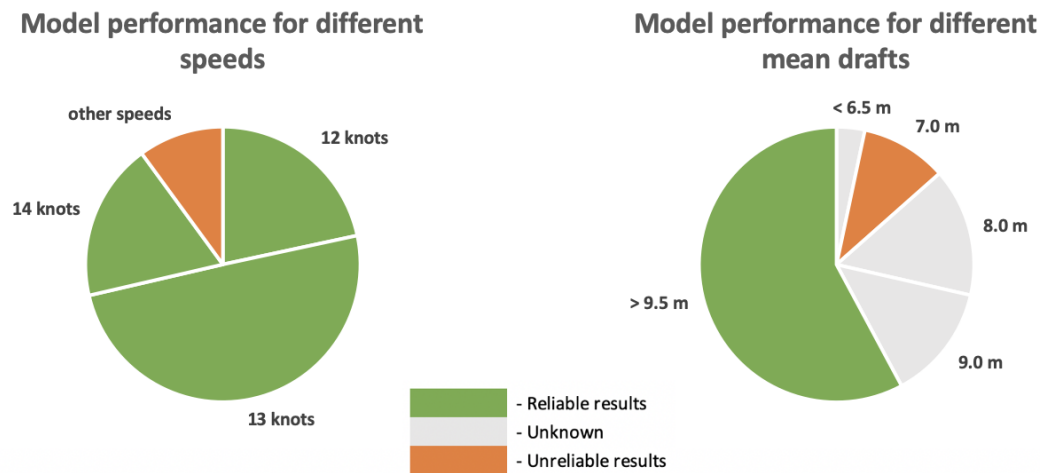
Figure 9.13: Model performance for different speeds and mean drafts, relative to the operational profile of the ship class of the case study.

9.6. Model performance compared to similar fuel models

The fuel model performance is compared to three similar models that all use a pure BBM approach and noon report data, as shown in the lower-left corner of 3.1. Details of the model have been covered in table 6.2. All three models refer to a different way of expressing model performance. To compare the models in a relative way, additional calculations and approximations have to be made.

The model of Du et al. (2019) uses 10 input variables to estimate the fuel consumption in tonnes per day for two 9000 TEU containerships. Model performance is expressed in RMSE using the first variant of formula 9.2. In order to compare this performance indicator, the normalized RMSE (nRMSE) is calculated, by dividing the RMSE with an estimation of the daily average fuel consumption. The distribution of noon report data entries is given for one of the ships (ship S2). Based on this, the average daily fuel consumption is determined to be 74 MT/day. Given an RMSE of 9.34 MT/day for this ship, the nRMSE will be 0.126.

Bal Besikci et al. (2016) describe a model to estimate the fuel consumption on MT/hr for a 266 m in length oil tanker using 7 input variables. A RMSE is found of using the second variant of formula 9.2. This formula variant reduces the RMSE with a factor of $\frac{1}{\sqrt{2}}$ compared to formula 9.2. Therefore the RMSE of this model is determined to be 0.192 MT/hr. The mean fuel consumption is given to be 1.89 MT/hr, resulting in a nRMSE of 0.102.

The model of Pedersen and Larsen (2009b) consider the fuel consumption and 9 input variables of a 110 000 DWT oil tanker and expresses the model performance in terms of relative errors. The model using noon report only, had an accuracy of 7.02 %. In the research, it was found that combining noon report data with hind cast weather data, would increase the accuracy to about 2%. However, available data set is split into 4 data sets with a limited time range, therefore the model is tested within a limited range of conditions. The accuracy is likely to decrease when new conditions are met.

Table 9.3 shows all known performance indicators of the three discusses models and the fuel model presented in this report. It is found that the fuel model presented in this report, performs more accurate than all three similar models. Most likely, the better model performance is due to the higher number of input variables and the quality of the used noon reports for training.

Table 9.3: **Model performance comparison.**

	RMSE	Mean of target value	nRMSE	RE
Fuel model	467 kW	5546 kW	0.0842	6.58%
(Pedersen and Larsen, 2009b)	-	-	-	7.02%
(Bal Besikci et al., 2016)	0.192 MT/hr	1.89 MT/hr	0.102	
(Du et al., 2019)	9.34 MT/day	74 MT/day	0.126	

$$RMSE = \begin{cases} \sqrt{\frac{1}{N}\sum_i^N(\hat{y_n}-y_n)^2} & \text{used by Du et al. (2019)} \\ \sqrt{\frac{1}{2N}\sum_n^N(\hat{y_n}-y_n)^2} & \text{used by Bal Besikci et al. (2016)} \end{cases} \tag{9.2}$$

The work of Parkes et al. (2018) shows the potential of using CM data and ANNs in estimating the shaft power. Data of three sister vessels over a period of approximately 2 years are combined. The presented model was able to estimate the shaft power with a relative error of 7.8%. According to the authors, the accuracy will likely be better within the region of sufficient data points and less accurate at the 'extreme' conditions. Similar behaviour has been observed in the effect of speed on power: the slope of the curve flattens at the highest possible speed.

9.7. Voyage fuel consumption estimation

Voyage fuel consumption can be estimated per defined time (or instance one day), by setting all conditions according to the actual load condition and weather conditions/forecast.

A demonstration of possible daily savings is given in table 9.5 for one day, assuming the conditions of table 9.4. It is assumed that the ship heading and load condition (either by mean draft or DWT) is known, as well as the weather and sea condition by forecast.

Table 9.4: **Input parameters for voyage fuel consumption estimation.**

Operational & Fouling		Conditions	
Mean draft	10.5 m	**Sea water temperature**	25 °C
Speed	13 knots	**Wind condition**	4 Bf - SE direction
Heading	270 °	**Sea condition**	3 Douglas - SE direction
Last hull cleaning	2 years	**Swell condition**	3 Douglas - S direction
Last propeller cleaning	180 days		

Furthermore, the specific fuel consumption (sfc) of the C-38 is assumed to be 179.2 $\frac{g}{kWh}$, which measured in a engine performance audit at 6240 kW or 79% MCR. The CO_2 conversion factor C_f is 3.2060 $\frac{t}{t}$ for MDO (approximate value for low-sulphur fuel oil) (IMO, 2014). The price (P_{fuel}) of MGO/MDO is around 600 USD/MT, which is the approximate fuel price of MGO in Singapore, November 2019 (Ship and Bunker, 2019).

9.8. Integration in voyage management

The voyage management of a ship can be split into two stages: The first stage starts when a voyage is scheduled and ends when the voyage commences, defined as voyage preparation. This stage is characterized by activities that prepares the voyage, including the development of the voyage scheduling and stowage plan.

Table 9.5: **Demonstrations of fuel, CO_2 and costs saving potential for an average single sailing day for three trim conditions.**

	trim = 1.5 m (reference)	trim = 0.5 m	trim = -0.5 m
Fuel consumption [t]	24.81	- 0.50	- 0.89
CO_2 [t]	79.53	- 1.59	- 2.85
Costs [USD]	14 884	- 298	- 553

The second stage is the actual voyage. Besides the transit at sea, this includes the loading and discharging in possibly multiple ports.

Because cargo allocation has a significant effect on the trim of the ship, trim optimization should be considered while making the stowage plan. It is the operator that proposes the initial stowage plan, therefore the process of trim optimization should start at the point where cargo is allocated, putting a responsibility at the operator.

It is the ship's crew that is responsible for the final loading condition of the ship and to consider the limitations to trim as defined in figure 5.1. Limitations regarding hull strength and stability, as well as operational safety (excluding course keeping and steering capacity) is embedded in the on-board loading computer. Besides that, the ship's crew has the possibility to (re-)allocate auxiliary loads such as fresh water, fuel or ballast water, to change the trim before and during the voyage.

The impact of trim optimization on the process of voyage management is illustrated by the business processes of both stages, with and without trim optimization. Figure 9.14a illustrates the first stage of voyage management (voyage preparation) excluding trim optimization and figure 9.14b illustrates the voyage preparation including trim optimization.

Trim optimization during the voyage will be one of the operational performances considered by the operators continuously during active voyage management. Figure 9.15a illustrates the process of (in-active) voyage management excluding trim optimization and figure 9.15b illustrates the process of active voyage management including trim optimization.
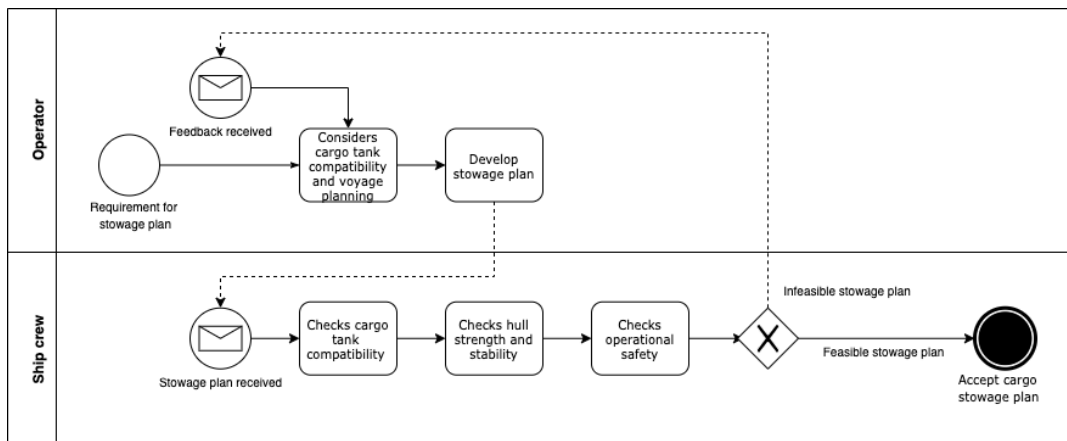
(a) Process of voyage preparation excluding trim optimization.
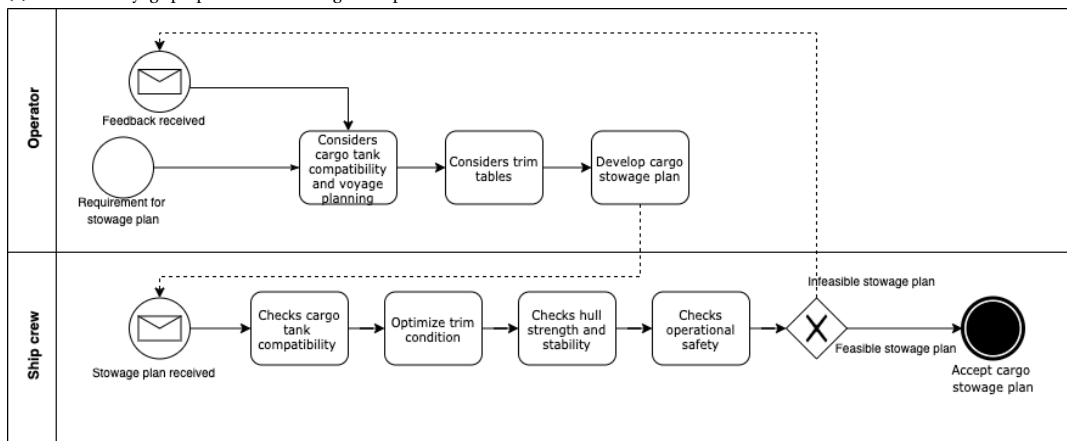
(b) Process of voyage preparation including trim optimization.

Figure 9.14: Process of voyage preparation.
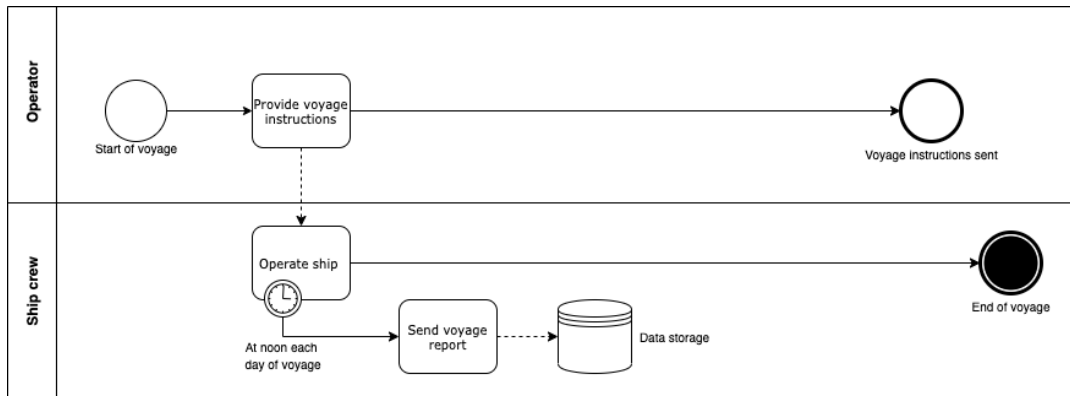
(a) Process of voyage management excluding trim optimization.
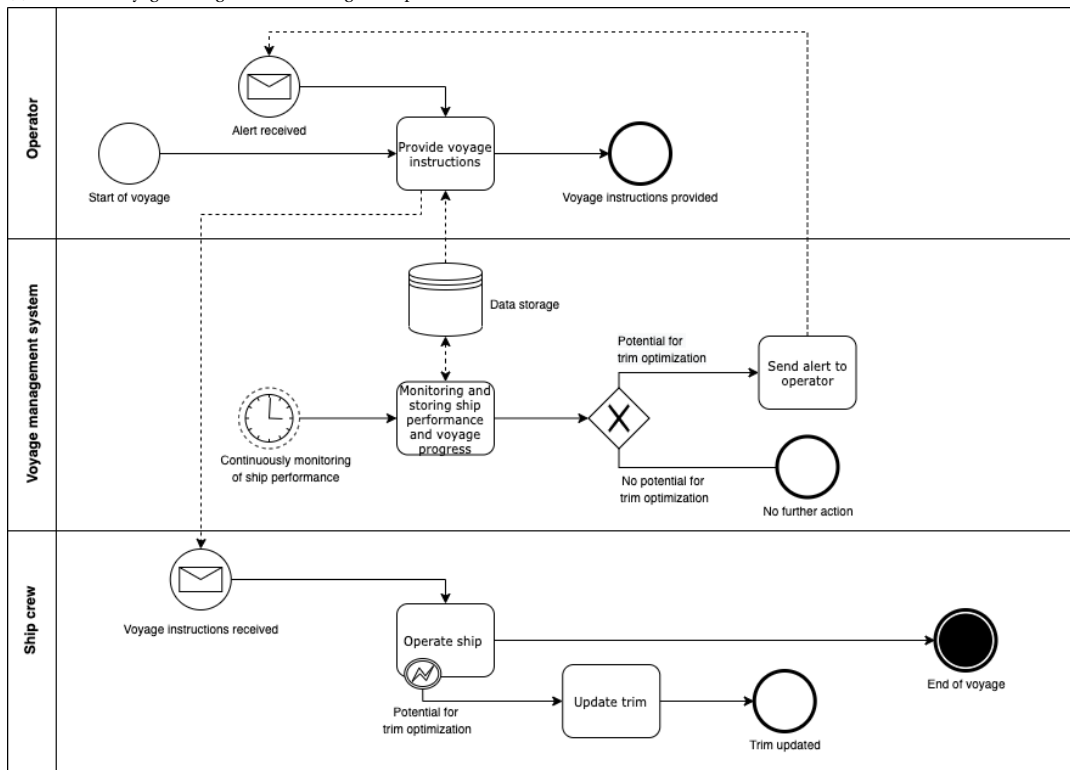
(b) Process of active voyage management including trim optimization.

Figure 9.15: Process of voyage management.

IV

Part IV: Conclusion and discussion

10

Conclusion

A model has been presented in this report to extract the effect of trim on required shaft power and fuel consumption, based on noon report data. Model requirements have been set to answer six research questions. The conclusions have been split into two parts, as defined in the research objective of section 2.7. First, the model requirements are evaluated and the research questions are answered. Based on this, the final conclusion on the research objective is drawn.

10.1. Conclusion on model requirements

10.1.1. Estimate the required power for propulsion, with sufficient accuracy to extract the effect of trim

The GBM-PLK model variant can estimate the required power with an accuracy of 6.58% for a random test set from the available noon report data. A linear trend is found between trim and power for all mean drafts, showing a potential reducing the required shaft power with 1 to 2 % for a change in trim of 0.5 m.

The most significant part of the noon report data (58%) represents draft conditions of 9.5 m and more, whereas other draft conditions are less frequently recorded. Similarly, speeds between 12 and 14 knots are most frequently sailed. Sea trial results show that the model performs more accurate for these conditions than for conditions represented by less noon reports. The effect of trim on shaft power is correctly extracted for these conditions, although the magnitude of the effect was found to be higher in the sea trial results for full load conditions.

For other speeds, the accuracy significantly drops, since the effect of speed on power is unrealistically embedded in the model, especially in non-calm water conditions. Model calibration based on sea trial results is required for accurate estimations of required shaft power for all speeds.

10.1.2. Able to generate trim tables considering the effect of dynamic factors

Trim tables can be generated considering specific conditions, including dynamic factors such as weather and fouling. The fuel model correctly extracts the effect of weather factors on required power for most cases. Distinction is made between the effect of wind, sea and swell from multiple directions. Hull- and propeller fouling is considered by the effect of days since last hull cleaning and days since last propeller polishing.

Validation by sea trials for two mean draft conditions, has shown that the trend is fairly accurate for a mean draft of 10.5 m, and would have advised the correct optimal trim, but the magnitude of the trend is smaller compared to the trend in the power recording of the sea trials. Sea trials at 7.0 m mean draft deviate from 1.0 m stern trim conditions with fuel model results, indicating that the model cannot provide accurate

results for this draft condition.

The model applicability is limited for draft conditions of 9.5 m and more, meaning that only part of the generated trim table should be used for trim optimization for the current state of model performance and validation. A few indications are observed that the model performs not accurate enough for lower draft conditions than 9.5 m:

- The model might be overtrained for draft conditions that are most frequently recorded, which affects the accuracy for other draft conditions;

- A very similar trend in the effect of trim on shaft power is extracted by the model for all draft conditions, while sea trial results show a different magnitude of the effect for different draft conditions;

- Results from the model scale towing tests show that the effect of trim on shaft power is very different for drafts between 8 and 9 m, which is not seen in the fuel model results.

10.1.3. Model should be based on available data within Stolt Tankers

The model estimated the required power based on available data within Stolt Tankers, of which noon report data represent to most significant part.

10.1.4. Model should deal with errors in voyage report data

The data pre-processing framework has been constructed and used effectively for a case study. However, due to the nature of noon reports, the quality of the noon report data remains a source of noise. As a consequence, noon report data performs well for finding trends, but the magnitude is likely to differ from actual effects. The main problems with using noon report data are:

- the discrepancy between the averaged recordings of shaft power and speed through water over a 24 hour period on one hand, and the snapshot of weather and sea conditions and the relative direction on the other;

- Human error in observing and recording required data fields of the noon reports. To find realistic trends between trim and required shaft power, accurate and daily updated static forward and aft drafts are a prerequisite, but are not always visible in the noon report data.

- Reliability on the range of recorded conditions. The small range of power recordings partly causes the weakly defined relations between speed and power;

10.1.5. Model should be able to be used for a range of ship types within the fleet

The fuel model and data pre-processing framework is constructed to be easily scalable to other ships of Stolt Tankers. A prerequisite is a similar or better quality of the noon report as used in the case study for results than can be used in practice. The additional parameters required for the power estimation of the WBM based on Lutzen and Kristensen (2013), is limited and can be easily acquired. Validation for other ship classes within the fleet is recommended.

10.2. Conclusion on research questions

10.2.1. What methods exist to generate trim tables?

Approaches to generate trim tables are either based on model results (model scale towing tests or CFD-simulations) or ship scale data (continuous data monitoring or noon report data). A model that estimates the shaft power for a given set of conditions based on noon report data has shown multiple advantages over

other approaches. It makes use of already available data on ship scale, is easily scalable to other ships and is able to consider weather and fouling effects on shaft power. The main disadvantage is that noon report data is generally considered to be noisy, caused by human error in observing and recording, the snapshot nature of recording and the limited variance in recorded conditions.

10.2.2. How can the required shaft power of a ship under specified conditions be estimated?

A gap in existing literature has been defined and answered, by combining a grey-box modelling approach with using noon report data to model the required shaft power under specified conditions.

For the black-box part, the data pre-processing framework has identified the most relevant parameters affecting required shaft power that are recorded within the noon reports and maintenance data, which are mean draft, ship speed (through water), trim, wind force, sea state, swell state, wind direction, sea direction, swell direction, days since last hull cleaning and days since last propeller cleaning. For the white box part, both the regression model of Holtrop and Mennen (1982) and Lutzen and Kristensen (2013) has been used. A multi-layer feed forward neural network is made to learn the relationships between these input variables and shaft power, by following a supervised learning method.

The model variant GBM-PHM, which uses the model of Holtrop and Mennen (1982) for resistance estimation and the model of Lutzen and Kristensen (2013) for estimations of propulsion characteristics, makes the model behaviour worse. This model has the risk to result in wrong conclusions regarding trim optimization. The model variant GBM-PLK improves the model accuracy compared to the BBM approach marginally (0.05%), but no clear indications have been observed that the GBM approach improves extrapolation qualities. However, it is believed that a GBM still may have advantages over a pure BBM, which include the prevention of unreasonable results, and the possibility to use less historical data than a pure BBM.

10.2.3. At which trim condition is the required shaft power minimized?

Model results show that the required shaft power is minimized by 0.5 m bow trim, with a linear effect between trim and shaft power. Depending on the speed and load condition, between 1% and 2% can be saved with a change in trim of 0.50 m.

Sea trial results indicate a similar trend for a full load condition between -0.50 m and +0.50 m trim. Bow trim is the optimal trim, with a surprisingly significant effect of up to approximately 6% to 8% in required shaft power can be saved with a change in trim of 0.50 m, even with additional ballast water.

For part load conditions, the fuel model behaves similar as in the full load condition. Sea trial results show a much smaller potential for power savings and a possible optimal trim at -0.5 m and 2.0 m stern trim, whereas the model results indicate that bow trim is optimal.

10.2.4. How accurate are trim tables from model scale test results?

The trend in effect of trim on required shaft power based on model scale towing tests results is consistent with sea trial results. However, the trend is an estimated factor of 2 smaller than the sea trial results, and the required shaft power is underestimated by more than 20% for speeds between 12 and 14 knots for the conditions validated by sea trials. Sea trials at around 8.5 m is to be performed to completely answer this question.

Shortcomings of the existing trim tables are the limited range of trim (up to 1.5 m stern trim) and draft (up to 10.0 m).

10.2.5. What limitations exist to trim a ship

Limitation in trim can be divided in limitations to load allocation, voyage-related limitations, hull strength and stability and operational safety (see figure 5.1).

10.2.6. How can the proposed method for trim optimization be integrated in the voyage management system?

Figure 9.14b and 9.15b show how trim optimization can be integrated in the voyage management system.

10.3. Conclusion on research objective

The objective of this research was:

> *To develop a method to decrease fuel consumption by trim optimization, by a dynamic fuel consumption estimation model based on available operational data, that can be integrated in the voyage management system of Stolt Tankers.*

Based on the model requirements and the answers on the research questions, it is concluded that an important step is made in extracting useful knowledge from noon report data and to use this to decrease fuel consumption by trim optimization. The model is able estimate the required power with an average accuracy of 6.58% for a random subset of the noon report data. Moreover, the fuel model is able to extract the trend of trim on required shaft power while considering dynamic effects, but the applicability is limited to draft conditions of 9.5 m and more and a speed range of 12 to 14 knots. Due to problems inherent to noon reports as data source, actual effect of trim and speed have a bigger magnitude than the extracted trend.

11

Discussion and research recommendations

11.1. Input data

Noon reports with bow trim are limited, not only for the case study ship, but this may be true for other ships within the fleet of Stolt Tankers as well. In order to generate trim tables that includes bow trim as well, noon reports with bow trim conditions are a prerequisite.

The recorded forward and aft draft conditions should represent actual draft conditions and therefore be updated daily. It has been found that this requirement is not always met. The draft condition at departure and arrival is generally determined for every voyage, since that is required to know regarding draft restrictions in port. A solution to flat lines may therefore be to take these draft conditions as a reference, and interpolate linearly to determine the draft conditions during the voyage. This approach can be validated with voyages for which the draft conditions are regularly updated.

To solve the mismatch in the noon reports between the snapshot of conditions and the average value of speed and shaft power, more frequent recordings would decrease the noise caused by this mismatch. Moreover, hindcast weather data excludes the source of human error in observing and recording weather and sea conditions, while automated recordings of shaft power would enable to match the shaft power with the weather data. However, this would not be noon report data anymore.

11.2. Model considerations

The extracted trends between trim and required shaft power are almost equal for all draft conditions. Considering the robust design of the ship in the case study, this might be true. However, sea trial results indicate a different magnitude of the effect of trim for different draft conditions. Moreover, the results from model scale towing tests indicate a different trend for a mean draft of 7.0 m, which is not yet validated by sea trials. It can not be concluded with confidence that the extracted trends by the fuel model is true for all mean drafts. A possible solution would be to group the noon reports for different draft conditions, and perform the analysis presented in the report for each group of mean drafts. The result would be a trend between trim and power for each group of mean draft, which would increase the interpretability of the GBM and enable to conclude if different trends exists for different groups of mean drafts. Since the number of noon reports will be less for each group of mean drafts, the number of groups of drafts should be limited.

Regarding the number of noon reports required to perform analyses, further research is required to understand the limit of noon reports required for the model to learn all relationships between the input variables and shaft power. Relevant literature (see section 6.3) have made conclusions regarding the effect of trim based on approximately 300 noon reports.

Power estimations of the WBM deviate significantly from the power recordings in the noon report data for speed below 12 knots and above 14 knots. A research opportunity is identified, to research the effect of a modified WBM on the performance of the GBM. The WBM modification can be done by including an estimation of the effect of weather conditions on the required shaft power in the WBM, which could improve the extrapolation qualities of the GBM. The model accuracy would then improve for speeds outside the region of 12 to 14 knots.

The specific fuel consumption (sfc) is assumed to be constant. However, this will be a function of engine speed, pitch setting of the CPP, maintenance level and will differ between ships. To estimate the fuel consumption more accurate, this assumption should be dropped and be determined as a function of the mentioned factors. The effect of hull and propeller fouling is considered by considering only the days since last hull cleaning and last propeller polishing. However, the actual degree of fouling is much more complex. Further model improvements may consider the geographical locations, consecutive days in warm water, consecutive non-sailing days, etc.

11.3. Model validation

The proposed speed calibration of the model is to be validated with more sea trial results. These sea trial results are not required to perform measurements at different trim conditions, but for fixed conditions and for a range of speeds.

Model results regarding the trend between trim and power are now validated by two sea trials, each on a different mean draft condition. Some changes in shaft power in the performed sea trials are now attributed to external effects such as an increase in weather parameters. More sea trial results would enforce these statements. Sea trials are especially required to validate the model behaviour within the region of 8 to 9 m mean draft. Results from model scale towing tests indicate that for this draft region, another trend between trim and shaft power exists than extracted by the fuel model. Sea trial(s) at this draft condition contribute to conclude which approach show the correct trend for this region of mean draft.

The model should be validated with noon report data and sea trial results conducted by a chemical tanker with a bulbous bow. The effect of the bulbous bow on the wave resistance depends on the mean draft and trim condition of the ship. Therefore, a non-linear but significant effect between trim and power may be expected. Further research has to be done to investigate if the model can extract a non-linear trend between trim and power with local minima, based on noon report data.

Bibliography

26th ITTC Specialist Committee on Uncertainty Analysis. *Fresh Water and Seawater Properties*. ITTC, 2 edition, 2011.

A. H. Abouelfadl and E. E. Y. Abdelraouf. The impact of optimizing trim on reducing fuel consumption. *Journal of Shipping and Ocean Engineering*, 6:179–184, 2016.

L. Aldous, T. Smith, R. Bucknall, and P. Thompson. Uncertainty analysis in ship performance monitoring. *Ocean Engineering*, 110:29–38, 2015.

The Naval Architect. Trim optimisation - don't blind me with science! [pdf file]. Retrieved from `https://www.dnvgl.com/maritime/energy-efficiency/better-fuel-savings-integrated-onboard-trim-solution.html`, September 2014. Accessed on 28-10-2019.

E. Bal Besikci, O. Arslan, O. Turan, and A. I. Olcer. An artificial neural network based decision support system for energy efficient ship operations. *Computers and Operations Research*, 66:383–401, February 2016.

V. Bertram. *Practical Ship Hydrodynamics*. Butterworth Heinemann, 2000.

N. Bialystocki and D. Konovessis. On the estimation of ship's fuel consumption and speed curve: A statistical approach. *Journal of Ocean Engineering and Science*, pages 157–166, 2016.

D. M. Bridgeland and R. Zahavi. *Business Modeling - A practical guide to realizing business value*. The MK/OMG Press. Morgan Kaufmann, 1st edition, 2009.

J. S. Carlton. *Marine propellers and propulsion*. Butterworth-Heinemann, fourth edition edition, 2018.

A. M. Castro, P. M. Carrica, and F. Stern. Full scale self-propulsion computations using discretized propeller for the kriso container ship kcs. *Computers and Fluids*, 51:35–47, 2011.

A. Coraddu, L. Oneto, F. Baldi, and D. Anguita. Vessels fuel consumption forecast and trim optimisation: A data analytics perspective. *Ocean Engineering*, 130:351–370, 2017.

I. N. da Silva, D. H. Spatti, R. A. Flauzino, L. H. B. Liboni, and S. F. dos Reis Alves. *Artificial Neural Networks - A Practical Course*. Springer International Publishing, 2017.

M. David and S. Gollasch. *Global Maritime Transport and Ballast Water Management*, volume 8. Springer, 2015.

DNV-GL. Eco assistent 4.1 [pdf file]. Retrieved from `http://production.presstogo.com/fileroot7/gallery/DNVGL/files/original/6a40ec4017884ae99d8c1ac206de8f96.pdf`, 2013. Accessed on 28-10-2019.

DNV-GL. Eco assistant 4 [pdf file]. Retrieved from `http://production.presstogo.com/fileroot6/gallery/DNVGL/files/original/f634b71f59815b62e04385ee5e4d07cd.pdf`, n.d. Accessed on 14-11-2019.

Meng Q. Du, Y. and, S. Wang, and H. Kuang. Two-phase optimal solutions for ship speed and trim optimization over a voyage using voyage report data. *Transportation Research Part B*, 122:88–114, 2019.

FORCE-Techology. Trim guidance in perspective. `https://forcetechnology.com/da/cases/trim-raadgivning`, n.d. Accessed on 14-11-2019.

Furuno. *Operator's manual Furuno Doppler sonar Model DS-60*. Furuno Electric Co. Ltd., 1 edition, 2010.

X. Gao, K. Sun, S. Shi, B. Wu, and Z. Zuo. Research on influence of trim on a container ship's resistance performance. In *3rd International Conference on Fluid Mechanics and Industrial Applications*, volume 1300. IOP Publishing, 2019.

A. Garcia, S. Ramirez-Gallego, J. Luengo, J.M. Benitez, and F. Herrera. Big data preprocessing: methods and prospects. *Big Data Analytics*, 1(9), 2016.

K. Govindan. Breaking new ground in operational performance. Retrieved from `https://www.wartsila.com/twentyfour7/innovation/breaking-new-ground-in-operational-performance`, February 2019. Accessed on 14-11-2019.

A. M. Grachev, D.I. Ignatov, and A. V. Savchenko. Compression of recurrent neural networks for efficient language modeling. *Applied Soft Computing Journal*, 79:354–362, 2019.

GreenFramework. Greenship efficiency software. Retrieved from `https://green-framework.com/greenshipefficiencysoftware`, n.d. Accessed on 14-11-2019.

W. Górski, T. Abramowicz-Gerigk, and Z. Burciu. The influence of ship operational parameters on fuel consumption. *Scientific Journals Maritime University of Szczecin*, 36(108), 2013.

S. A. Harvald. *Resistance and Propulsion of Ships*. John Wiley and Sons, 1983.

Herbert-ABS. Trim and draft optimization [pdf file]. Retrieved from `https://static1.squarespace.com/static/59c5518a2994ca9ad2ce87ca/t/5a62337e53450aa0b392cb82/1516385155079/PerfOpt.pdf`, n.d. Accessed on 13-11-2019.

J. Holtrop and G. G. J. Mennen. An approximate power prediction method. *International Shipbuilding Progress*, 29(335):166–170, 1982.

HSVA. *Model Tests with the Stolt Chemical Tanker Trim Variations*. Hamburgische Schiffbau-Versuchanstalt GMBH, May 2014.

M. N. Iakovatos, D. E. Liarokapis, and G. D. Tzabiras. Experimental investigation of the trim influence on the resistance characteristics of five ship models. *Developments in Maritime Transportation and Exploitation of Sea Resources*, 2014.

IMO. International convention on load lines. Technical report, IMO, December 1966.

IMO. Stability information manual. `https://static1.squarespace.com/static/579a1ee6e6f2e1648e641817/t/579a5e07d1758ed7db33360f/1469734409802/Trim+and+stability-+standard.doc`, 2008.

IMO. Third imo ghg study 2014. `http://www.imo.org/en/OurWork/Environment/PollutionPrevention/AirPollution/Pages/Greenhouse-Gas-Studies-2014.aspx`, 2014. Accessed on 16-10-2019.

IMO. Low carbon shipping and air pollution control. `http://www.imo.org/en/MediaCentre/HotTopics/GHG/Pages/default.aspx`, 2019a. Accessed on 25-12-2019.

IMO. Carriage of chemicals by ship. `http://www.imo.org/en/OurWork/Environment/PollutionPrevention/ChemicalPollution/Pages/Default.aspx`, 2019b. Accessed on 18-12-2019.

Ship Focus Intelligence. World's top chemical tanker operators [pdf file]. Retrieved from `https://www.shipsfocus.com/wp-content/uploads/2019/03/Worlds-Top-Chemical-Tanker-Operators-Rankings-2019.pdf`, 2019. Accessed on 5-11-2019.

H. Islam and C. Guedes Soares. Effect of trim on container ship resistance at different ship speeds and drafts. *Ocean Engineering*, 183:106–115, 2019.

H. Jasak, V. Vukcevic, I. Gatin, and I. Lalovic. Cfd validation and grid sensitivity studies of full scale ship self propulsion. *International Journal of Naval Architecture and Ocean Engineering*, 11:33–43, 2019.

M. Khare and S.M. Shiva Nagendra. *Artificial Neural Networks in Vehicular Pollution Modellig*. Springer, 2007.

K. Kijima, K Katsuno, Y. Nakiri, and Y. Furukawa. On the manoeuvring performance of a ship with the parameter of loading condition. In *Autumn Meeting of the Society of Naval Architects of Japan*, November 1990.

R. Kishev, S. Georgiev, S. Kirilova, and E. Milanov. Global view on ship trim optimization. `https://www.academia.edu/14503905/Global_View_on_Ship_Trim_Optimization`, n.d.

H. Klein Woud and D. Stapersma. *Design of Propulsion and Electric Power Generation Systems*. IMarEST, 2012. Original work published 2002.

G. Kuiper and S. Bernaert. Hydromechanica 3 - resistance and propulsion 1. Faculty of Mechanical, Maritime and Materials Engineering, Delft University of Technology, 2002.

J. Labanti, H. Islam, and C. Guedes Soares. Cfd assessment of ropax hull resistance with various initial drafts and trim angles. In *Maritime Technology and Engineering III: Proceedings of the 3rd International Conference on Maritime Technology and Engineering*. MARTECH, July 2016.

L. Larsson and H. C. Raven. *Ship Resistance and Flow*. The Principles of Naval Architecture Series. The Society of Naval Architects and Marine Engineers, 2010.

L. þ. Leifsson, H. Sævarsdóttir, S. þ. Sigurðsson, and A. Vésteinsson. Grey-box modeling of an ocean vessel for operational optimization. *Simulation Modelling Practice and Theory*, 16:923–932, 2008.

R. Lu, O. Turan, E. Boulougouris, C. Blanks, and A. Incecik. A semi-empirical ship operational performance prediction model for voyage optimization towards energy efficient shipping. *Ocean Engineering*, 110:18–28, 2015.

M. Lutzen and H. O. Kristensen. Prediction of resistance and propulsion power of ships [pdf file]. Retrieved from `https://www.danishshipping.dk/en/services/beregningsvaerktoejer/download/Basic_Model_Linkarea_Link/163/wp-2-report-4-resistance-and-propulsion-power.pdf`, May 2013. Accessed on 18-11-2019.

M. Lutzen and H. O. H. Kristensen. A model for prediction of propulsion power and emissions - tankers and bulk carriers. In *World Maritime Technology Conference*, Saint-Petersburg, Russian Federation, 2012.

C. Ma, C. Zhang, X. Chen, Y. Jiang, and F. Noblesse. Practical estimation of sinkage and trim for common generic monohull ships. *Ocean Engineering*, 126:203–216, 2016.

MAN Diesel and Turbo. Basic principles of ship propulsion [pdf file]. Retrieved from `https://spain.mandieselturbo.com/docs/librariesprovider10/sistemas-propulsivos-marinos/basic-principles-of-ship-propulsion.pdf?sfvrsn=2`, December 2011. Accessed on 19-11-2019.

Marorka. Data is revolutionising the maritime industry. Retrieved from `http://www.marorka.com/products/`, n.d. Accessed on 14-11-2019.

Q. Meng, Y. Du, and Y. Wang. Shipping log data based container ship fuel efficiency modeling. *Transportation Research Part B*, 83:207–229, 2016.

MEPC. Resolution msc.267(85). adoption of the international code on intact stability, 2008. Technical report, IMO, December 2008.

MEPC. Energy efficiency technologies information portal. `https://glomeep.imo.org/resources/energy-efficiency-techologies-information-portal/`, n.d.

H. Mikkelsen, M. L. Steffensen, C. Ciortan, and J. H. Walther. Ship scale validation of cfd model of self-propelled ship. In R. Bensow and J. Ringsberg, editors, *8th International Conference on Computational Methods in Marine Engineerding*, volume MARINE 2019, 2019.

A. F. Molland. *The Maritime Engineering Reference Book*. Butterworth-Heinemann, 2008.

A. F. Molland, S. R. Turnock, and D. A. Hudson. *Ship resistance and propulsion. Practical estimation of ship propulsive power*. Cambridge University Press, first edition edition, 2011.

M. W. C. Oosterveld and P. Van Oossanen. Further computer-analyzed data of the wageningen b-screw series. In *International shipbuilding progress - Shipbuilding and marine engineering monthly*, 251, Rotterdam, Holland, July 1975.

C. Ozturk and D. Karaboga. Hybrid artificial bee colony algorithm for neural network training. In *2011 IEEE Congress of Evolutionary Computation (CEC)*. IEEE, June 2011.

A. I. Parkes, A. J. Sobey, and D. A. Hudson. Physics-based shaft power prediction for large merchant ships using neural networks. *Ocean Engineering*, 166:92–104, 2018.

B. P. Pedersen and J. Larsen. Modeling of ship propulsion performance. In *Proceedings of the World Maritime Technology Conference*, Mumbai, India, 2009a.

B. P. Pedersen and J. Larsen. Prediction of full-scale propulsion power using artificial neural networks. In *Proceedings of the 8th international conference on computer and IT applications in the maritime industries (COMPIT'09)*, pages 537–550, Budapest, Hungary, 2009b.

J. P. Pedersen and J. Larsen. Gaussian process regression for vessel performance monitoring. In *12th International conference on computer and IT applications in the maritime industries (COMPIT 13)*, Cortona, Italy, 2013.

L. P. Perera, B. Mo, P. C. Jonvik, L. A. Kristjansson, and J. O. Svardal. Evaluations on ship performance under varying operational conditions. In *Proceedings of the 34th International Conference of Ocean, Offshore and Arctic Engineering*, May 2015a.

L. P. Perera, B. Mo, and L. A. Kristjánsson. Identification of optimal trim configurations to improve energy efficiency in ships. In *In Proceedings of the 10th IFAC Conference on Manoeuvring and Control of Marine Craft (MCMC2015)*, pages 267–272, 2015b.

J. P. Petersen, D. J. Jacobsen, and O. Winther. Statistical modelling for ship propulsion efficiency. *Journal of Marine Science and Technology*, 17(1):30–39, March 2012.

D. Ponkratov and C. Zegos. Validation of ship scale cfd self-propulsion simulation by the direct comparison with sea trials results. In *4th International Symposium on Marine Propulsors*, Austin, Texas, USA, June 2015.

J. Prpic-Orsic and O. M. Faltinsen. Estimation of ship speed loss and associated co$_{(}$2) emissions in a seaway. *Ocean Engineering*, 44:1–10, 2012.

A. Radonjic and K. Vukadinovic. Application of ensemble neural networks to prediction of towboat shaft power. *Journal or Marine Science and Technology*, 20:64–80, 2015.

A. M. Rather, A. Agarwal, and V. N. Sastry. Recurrent neural network and a hybrid model for prediction of stock returns. *Expert Systems with Applications*, 42:3234–3241, 2015.

M. Reichel, A. Minchev, and N. L. Larsen. Trim optimisation - theory and practice. *International Journal on Marine Navigation and Safety of Sea Transportation*, 8(3), 2014.

Resistance Committee of the 27th ITTC. *ITTC Recommended Procedures - General Guideline for Uncertainty Analysis in Resistance Tests*. ITTC, 2 edition, 2014.

A. A. Safaei, H. Ghassemi, and M. Ghiasi. Vlcc's fuel consumption prediction modeling based on noon report and automatic identification system. *Cogent Engineering*, 6, 2019.

S. Sherbaz and W. Duan. Ship trim optimization: Assessment of influence of trim in resistance of moeri container ship. *The Scientific World Journal*, 2014.

Ship and Bunker. Singapore buker prices. `https://shipandbunker.com/prices/apac/sea/sg-sin-singapore`, 2019. Accessed on 26-11-2019.

O. Soner, E. Akyuz, and M. Celik. Statistical modelling of ship operational performance monitoring problem. *Journal of Marine Science and Technology*, 2019.

Specialist Committee on Performance of Ships in Service 27th ITTC. *Analysis of Speed/Power Trial Data*. ITTC, 1 edition, 2014.

H. Stadtler. Stowing seagoing chemical tankers: An example of solving some semi-structured decision problems. *European Journal of Operational Research*, 14(3):279–287, 1983.

D. Stapersma. Lecture notes wb4408a - diesel engines volume 1, performance analysis. Delft University of Technology, 2002.

B. Starke and J. Bosschers. Analysis of scale effects in ship powering performance using a hybrid rans-bem approach. In 29th *Symposium on Naval Hydrodynamics*, pages 26–31, Gothenburg, Sweden, August 2012.

D. Svozil, V. Kvasnicka, and J. Pospichal. Introduction to multi-layer feed-forward neural networks. *Chemometrics and Intelligent Laboratory Systems*, 39:43–62, 1997.

R. L. Townsin, Y.J. Kwon, M. S. Baree, and D. Y. Kim. Estimating the influence of weather on ship performance. *RINA Transactions*, 135:191–209, 1993.

UNCTAD. Review of maritime transport 2019 [pdf file]. Retrieved from `https://unctad.org/en/PublicationsLibrary/rmt2019_en.pdf`, 2019. Accessed on 4-11-2019.

United Nations. The paris agreement. `https://unfccc.int/process-and-meetings/the-paris-agreement/the-paris-agreement`, 2015. Accessed on 25-12-2019.

D. Uzun, Y. K. Demirel, A. Coraddu, and O. Turan. Time-dependent biofouling growth model for predicting the effects of biofouling on ship resistance and powering. *Ocean Engineering*, 191, 2019.

E. van Ballegooijen, T. Helsloot, and M. Timmer. Experience with full-scale thrust measr=urements in dynamic trim optimisation. In V. Bertram, editor, 3rd *Hull Performance and Insight Conference*, volume HullPIC'18, March 2018.

J. J. J. van den Boom, H. Huisman, and F. Mennen. New guidelines for speed/ power trials [pdf file]. Retrieved from `https://www.marin.nl/storage/uploads/20168/files/STA_article_SWZ_Maritime_Jan2013_(part_1).pdf`, January 2013. Accessed on 20-11-2019.

B. M. Wilamowski. Neural network architectures and learning algorithms. *IEEE Industrial Electronics Magazine*, 3(4):56–63, 2009.

L. Yang, G. Chen, N. G. M. Rytter, J. Zhao, and D. Yang. A genetic algorithm-based grey-box model for ship fuel consumption prediction towards sustainable shipping. *Annals of Operations Research*, pages 1–27, 2019.

J. Yuan and V. Nian. Ship energy consumption prediction with gaussian process metamodel. *Energy Procedia*, 152:655–660, 2018.

P. Zhang. *Advanced Industrial Control Technology*. Elsevier Inc., The Boulevard, Langford Lane, Kidlington, Oxford, UK, first edition, 2010.

A

Data proof of concept

Table A.1: **Training data used for the proof of concept.**

Sample nr.	Δ [t]	V_S [kn]	FC [MT/day]
1	22000	8.0	6.8284
2	25000	9.0	10.2812
3	20000	12.0	17.6496
4	28000	13.0	29.4305
5	25000	12.0	21.0530
6	20000	10.0	11.2559
7	30000	8.0	9.2016
8	26000	14.0	32.0282
9	30000	11.0	20.9359
10	27000	9.0	11.8344
11	23000	6.0	3.7569
12	23000	10.0	12.2323
13	26000	12.0	22.5856
14	29000	14.0	36.2794
15	28000	12.0	24.1556
16	21000	10.0	11.2829
17	28000	9.0	12.0539
18	25000	11.0	17.5084
19	22000	15.0	32.2578
20	27000	8.0	8.2755
21	21000	9.0	9.3284
22	25000	10.5	15.1440
23	23500	11.5	17.5913
24	24500	13.5	27.6531
25	26500	14.5	35.7349
26	27000	10.0	14.8967
27	29000	9.5	14.0997
28	30000	11.5	22.6449
29	20000	12.5	19.4850
30	22500	7.0	5.0935
31	21500	14.5	29.6900
32	20500	8.5	8.6465
33	28500	9.5	14.0330
34	29000	10.5	17.3597
35	26500	11.0	18.2367
36	25000	9.0	10.3542
37	24500	14.0	30.5903
38	25500	13.0	27.0289
39	27500	12.0	22.8966
40	28000	12.5	26.1311

B

Description of cleaned data

Load in DWT of C-38
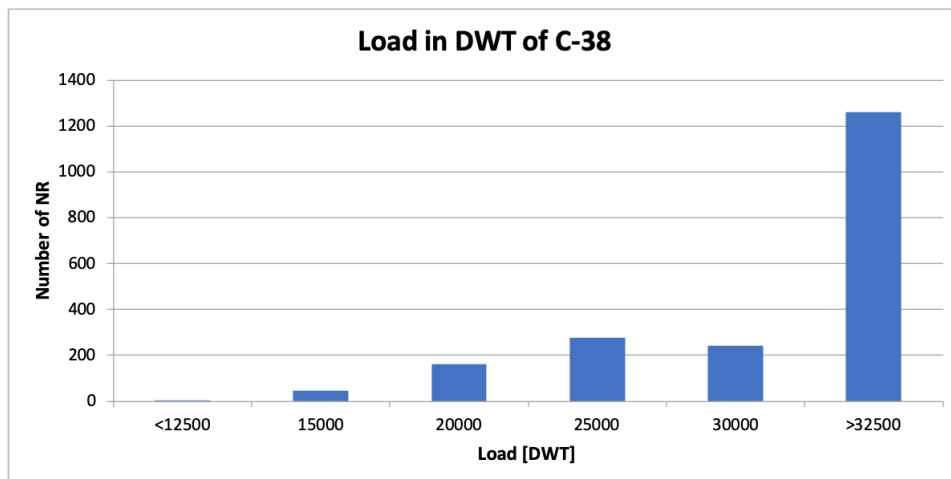
Figure B.1: Frequency histogram of loading condition in DWT.

Mean draft of C-38
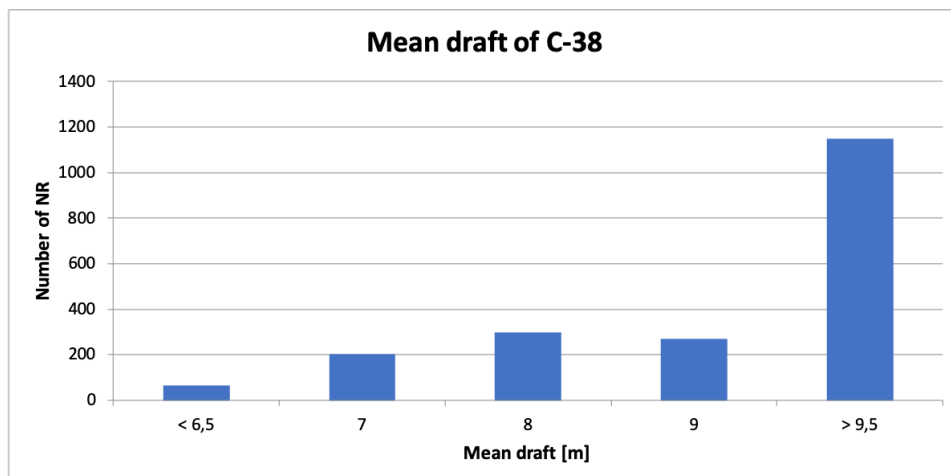
Figure B.2: Frequency histogram of draft in metres.
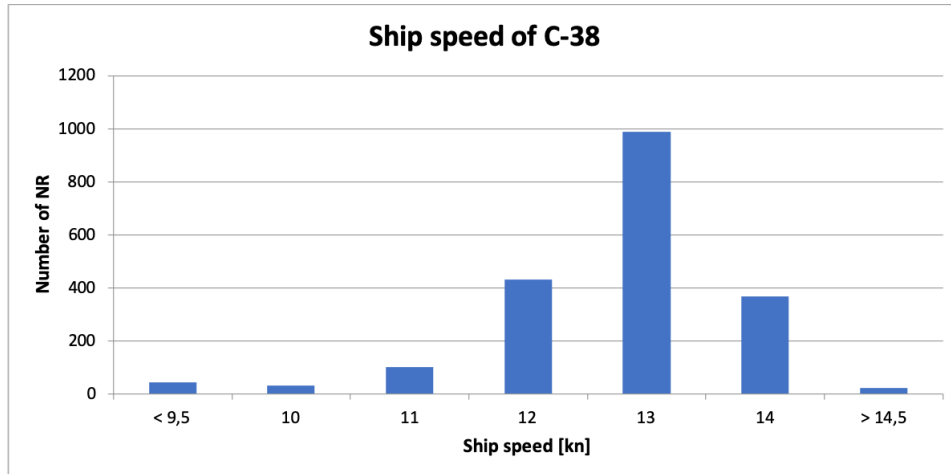
Figure B.3: Frequency histogram of ship speed through water in knots.
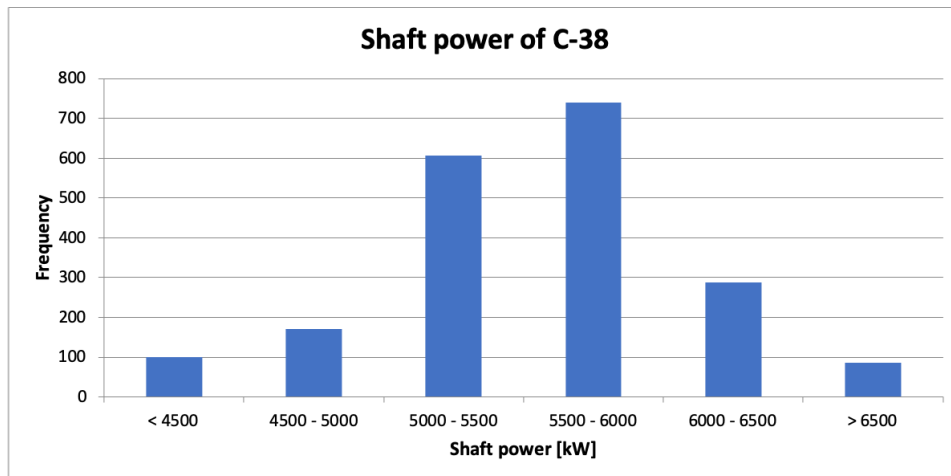
Figure B.4: Frequency histogram of shaft power in kW.
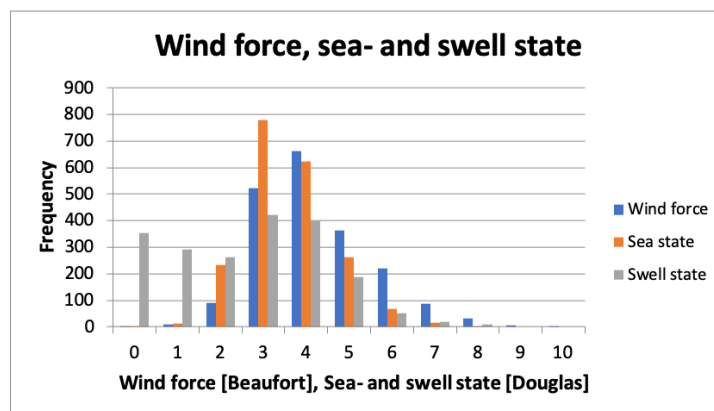
Figure B.5: Frequency histogram of windforce on the scale of Beaufort and sea- and swell state on the scale of Douglas.
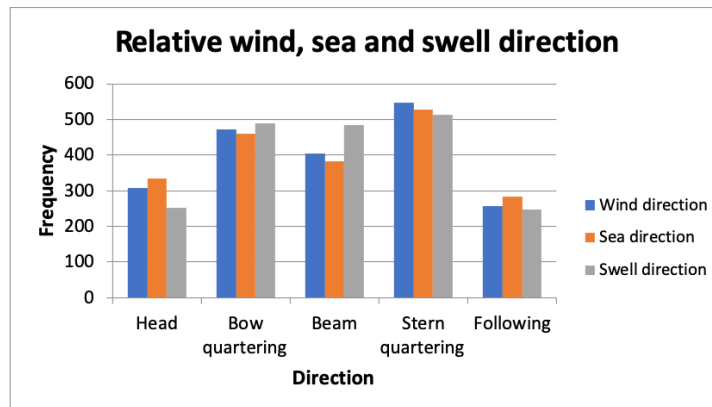
Figure B.6: Frequency histogram of wind, sea and swell directions.
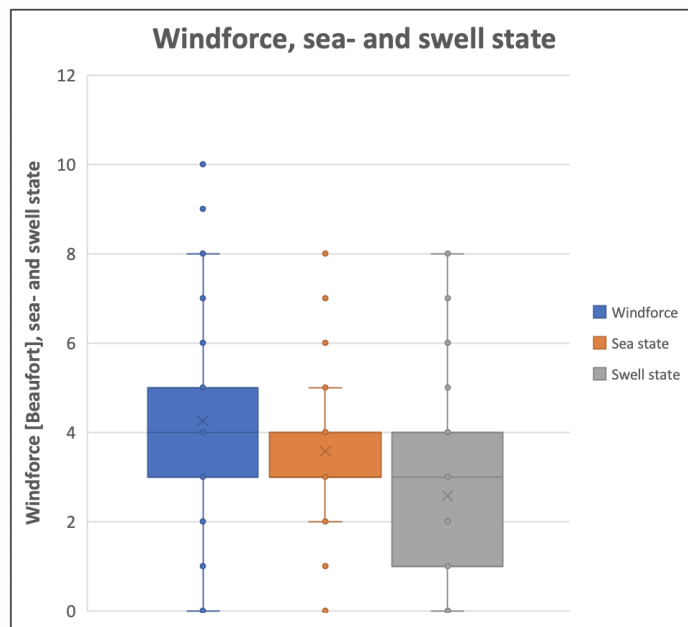
Figure B.7: Boxplot of windforce and sea- and swell state.
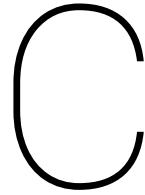
Approximations in white box models

Table C.1: **Sea water density and kinematic viscosity at standard salinity, together with approximated values for the kinematic viscosity by Lutzen and Kristensen (2013). This function approximates the kinematic viscosity as a function of sea water temperature and density. It can be observed that similar values are approximated as the reference values from 26th ITTC Specialist Committee on Uncertainty Analysis (2011).**

Sea water temperature [$°C$]	Kinematic viscosity [$\frac{m^2}{s}$]	Kinematic viscosity [$\frac{m^2}{s}$]	Density [$\frac{kg}{m^3}$]
	Lutzen and Kristensen (2013)	26th ITTC Specialist Committee on Uncertainty Analysis (2011)	26th ITTC Specialist Committee on Uncertainty Analysis (2011)
1	1.782E-06	1.793E-06	1028.09
5	1.564E-06	1.576E-06	1027.72
10	1.354E-06	1.360E-06	1027.00
15	1.188E-06	1.189E-06	1026.02
20	1.053E-06	1.051E-06	1024.81
25	9.410E-07	9.371E-07	1023.39
30	8.454E-07	8.425E-07	1021.77
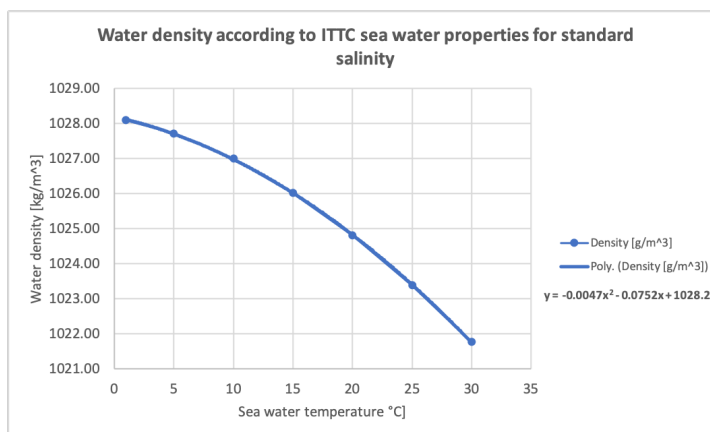
Figure C.1: Sea water density as a function of sea water temperature for standard salinity, based on reference values of 26th ITTC Specialist Committee on Uncertainty Analysis (2011).
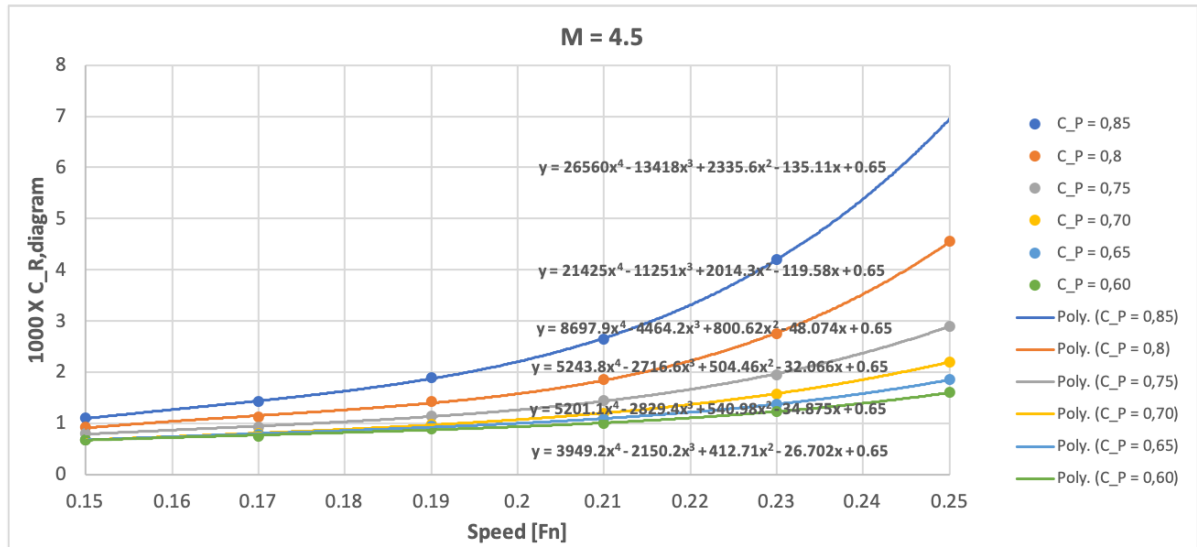
Figure C.2: Residual resistance coefficient for M = 4.5.
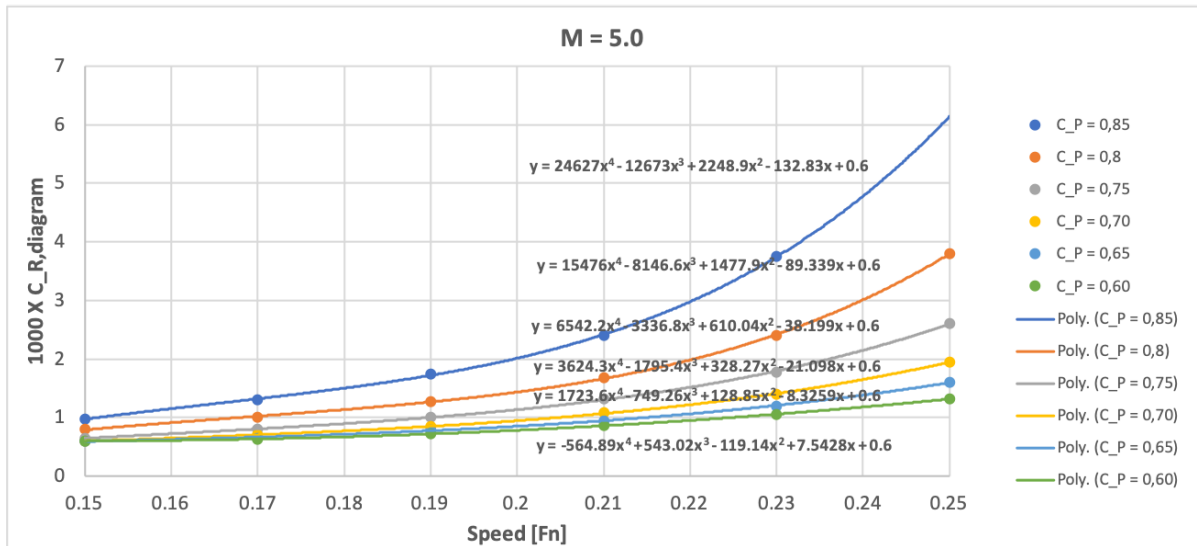
Figure C.3: Residual resistance coefficient for M = 5.0.
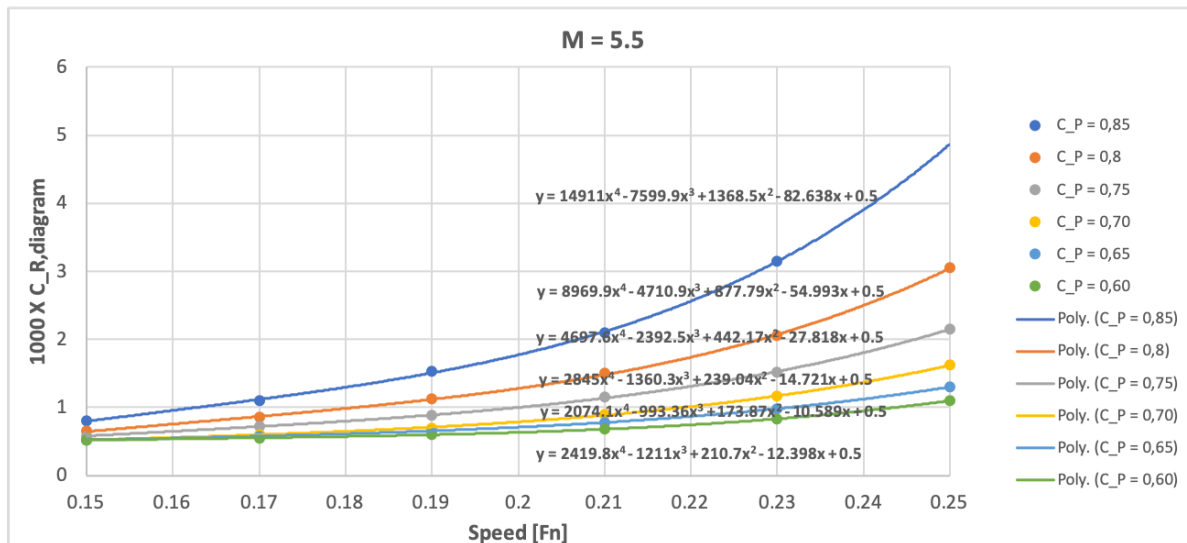
Figure C.4: Residual resistance coefficient for M = 5.5.
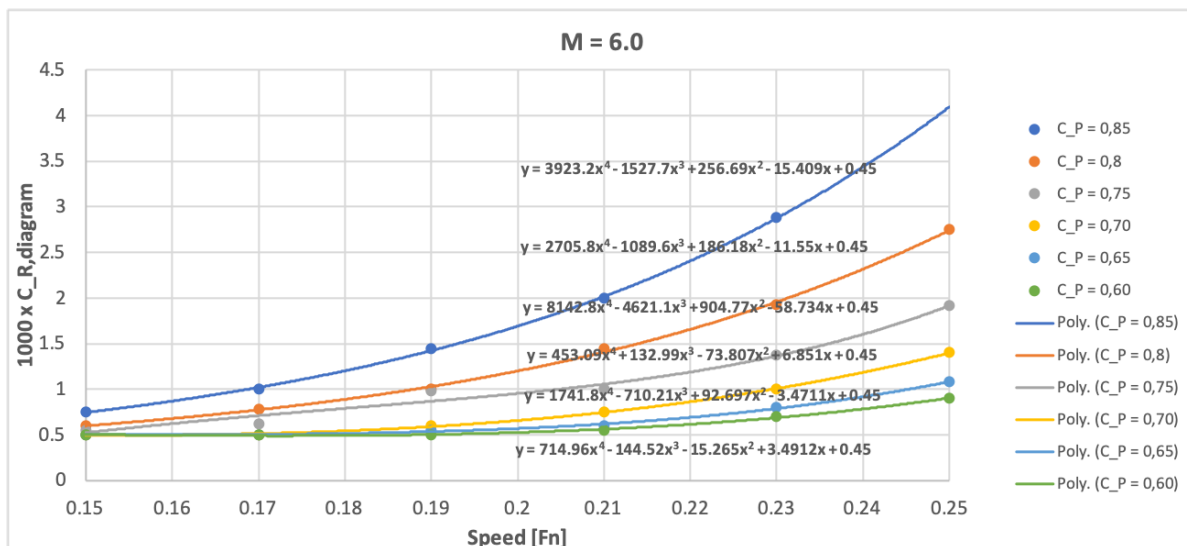
Figure C.5: Residual resistance coefficient for M = 6.0.
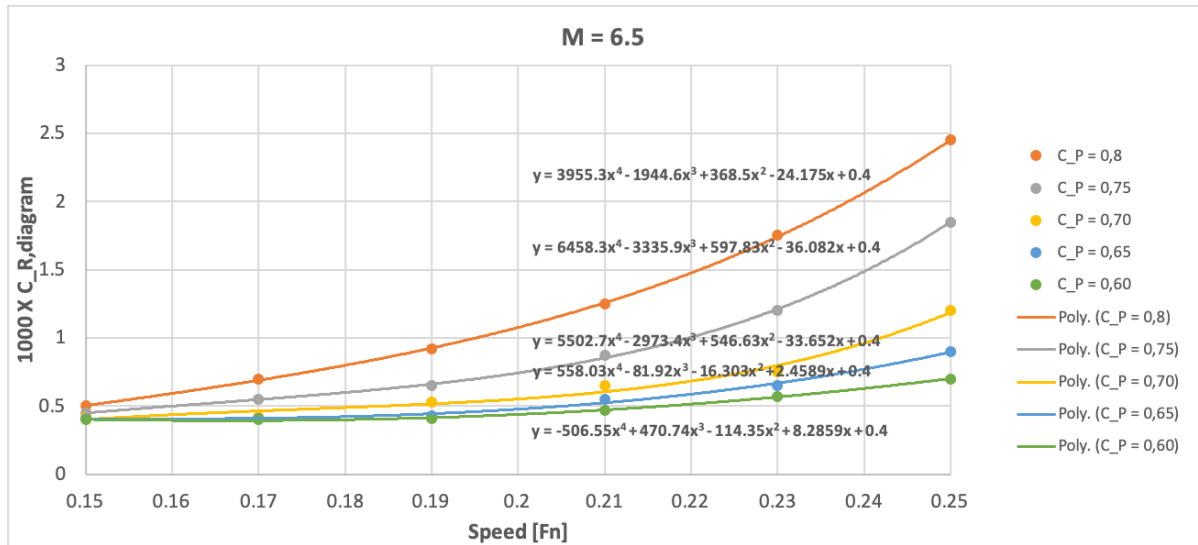
Figure C.6: Residual resistance coefficient for M = 6.5.
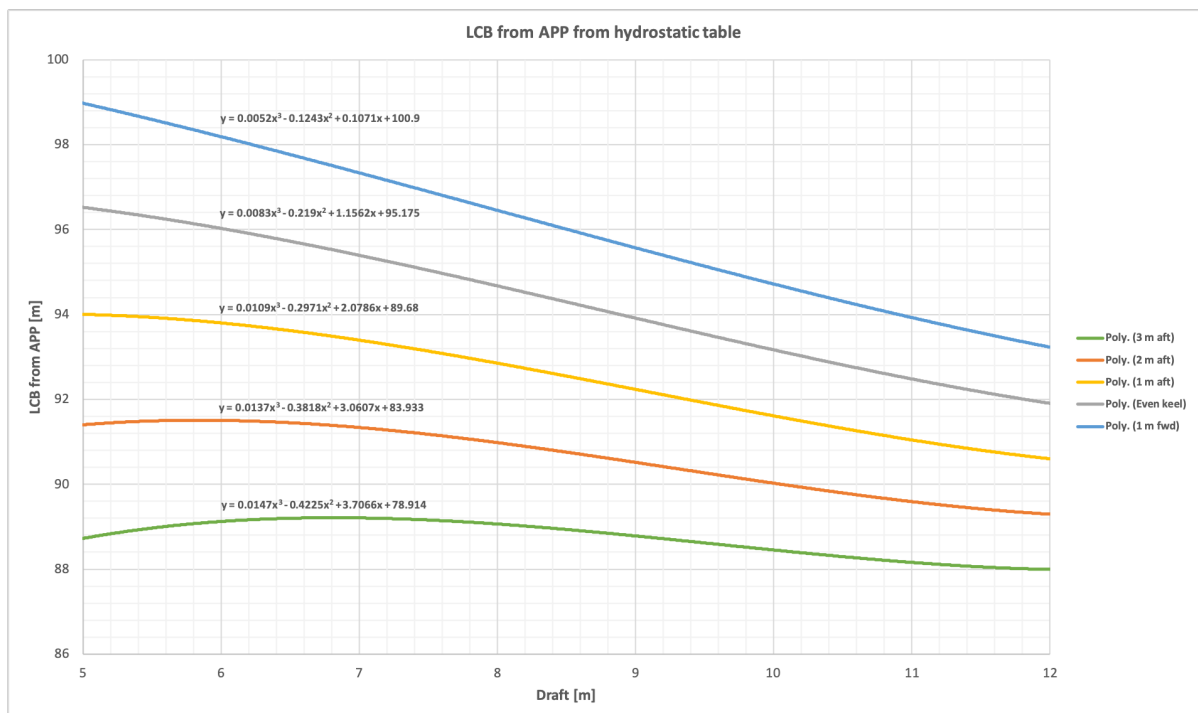
Figure C.7: Length centre of buoyancy (LCB) of the C38 ship class in metres, measured from the aft perpendicular (as defined in the hydrostatic tables of the ship).
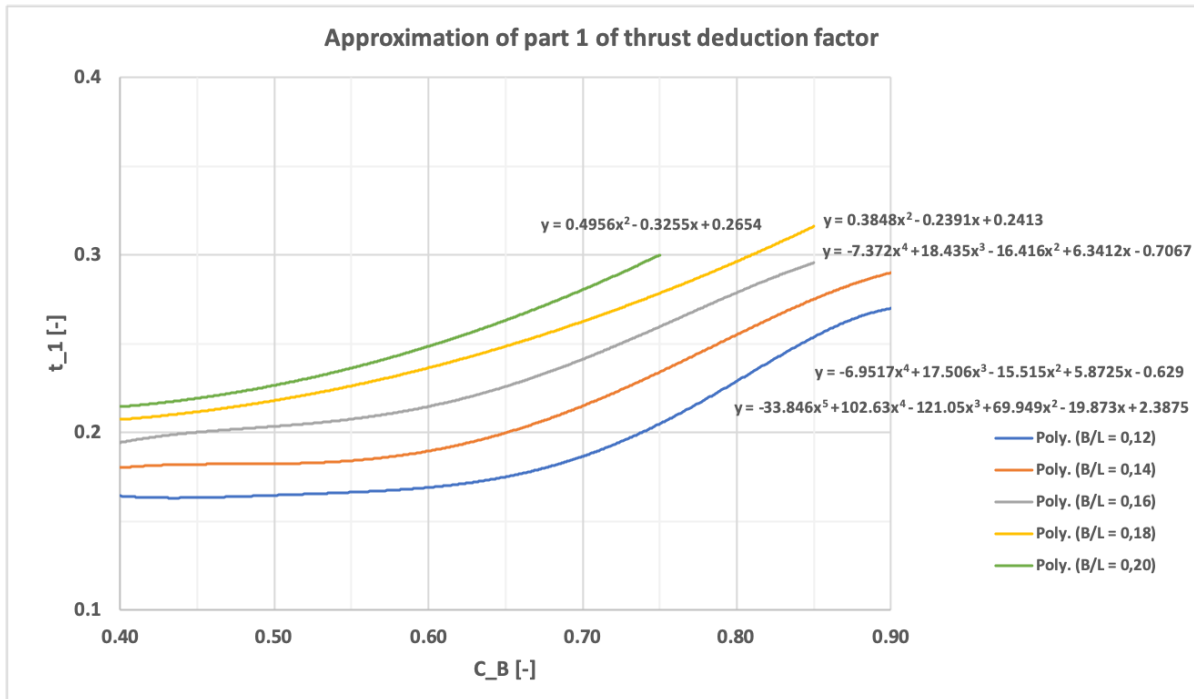
Figure C.8: Approximation of first part of thrust deduction factor of the method of Lutzen and Kristensen (2013).
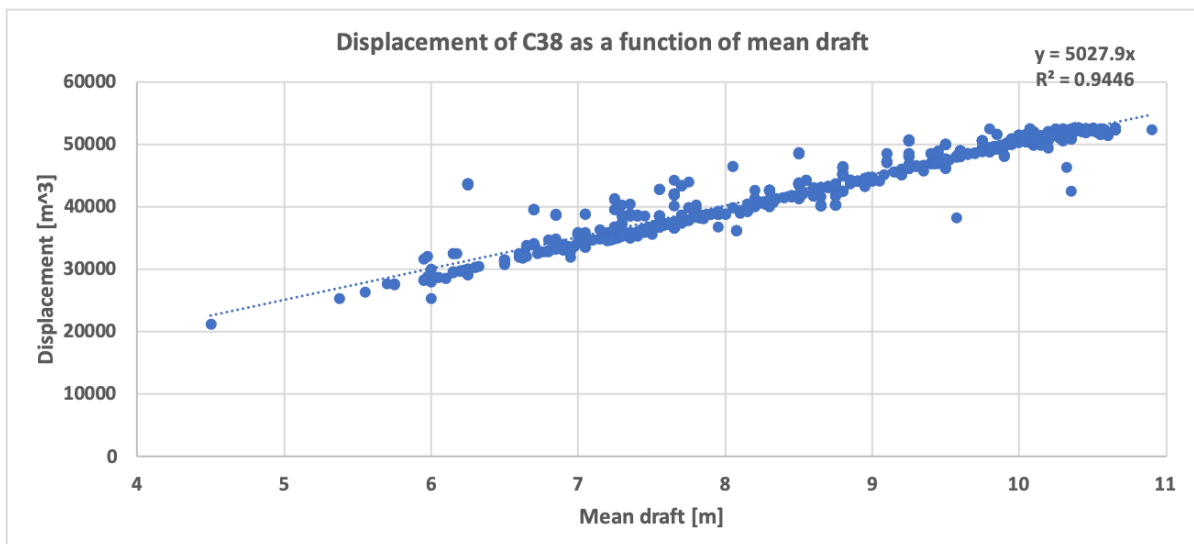
Figure C.9: Function to estimate displacement as a function of mean draft.

D

Data pre-processing
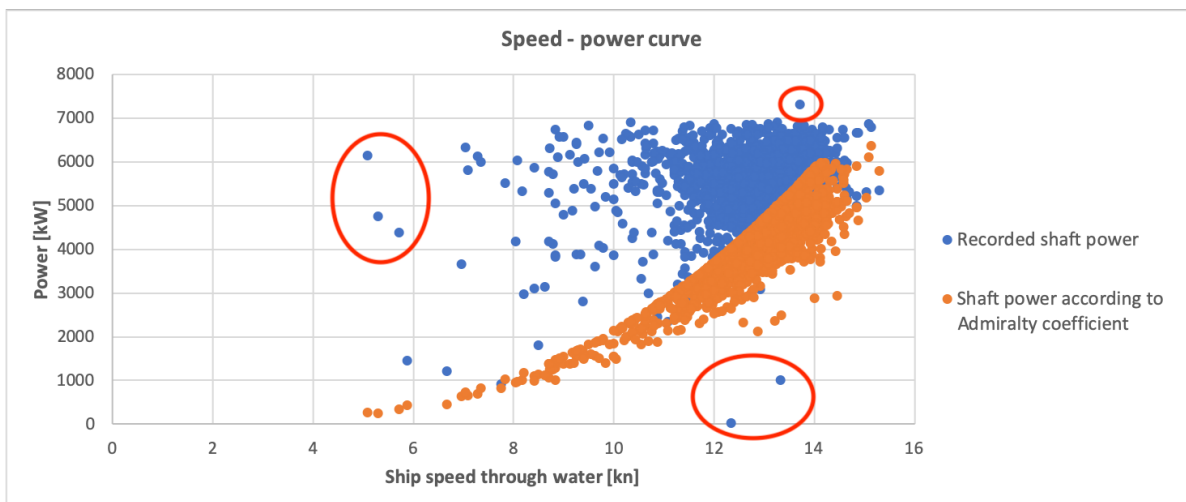
Figure D.1: Speed-power curve, showing the shaft power and speed as recorded in the noon reports in blue, and the estimated shaft power according to the Admiralty coefficient in orange. Outliers are marked in the red ovals.
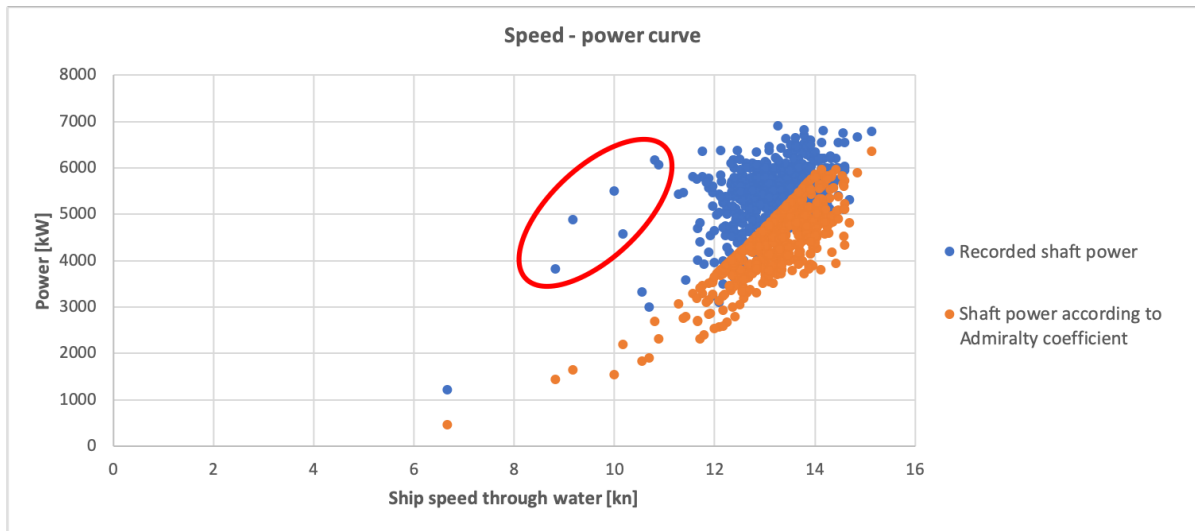
Figure D.2: Speed-power curve, showing the shaft power and speed as recorded in the noon reports in blue, and the estimated shaft power according to the Admiralty coefficient in orange. Outliers are marked in the red ovals.
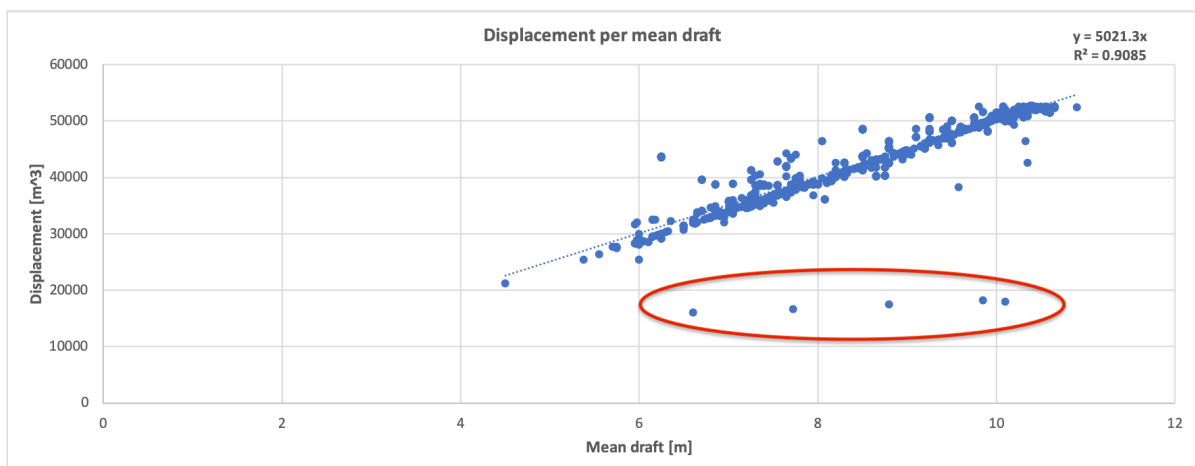
Figure D.3: Displacement as a function of mean draft. Deleted datapoints are indicated in red ovals.

E

Performance of network topologies

Table E.1: **Performance of different network topologies of the GBM-PHM model variant.**

1 hidden layer

Number of neurons	RE [%]	STD	Speed per training	Remark
3	6.8033	0.40262	<1 sec	Clustered results
6	6.7628	0.46252	<1 sec	Clustered results
9	6.6523	0.46216	<1 sec	
12	6.5989	0.44434	<1 sec	
15	6.6634	0.4251	<1 sec	
18	6.6178	0.43056	<1 sec	
21	6.7173	0.46407	<1 sec	
24	6.7799	0.40569	<1 sec	
27	6.7043	0.42611	<1 sec	
30	6.7222	0.46045	<1 sec	
50	6.7623	0.44513	<5 sec	
75	6.9112	0.45686	<10 sec	

2 hidden layers

Number of neurons	RE [%]	STD	Speed per training	Remark
3	6.8844	0.45409	<1 sec	Clustered results
6	6.708	0.45252	<1 sec	
9	6.7349	0.42587	<1 sec	
12	6.6877	0.45559	<1 sec	
15	6.7487	0.41993	<1 sec	
18	6.7698	0.45428	<1 sec	
21	6.6751	0.38031	<2 sec	
24	6.7529	0.38571	<3 sec	
30	6.8917	0.43597	<5 sec	
50	6.8163	0.42322	<1 min	K = 25

3 hidden layers

Number of neurons	RE [%]	STD	Speed per training	Remark
3	6.8697	0.58365	<1 sec	Flat line observed
6	6.8136	0.54921	<1 sec	
9	6.5964	0.5344	<1 sec	
12	6.7173	0.46672	<3 sec	
15	6.6504	0.46626	<3 sec	

4 hidden layers

Number of neurons	RE [%]	STD	Speed per training	Remark
3	6.9705	0.61627	<1 sec	Clustered results
6	6.6611	0.48725	<1 sec	Clustered results
9	6.7683	0.55963	<2 sec	
12	6.8036	0.52996	<5 sec	
15	6.851	0.58832	<5 sec	

Table E.2: **Performance of different network topologies of the GBM-PLK model variant.**

1 hidden layer

Number of neurons	RE [%]	STD	Speed per training k	Remark
3	6.9326	0.44669	<1 sec	Clustered results
6	6.672	0.39466	<1 sec	
9	6.6221	0.44762	<1 sec	
12	6.6454	0.3882	<1 sec	
15	6.5768	0.45184	<1 sec	
18	6.6393	0.41847	<1 sec	
21	6.6735	0.45523	<1 sec	
24	6.6624	0.43528	<1 sec	
27	6.6227	0.42849	<1 sec	
30	6.6532	0.46439	<1 sec	
50	6.7076	0.47716	<2 sec	
75	6.7889	0.52781	<3 sec	

2 hidden layers

Number of neurons	RE [%]	STD	Speed per training	Remark
3	6.857	0.46406	<1 sec	Clustered results
6	6.638	0.45059	<1 sec	Clustered results
9	6.6795	0.46823	<1 sec	
12	6.6824	0.47008	<1 sec	
15	6.7395	0.48276	<1 sec	
18	6.8197	0.46978	<1 sec	
21	6.6499	0.40354	<1 sec	
24	6.7489	0.44692	<2 sec	
30	6.9949	0.49822	<3 sec	
50	6.9137	0.53388	<1 min	K = 25

3 hidden layers

Number of neurons	RE [%]	STD	Speed per training	Remark
3	6.9735	0.48842	<1 sec	Clustered results
6	6.7588	0.43283	<1 sec	
9	6.6794	0.42128	<2 sec	
12	6.6867	0.52534	<3 sec	
15	6.8043	0.44942	<3 sec	

4 hidden layers

Number of neurons	RE [%]	STD	Speed per training	Remark
3	7.0585	0.79021	<1 sec	Clustered results
6	6.8835	0.59803	<1 sec	Clustered results
9	6.7889	0.48383	<2 sec	
12	6.7841	0.61062	<5 sec	
15	7.0065	0.83978	<5 sec	

Table E.3: **Performance of different network topologies of the BBM model variant.**

1 hidden layer

Number of neurons	RE [%]	STD	Speed per training k	Remark
3	6.8705	0.38525	<1 sec	
6	6.7438	0.42813	<1 sec	
9	6.6679	0.45716	<1 sec	
12	6.6404	0.47535	<1 sec	
15	6.6868	0.50566	<1 sec	
18	6.6737	0.41893	<1 sec	
21	6.6726	0.51184	<1 sec	
24	6.7152	0.43576	<1 sec	
27	6.6316	0.41727	<1 sec	
30	6.6768	0.48192	<1 sec	
50	6.8105	0.46171	<2 sec	
75	6.9562	0.5359	<3 sec	

2 hidden layers

Number of neurons	RE [%]	STD	Speed per training	Remark
3	6.8132	0.43951	<1 sec	
6	6.7492	0.45239	<1 sec	
9	6.7126	0.51982	<1 sec	
12	6.6498	0.40532	<1 sec	
15	6.7173	0.51255	<1 sec	
18	6.7364	0.40972	<1 sec	
21	6.7542	0.45709	<1 sec	
24	6.8176	0.51279	<2 sec	
30	6.9535	0.50868	<3 sec	
50	6.91	0.49474	<1 min	K = 25

3 hidden layers

Number of neurons	RE [%]	STD	Speed per training	Remark
3	6.9428	0.51851	<1 sec	
6	6.7983	0.56357	<1 sec	
9	6.6607	0.47356	<2 sec	
12	6.6982	0.6432	<3 sec	
15	6.7344	0.45044	<3 sec	

4 hidden layers

Number of neurons	RE [%]	STD	Speed per training	Remark
3	7.1548	0.74004	<1 sec	Clustered results
6	6.804	0.60284	<1 sec	Clustered results
9	6.7405	0.55927	<2 sec	
12	6.8616	0.56508	<5 sec	
15	6.9081	0.86442	<5 sec	Flat line observed

F
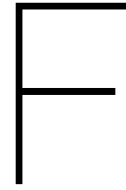
Brief survey to ship crew

A small survey was sent to the crew of the C38 and D37 ship class in January and February 2020, to find out if the already existing trim tables are available on board of the ships. This initial survey covers question 1, 2 and 3.

Additionally, question 4 and 5 was sent to the crew of the C38 ship class, and one of the ships within the D37 ship class as well.

From most ships, a reply has been received. When no reply was received, the vessel name is left out in the list of answers.

Overview of questions:

1. Are these trim tables available on board of your ship?

2. Are you using these trim tables?

    (a) If yes, could you explain how you use these trim tables?

    (b) If no, what limits you in using trim tables?

3. Do you have any additional comments regarding trim optimization?

4. In the noon reports, the forward and aft draft is recorded. How do you determine this forward and aft draft while sailing at sea?

5. It is known that the ship will trim forward when sailing compared to the static trim in port. How much does the ship trim forward while sailing 10-11-12-13-14-15 knots, compared to static trim?

F.1. Are these trim tables available on board of your ship?

F.1.1. C38 ship class

- Pride: No such table onboard. I always sail with at least 0.5m trim when fully loaded as it is optimum for best steering.

- Integrity: The trim table you attached I did not find here on board – but being only a short term reliever I might have missed to find it. However found a similar table in C

- Tenacity: Not sure what to reply to this as we have to many unknown during loading as they change qty and stowage several times during preparation for the full load and at the end we are just what we are and that is at best full cgo even keel and no ballast and no list.

- Loyalty: We(Choff, Cheng & I), have never seen the attached table, where can we find it?

- Excellence: Never seen this trim table. Where can I find it?

F.1.2. D37 ship class

- Innovation: Would presume so, but can't find them at this time.

- Confidence: Having not personally been aware of this issue I have done some digging. The normal SMT apparently always use this practice when fully loaded. However this only counts for half of the voyage. I could not find any information is the Stability booklets but the Chief Eng pointed me in the direction of a Performance Memo from 2004. It goes into great depth about the saving to be made using optimum trim.

- Invention: We have trim tables included in the maneuvering manual received from the Danyard.

- Efficiency: Yes, these trim tables available on board of my ship and I have been using it on this Class.

- Capability: Has not received this question.

- Concept: Unfortunately cannot help you with jour project. New to this ship, did some research with no results. No.

- Effort: No response received.

F.2. Are you using these trim tables?

F.2.1. C38 ship class

- Pride: No.

- Integrity: so far I did not, but actually it is well known that trim by the head increases speed or reduces engine load. I have not much experience on C38 class but e.g. D37's trim about 1 – 1.5 m by the head when running full sea speed when static trim is zero (even keel). C38 might be similar, I will check once underway with our good ship and revert if needed. how to use tables – as per above, tables show at 10m draft, 13 kn speed and 0.5 m fwd trim engine load reduces approx. 100kw, resulting in either less consumption or higher speed. what limits us – as per above

- Tenacity: Panama has a issue also if the ship is by head so has the Houston pilots as they have declared C38's has to be minimum 0.5 mtr by stern trim. From way back we have always said we are doing best speed etc if we are by head so that would be the best but how feasible it is to make this a trend is not for me to predict. As we discharge we sometimes can add ballast to be by the head but not sure if carrying ballast around justify the savings of fuel. As now we have loaded in 4 ports but only aft and fwd so not able to make any change to that. This is again due to nature of cgo we carry, fwd section low flash and no heat required and aft part heated cgo (low and high heat) and reason for this is that cgo is noit ready in some of the ports or they have specific requirements in reg to last 3 cgo's in the tank , heat adjacent etc etc.

- Loyalty: In the CargoMax software there is a feature for this, with choices of speed at constant draft. (see below). Normally, it is not of much use, as we first and foremost struggle to get as much cargo we can onboard minding the draft restrictions. This means loading as close to even keel as possible, with minimum ballast.

- Excellence: Usually we need to minimize trim to minimize draft especially with our UKC policy.

F.2.2. D37 ship class

- Innovation: Once a decade.Looked up what optimal trim is: as your screenshot already indicated it's best to be around 0.5m by the head for pretty much any draft. Question: is this table for dynamic or static trim? (when even keel statically, the ship runs by the head when moving...)

- Confidence: The major factor in not planning for this is cargo distribution.

- Creativity: Not sure what to reply to this as we have to many unknown during loading as they change qty and stowage several times during preparation for the full load and at the end we are just what we are and that is at best full cgo even keel and no ballast and no list.

- Invention: I have not been looking too much these tables but it is well known fact that D37 class ships in loaded condition go faster in condition of half meter forward trim to even keel. We have been trying to keep trim close to even keel in loaded conditions during ocean crossings. Also in lighter conditions on any longer voyages we are trying to keep trim minimized trying to find best balance between the amount ballast water onboard, stresses on the hull and gain achieved in speed or fuel saving.

- Efficiency: Yes, I understand and could explain how to use them.

- Concept: N/A

F.3. Do you have any additional comments regarding trim optimization?

F.3.1. C38 ship class

- Pride: Also, forget 14 and 15 knots as it's not often we get that speed unless it's flat calm or there's a heavy current since we have so little power the slightest current or wind from ahead slows us down significantly. I was here for sea trials and having seen how they were run and having now been here for 4 years I have no confidence whatsoever in sea trial figures.

- Tenacity: Saving fuel would be best if we did not squeeze the last knot out of the hull as the fuel use is dropping drastically as we drop speed 1-2 knots.

F.3.2. D37 ship class

- Innovation: Trim is not all we look at. It's a dynamic mix of sea conditions, bending and shear force conditions, tank cleaning ops, cargo adjacent to ballast tanks, planned work in ballast tanks, ballast exchange, etc. Often we choose to optimize prior factors before looking at optimum trim for energy consumption. We trim her optimally when we can...

- Invention: Stresses on the hull are becoming an issue if trying to reduce trim too much on lighter conditions. Best of coarse is when you manage to optimize trim with cargo instead of taking additional ballast where you loose always some of the gain for the extra weight taken.

- Efficiency: Not much to comment, Robert. It's a cut clear case that it saves money. In the past I've been playing with the trim and put a tracker on the RPM's , Prop power and Prop torque. It's more fun when it's visible. If we could add a tracker for USD then it would be even greater...J We are alongside at the moment, but this is what it would look like...

F.4. In the noon reports, the forward and aft draft is recorded. How do you determine this forward and aft draft while sailing at sea?

F.4.1. C38 ship class

- Pride: We update drafts based on weights in Cargomax and bunkers burned, water made every few days. No other method is accurate as the ship will be rolling and pitching in the seaway.

- Integrity: Drafts at sea while underway are taken from c/max calculations. As far I know there are no tables, calculations available for fwd trim changes at various speed. I have not sufficient experience on C-38 class vessels.

- Tenacity: As you say we are recording the drafts in the noon reports and sure we do but after leaving Panama for crossing Pacific we have full cgo and enough fuel to reach the other side so adding ballast to be by head is not a option as normaly at the max mark.

- Loyalty: We are recording actual static drafts from the CargoMax.

F.4.2. D37 ship class

- Innovation: Choff via cargomax. Noon reports on sea passages are not updated regularly with changing drafts due to ballasting, water and fuel consumption and do not reflect actual conditions during sea passage at this time.

F.5. It is known that the ship will trim forward when sailing compared to the static trim in port. How much does the ship trim forward while sailing 10-11-12-13-14-15 knots, compared to static trim?

F.5.1. C38 ship class

- Pride: Have no exact idea how much the ship will trim and it depends on our loaded condition. I have seen about half a meter when loaded on pilotage but on ocean passages I can't say. My primary concern with the C38 class is steering and as long as I have at least 0.5m stern trim for optimum steering on pilotage I'm happy. This class of ship should NEVER be trimmed by the head when underway.

- Integrity: To determine fwd trim changes also draft/displacement must be considered as well as sea conditions. Actually it is not possible, at least for me, to answer this question. I do not have sufficient experience on C-38 class vessels and it would be guessing only.

- Tenacity: Trimming fwd when at sea we can only go 14 knots and that is only on a good day. I would say anything from 0.5 mtr to 1 mtr at full speed.

- Loyalty: Have looked for the information in the Sea Trials and didn't find such information, therefor I have the same question where to find the information.

F.5.2. D37 ship class

- Innovation: Around full speed (14-16 kn) in open sea and fully loaded these ships trim 0.6 to 0.8m by the head (based on experience). At lesser speed I presume it's a square root function of the speed less, but don't have actual figs for you.

G

Sea trial instructions

G.1. Introduction

Trim optimization is one of the incentives being researched within Fleet Support to improve the fuel efficiency of all ships in the fleet. In the past months, a model has been established to generate trim tables based on noon report data. The research is reaching its validation phase on the first ship class. Data from the C38 ship class is used as a case study. Before this new model to generate trim tables can be used with confidence in trim optimization, the generated trim tables have to be validated with operational data, measured in equal weather conditions. The only way to do this, is to conduct a number of tests while the ship is at sea during a voyage.

The effect of trim should be validated for multiple draft conditions and for different speeds. To be able to test at different draft conditions in a limited amount of time and to obtain a sufficient number of validation points, all 6 ships of the C38 class should be involved in this validation phase.

This document consists of two parts. The first part gives an explanation on how the trim tables are generated. The second part is a proposal to perform a number of tests, used to validate the generated trim tables.

G.2. Part I: Explanation of generated trim tables

The established model uses machine learning on a number of variables that are available from noon reports, of which it is known that it affects the required shaft power or the resulting speed through water. A correlation analysis has been done to confirm these expected relationships.

The model acts as a black box, that learns the relationships between the input data (listed below) and the output data (required shaft power), by providing the model with historical noon report data. After a number of learning iterations, the model has learned these relationships and can be used to estimate the shaft power for any input condition. See figure G.1 for an overview of the model.

- Draft forward and aft (and trim)
- Displacement
- Speed through water
- Wind force + direction (ship relative)
- Sea state + direction (ship relative)
- Swell state + direction (ship relative)

- Days since last hull cleaning

- Days since last propeller polishing
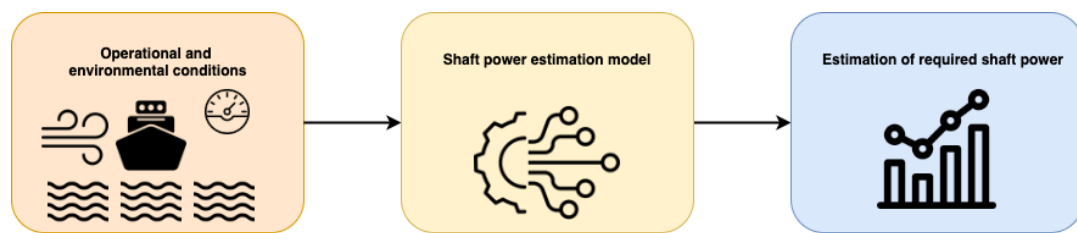
Figure G.1: Model overview to estimate shaft power. When all conditions are fixed, while draft and trim is varied, trim tables can be generated. The benefit of this model is that it can include the effect of weather and sea conditions on the ship performance, meaning that the generated trim table is adapted to that specific condition. Based on these conditions, an estimate of the fuel consumption for propulsion can be made as well. .

Limitations in trim and how trim optimization can be integrated in the (active) voyage management system is part of the research as well, but will not be covered in this validation.

G.3. Part II: Validation

G.3.1. Safety first

Safety remains the first priority during these tests. It should be to the ship crew's decision if the proposed combination of draft and resulting sailing condition are safe to operate. This includes to maintain sufficient hull strength, stability, propeller immergence, freeboard, visibility and maneuverability. If for any reason it is not safe to conduct a certain test, it should not be done.

G.3.2. Timeframe

Tests should be conducted as soon as reasonably possible. The goal is to collect the sea trial results before the first of May 2020. If the sea trials could not have been performed for any reason before this date, these should still be performed and will be considered separately.

G.3.3. Conditions

To prevent noise in measurements and because trim optimization will only be effective in relatively calm water conditions, the condition for measurements should comply with the following:

- Sea state must be less or equal to 3

- Swell state must be less or equal to 2

- Velocity of the current should be less or equal to 1.5 knots

- Shaft generator should be turned OFF

- Maintain a steady course with autopilot on fixed heading

- The counter rudder angle to maintain the steady course, shall not exceed 5 degrees. If this occurs during the sea trial, please abort or postpone the sea trial

- Ship speed through water should increase, starting with 11 knots, finishing with 14 knots

G.3.4. How to trim

Trim is defined as the static trim condition as indicated by the loading computer. The trim condition may be changed by re-allocating tank loads that can be pumped to different tanks, or by adding or discharging ballast water. Other solutions may exist as well, but will all be subject to the loading situation.

G.3.5. Sea trials to be performed

Separate to this instruction, an Excel file is sent. This file provides the table to log the measurements for all relevant combinations of trim and speed. It will not be possible to perform sea trials for each condition of the table, since the freedom in trimming the ship will be limited, as well as the time to perform the tests.

   The most effective way to perform the tests, is to test at the most possible forward trim condition, and the most possible aft trim condition, with steps of 0.25 or 0.50 meters in between. The more conditions tested, the better the generated trim tables can be validated.

   Sea trials are usually repeated in opposite direction, to average the effect of current and weather. The developed model will be able to account for these effects, therefore one test run for each combination of trim and speed is sufficient.

G.3.6. How to perform the tests

The grey part of the table indicates the possible test conditions. Each test condition should be performed as follows:

1. Adjust the trim condition as close as possible to the indicated trim condition.

2. Adjust the ship speed through water as close as possible to the target speed.

3. Measurements should only be started after a constant ship speed and a fairly constant shaft power is reached.

4. Fill in the VESSEL (blue) and WEATHER (green) section.

5. Measurement of the average required shaft power should be performed over a period of at least 15 minutes.

6. Fill in the average shaft power and engine speed in the POWER (orange) section.

7. Fill in the maximum observed counter rudder angle in the RUDDER (blue) section.

8. Remarks can be added on the right yellow part of the table.

9. Repeat for other speeds.

G.3.7. Remarks

We would also welcome additional feedback from visual observations made during the tests. Where there any noticeable differences observed during the test runs, compared with previous tests runs? Observations could be seen for instance in rudder orders (magnitude and quantity) by the auto pilot, large fluctuations/variations noted or observed in % pitch or kW measured on the shaft.

   We would like to understand and hear your feedback if all conditions have shown similar behaviours for the machineries, or if there are differences observed in the trim conditions that may also impact items such as course keeping, maintenance (wear and tear), etc.

G.3.8. Final note

Please send the results, or any questions regarding this manual or the Excel file, to Robert Zwart (RZW@stolt.com) with your operator and superintendent in CC.

Thank you for performing the required sea trials. After all information is processed, we will send an e-mail with the results of the validation.

H

Sea trial results

Ship name	Stolt Loyalty
Local date (dd/mm/yyyy)	18/04/2020 and 19/04/2020
Initial draft forward (m)	10,3
Initial draft aft (m)	10,6

TRIAL CONDITION		VESSEL							WEATHER							POWER		RUDDER	REMARKS
Trim condition	Speed trough water (log speed) knots	Actual ship speed through water (log speed) knots	SOG knots	Loading (DWT) tonnes	Ship's heading degrees	Draft forward metres	Draft aft metres	Draft mean metres	Seawater temperature degree Celsius	Windforce Beaufort	Wind direction N-NNE-NE...	Sea state Douglass	Sea direction N-NNE-NE...	Swell state Douglass	Swell direction N-NNE-NE...	Shaft power kW	Engine speed rpm / pitch	Maximum observerd counter rudder angle degrees	
-0.50 m (forward trim)	11	11	10	39938	302	10,8	10,3	10,55	30	1	NW	1	NW	1	SSW	2700	74/90%	2	
	12	12	11,1	39938	302	10,8	10,3	10,55	30	1	NW	1	NW	1	SSW	3723	83/90%	2	
	13	13	12,1	39938	302	10,8	10,3	10,55	30	1	SW	1	S	1	SSW	4720	89/90%	3	
	14	14	13,2	39938	308	10,8	10,3	10,55	30	1	SW	1	S	1	SSW	5953	96/90%	3	
-0.25 m (forward trim)	11	11	10,2	39719	306	10,65	10,4	10,525	30	1	NW	1	NW	1	SSW	2780	75/90%	3	
	12	12	11	39719	302	10,65	10,4	10,525	30	1	NW	1	NW	1	SSW	3822	83/90%	2	Slight vibration
	13	13	12,1	39719	302	10,65	10,4	10,525	30	0	CALM	1	NW	1	SSW	5037	91/90%	2	
	14	14	13,2	39719	296	10,65	10,4	10,525	30	0	CALM	1	NW	1	SSW	6106	96/91%	3	
even keel	11	11	10,3	39470	295	10,47	10,47	10,47	31	1	E	1	NE	1	SSW	2901	76/90%	3	
	12	12	11,3	39470	295	10,47	10,47	10,47	31	1	E	1	NE	1	SSW	4005	84/90%	2	Slight vibration
	13	13	12,3	39470	295	10,47	10,47	10,47	31	1	N	1	N	1	SW	5143	92/90%	3	
	14	14	13,1	39470	295	10,47	10,47	10,47	30	0	CALM	1	N	1	SSW	6327	96/92%	3	
0.25 m (stern trim)	11	11	11	39222	295	10,3	10,55	10,425	29	3	NW	2	NW	2	SW	3255	78/90%	2	
	12	12	11,7	39222	295	10,3	10,55	10,425	30	3	NW	2	NW	2	SW	4316	86/90%	2	
	13	13	12,8	39222	296	10,3	10,55	10,425	30	3	NW	2	NW	2	SW	5466	92/90%	2	
	14	14	13,8	39222	296	10,3	10,55	10,425	30	3	NW	2	NW	2	SW	6781	96/94%	3	
0.50 m (stern trim)	11	11	11,4	39509	296	10,2	10,7	10,45	30	3	WNW	2	NW	2	SW	3439	79/90%	3	
	12	12	12,1	39509	296	10,2	10,7	10,45	30	3	WNW	2	NW	2	SW	4388	86/90%	2	
	13	13	13	39509	296	10,2	10,7	10,45	30	3	WNW	2	NW	2	SW	5908	95/89%	3	
	14	13,8	14	39509	296	10,2	10,7	10,45	30	3	WNW	2	NW	2	SW	6787	96/93%	2	Not able to reach 14kn STW

Figure H.1: Sea trial results as received from Stolt Loyalty.

STOLT INTEGRITY
Local date (01/05/2020)
Initial draft forward (m) 6.0
Initial draft aft (m) 8.0

TRIAL CONDITION		VESSEL							WEATHER								POWER		RUDDER	REMARKS
Trim condition	Speed trough water (log speed) knots	Actual ship speed through water (log speed) knots	SOG knots	Loading (DWT) tonnes	Ship's heading degrees	Draft forward metres	Draft aft metres	Seawater temperature degree Celsius	Windforce Beaufort	Wind direction N-NNE-NE...	Sea state Douglass	Sea direction N-NNE-NE...	Swell state Douglass	Swell direction N-NNE-NE...	Shaft power kW	Engine speed rpm	Maximum observerd counter rudder angle degrees	
-0.50 m (forward trim)	11	11	11,7	20019	23	7,25	6,75	19	4	SE	3	SE	LOW	E	2595	76,3	3	
	12	12	12,8	20019	23	7,25	6,75	19	4	SE	3	SE	LOW	E	3325	80,5	3	
	13	13	13,8	20019	23	7,25	6,75	19	4	SE	3	SE	LOW	E	4350	87,4	3	
	14	14	14,8	20019	23	7,25	6,75	19	4	SE	3	SE	LOW	E	5830	95,8	3	
even keel	11	11	11,4	20019	58	7	7	21	4	SE	3	SE	LOW	E	2695	76,3	3	
	12	12	12,5	20019	58	7	7	21	4	SE	3	SE	LOW	E	3460	81	3	
	13	13	13,5	20019	58	7	7	21	4	SE	3	SE	LOW	E	4565	88,5	3	
	14	14	14,5	20019	58	7	7	21	4	SE	3	SE	LOW	E	5970	96,3	3	
0.50 m (stern trim)	11	11	11,5	20019	59	6,75	7,25	22	4	SE	3	SE	LOW	E	2685	76,2	3	
	12	12	12,6	20019	59	6,75	7,25	22	4	SE	3	SE	LOW	E	3445	81,3	2	
	13	13	13,5	20019	59	6,75	7,25	22	4	SE	3	SE	LOW	E	4500	88,5	3	
	14	14	15,0	20019	59	6,75	7,25	22	4	SE	3	SE	LOW	E	6060	96,8	3	
1.00 m (stern trim)	11	11	11,5	20019	58	6,5	7,5	24	5	SE	3	SE	LOW	E	2975	77	5	
	12	12	12,5	20019	58	6,5	7,5	24	5	SE	3	SE	LOW	E	3585	81,7	4	
	13	13	13,6	20019	58	6,5	7,5	24	5	SE	3	SE	LOW	E	4775	89,4	3	
	14	14	14,6	20019	58	6,5	7,5	24	5	SE	3	SE	LOW	E	6390	98	2	
1.50 m (stern trim)	11	11	11,4	20019	57	6,25	7,75	24	3	SE	3	SE	LOW	E	2975	77	4	
	12	12	12,5	20019	57	6,25	7,75	24	3	SE	3	SE	LOW	E	3385	81	2	
	13	13	13,5	20019	57	6,25	7,75	24	3	SE	3	SE	LOW	E	4480	88,4	2	
	14	14	14,6	20019	57	6,25	7,75	24	3	SE	3	SE	LOW	E	5985	96,9	2	
2.00 m (stern trim)	11	11	12,7	20019	57	6	8	26	4	SE	3	SE	LOW	E	2625	76,3	4	
	12	12	13,8	20019	57	6	8	26	4	SE	3	SE	LOW	E	3370	80,9	2	
	13	13	14,9	20019	57	6	8	26	4	SE	3	SE	LOW	E	4340	87,7	2	
	14	14	15,9	20019	57	6	8	26	4	SE	3	SE	LOW	E	5990	96,8	2	

Figure H.2: Sea trial results as received from Stolt Integrity.

Ship name	STOLT EXCELLENCE
Local date (dd/mm/yyyy)	27/04/2020
Initial draft forward (m)	10,05
Initial draft aft (m)	10,55

TRIAL CONDITION	VESSEL							WEATHER							POWER		RUDDER	REMARKS
Trim condition	Speed trough water (log speed) knots	Actual ship speed through water (log speed) knots	SOG knots	Loading (DWT) tonnes	Ship's heading degrees	Draft forward metres	Draft aft metres	Seawater temperature degree Celsius	Windforce Beaufort	Wind direction N-NNE-NE...	Sea state Douglass	Sea direction N-NNE-NE...	Swell state Douglass	Swell direction N-NNE-NE...	Shaft power kW	Engine speed rpm	Maximum observerd counter rudder angle degrees	
0.50 m (stern trim)	11	10,9	11,2	38691	287	10,05	10,55	19	2	WNW	1	WNW	2	SSE	3112	77/90	3	
	12	12,1	12,4	38691	290	10,05	10,55	19	2	WNW	1	WNW	2	SSE	4152	84/92	2	
	13	13	13,5	38691	285	10,05	10,55	19	2	WNW	1	WNW	2	SSE	5412	91/92	2	
	14	13,8	14,3	38691	290	10,05	10,55	19	2	WNW	1	WNW	2	SSE	6736	92/98	2	

Figure H.3: Sea trial results as received from Stolt Excellence.

Speed calibration table

Table I.1: **Table showing calibration values for various speeds and drafts. Values are based on sea trial results for mean draft conditions of 7.0 m and 10.5 m (marked with "*") and for speeds of (close to) 11, 12, 13 and 14 knots.**

Speed [kn]	Mean draft [m]								
	6.5	7.0*	7.5	8.0	8.5	9.0	9.5	10.0	10.5*
10.00	-1926	-1898	-1870	-1842	-1815	-1787	-1759	-1731	-1704
10.10	-1978	-1938	-1898	-1857	-1817	-1777	-1737	-1696	-1656
10.20	-2026	-1973	-1921	-1869	-1817	-1765	-1712	-1660	-1608
10.30	-2068	-2004	-1941	-1877	-1814	-1750	-1686	-1623	-1559
10.40	-2105	-2031	-1956	-1882	-1807	-1733	-1659	-1584	-1510
10.50	-2137	-2053	-1968	-1883	-1799	-1714	-1629	-1544	-1460
10.60	-2164	-2070	-1976	-1881	-1787	-1692	-1598	-1503	-1409
10.70	-2187	-2083	-1979	-1876	-1772	-1668	-1565	-1461	-1357
10.80	-2204	-2091	-1979	-1867	-1754	-1642	-1530	-1417	-1305
10.90	-2216	-2095	-1975	-1854	-1734	-1613	-1493	-1373	-1252
11.00	-2222	-2094	-1966	-1838	-1711	-1583	-1455	-1327	-1199
11.10	-2224	-2089	-1954	-1819	-1684	-1549	-1414	-1279	-1144
11.20	-2221	-2080	-1938	-1797	-1655	-1514	-1372	-1231	-1089
11.30	-2213	-2065	-1918	-1771	-1623	-1476	-1328	-1181	-1034
11.40	-2199	-2047	-1894	-1741	-1588	-1436	-1283	-1130	-977
11.50	-2181	-2023	-1866	-1708	-1551	-1393	-1236	-1078	-920
11.60	-2158	-1996	-1834	-1672	-1510	-1348	-1186	-1025	-863
11.70	-2129	-1963	-1798	-1632	-1467	-1301	-1135	-970	-804
11.80	-2095	-1927	-1758	-1589	-1420	-1252	-1083	-914	-745
11.90	-2057	-1885	-1714	-1542	-1371	-1200	-1028	-857	-685
12.00	-2013	-1840	-1666	-1493	-1319	-1145	-972	-798	-625
12.10	-1964	-1789	-1614	-1439	-1264	-1089	-914	-739	-564
12.20	-1910	-1734	-1558	-1382	-1206	-1030	-854	-678	-502
12.30	-1852	-1675	-1499	-1322	-1146	-969	-792	-616	-439
12.40	-1788	-1611	-1435	-1258	-1082	-906	-729	-553	-376
12.50	-1719	-1543	-1367	-1191	-1015	-840	-664	-488	-312
12.60	-1645	-1470	-1295	-1121	-946	-772	-597	-422	-248
12.70	-1565	-1393	-1220	-1047	-874	-701	-528	-355	-183
12.80	-1481	-1311	-1140	-969	-799	-628	-458	-287	-117
12.90	-1392	-1224	-1056	-889	-721	-553	-385	-218	-50
13.00	-1298	-1133	-969	-805	-640	-476	-311	-147	17
13.10	-1198	-1038	-877	-717	-556	-396	-236	-75	85
13.20	-1094	-938	-782	-626	-470	-314	-158	-2	154
13.30	-984	-833	-682	-531	-380	-230	-79	72	223
13.40	-870	-724	-579	-434	-288	-143	3	148	293
13.50	-750	-611	-472	-332	-193	-54	86	225	364
13.60	-626	-493	-360	-228	-95	38	170	303	436
13.70	-496	-370	-245	-119	6	131	257	382	508
13.80	-361	-243	-126	-8	110	227	345	463	581
13.90	-221	-112	-2	107	216	326	435	545	654
14.00	-76	24	125	225	326	427	527	628	728
14.10	74	165	256	347	438	530	621	712	803
14.20	229	310	391	472	554	635	716	797	879
14.30	389	460	530	601	672	743	813	884	955
14.40	554	614	673	733	793	853	912	972	1032
14.50	724	772	821	869	917	965	1013	1061	1109
14.60	899	936	972	1008	1044	1080	1116	1152	1188
14.70	1080	1103	1127	1150	1173	1197	1220	1243	1267
14.80	1265	1275	1286	1296	1306	1316	1326	1336	1346
14.90	1456	1452	1448	1445	1441	1438	1434	1430	1427
15.00	1651	1633	1615	1597	1580	1562	1544	1526	1508

J

Trim results from model tests

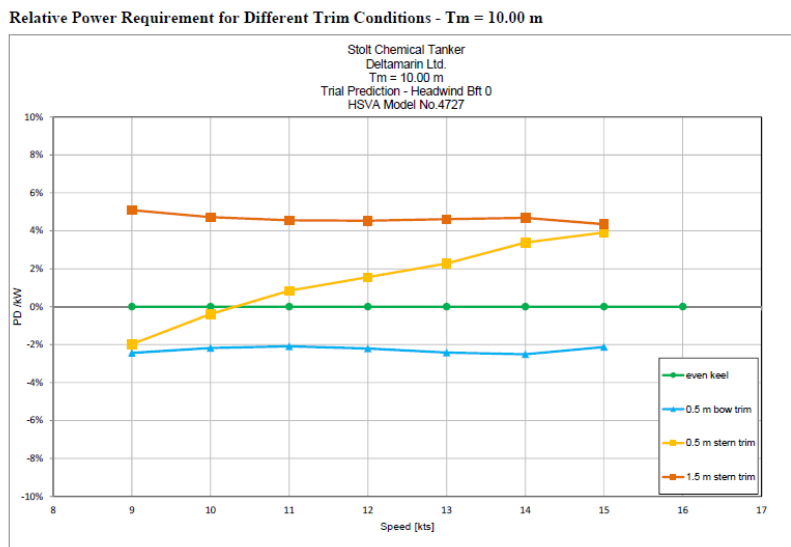Relative Power Requirement for Different Trim Conditions - Tm = 10.00 m

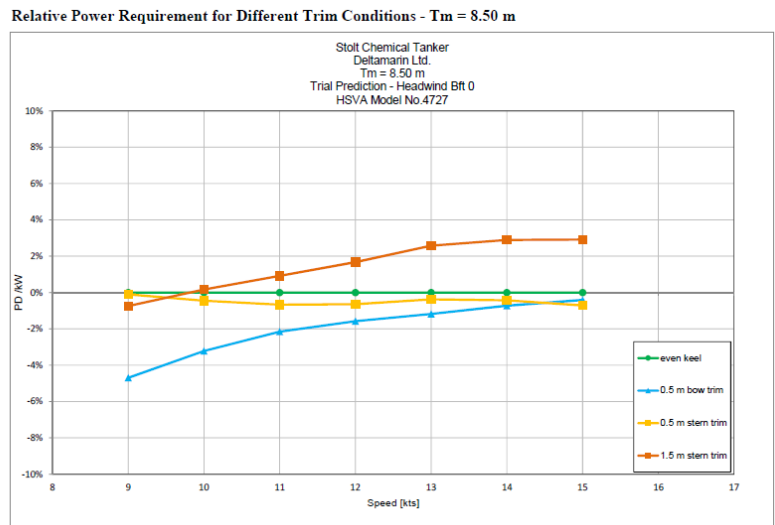Figure J.1: Graph of model scale towing test results for T = 10.0 m.

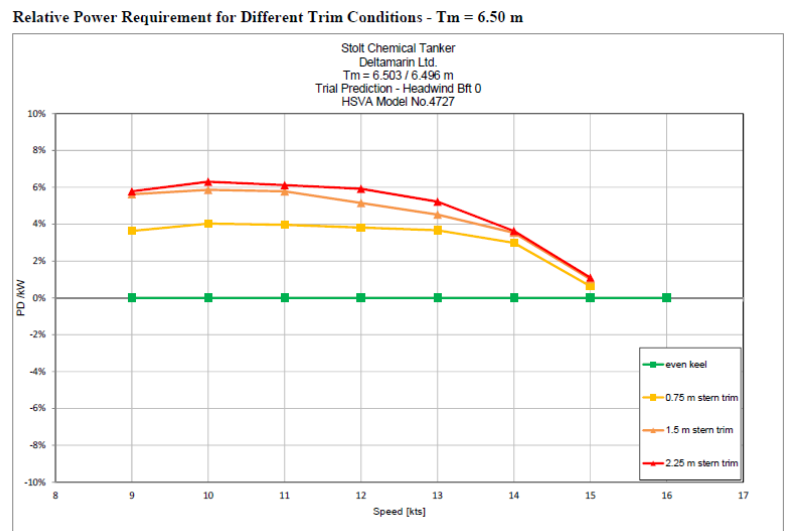Figure J.2: Graph of model scale towing test results for T = 8.50 m.

Figure J.3: Graph of model scale towing test results for T = 6.0 m.